UNLV University Libraries
University of Nevada, Las Vegas

UNLV Theses, Dissertations, Professional Papers, and Capstones

12-1-2013

Feasibility of the Use of Ultrasound Measurements for Grade Verification of the Performance Grade Asphalt Binders

Mehdi Khalili
University of Nevada, Las Vegas, khalilim@unlv.nevada.edu

Follow this and additional works at: https://digitalscholarship.unlv.edu/thesesdissertations

 Part of the Civil Engineering Commons, Engineering Science and Materials Commons, and the Materials Science and Engineering Commons

Repository Citation

Khalili, Mehdi, "Feasibility of the Use of Ultrasound Measurements for Grade Verification of the Performance Grade Asphalt Binders" (2013). *UNLV Theses, Dissertations, Professional Papers, and Capstones*. 2000.
https://digitalscholarship.unlv.edu/thesesdissertations/2000

This Dissertation is protected by copyright and/or related rights. It has been brought to you by Digital Scholarship@UNLV with permission from the rights-holder(s). You are free to use this Dissertation in any way that is permitted by the copyright and related rights legislation that applies to your use. For other uses you need to obtain permission from the rights-holder(s) directly, unless additional rights are indicated by a Creative Commons license in the record and/or on the work itself.

This Dissertation has been accepted for inclusion in UNLV Theses, Dissertations, Professional Papers, and Capstones by an authorized administrator of Digital Scholarship@UNLV. For more information, please contact digitalscholarship@unlv.edu.

FEASIBILITY OF THE USE OF ULTRASOUND MEASUREMENTS FOR GRADE VERIFICATION OF THE PERFORMANCE GRADE ASPHALT BINDERS

By

Mehdi Khalili

Bachelor of Science in Civil Engineering
Zanjan University, Iran
2004

Master of Science in Civil Engineering
ShahidChamran University, Iran
2006

A dissertation submitted in partial fulfillment
of the requirements for the

Doctor of Philosophy - Civil and Environmental Engineering

Department of Civil and Environmental Engineering
Howard R. Hughes College of Engineering
The Graduate Collage

University of Nevada, Las Vegas
December 2013

Copyright by Mehdi Khalili, 2014
All Rights Reserved

UNLV
UNIVERSITY OF NEVADA LAS VEGAS

THE GRADUATE COLLEGE

We recommend the dissertation prepared under our supervision by

Mehdi Khalili

entitled

Feasibility of the Use of Ultrasound Measurements for Grade Verification of the Performance Grade Asphalt Binders

is approved in partial fulfillment of the requirements for the degree of

Doctor of Philosophy in Engineering - Civil and Environmental Engineering

Department of Civil& Environmental Engineering and Construction

Moses Karakouzian, Ph.D., Committee Chair
SamaanLadkany, Ph.D., Committee Member
Douglas Rigby, Ph.D., Committee Member
Mohamed Kaseko, Ph.D., Committee Member
Ashok Singh, Ph.D., Graduate College Representative
Kathryn HausbeckKorgan, Ph.D., Interim Dean of the Graduate College

December 2013

Abstract

This research investigates the feasibility of application of high frequency immersion ultrasonic measurement (UM) to discriminate different performance grade (PG) asphalt binders. PG asphalt binder is one of the main components of hot mix asphalt used for roadway construction. UT may provide an inexpensive alternative to sophisticated tests currently used for quality control of PG asphalt binders. Nine different PG asphalt binders used were selected for this investigation. Velocity (V) and integrated response (IR) of the ultrasonic wave were measured. The IR is a measure of the ratio of ultrasonic energy transmitted into the material to the ultrasonic energy reflected from the surface of material, in decibels. The physical properties of PG asphalt binders are temperature sensitive. Accordingly, the UM was performed at five temperatures. The results indicate that velocity decrease with increase in temperature of the asphalt binder. UT could distinguish between modified and non-modified asphalt binders. Discriminant Function Analysis was used to predict the grade of the performance grade asphalt binders using the UM.

Acknowledgments

For the past four years Dr. Moses Karakouzian has been my academic hero, my educational support, my advisor and one of my best friends. His support was not limited to academic issues. He was like a father I was missing in these years. This could not be done without his rightful sight and domination in the field of construction materials. I am very glad that I could work with him, and learn from him, and it is the fortunate that it can continue.

Thanks to the committee members and special thanks to Dr. Ashok Singh for the help with the statistical analysis of this research.

Thanks to Dr. Michael Dunning and Mr. Ray Waters at the Clark County Public works, and also Mr. Aaron Clippers and Mr. Jesse Oakley at the Material Division of the Nevada DOT at Las Vegas.

Dedication

To my family; my father, who gave me thoughtful advice throughout my education and taught me the lessons of life, my mother, who supported me emotionally and taught me the lessons of love. To mybrother and sister, to whom I wish all the success and love they deserve.

My wife, my best friend, and my love; Sara. She was the one who encouraged me to continue the education and stayed by me in its ups-and-downs.

Table of Contents

List of Tables

List of Figures

1. CHAPTER 1 :INTRODUCTION AND PROBLEM STATEMENT

1.1 Introduction

Asphalt binders have been used for many years in Hot Mix Asphalt (HMA) as part of empirical or mechanistic mix designs. The quality control of pavement materials, especially for asphalt binders, requires the extensive use of laboratory and field testing. These tests are time consuming, and they require expensive equipment as well as skillful technicians. The laboratory tests related to an asphalt binder are based on physical properties that show how it will perform as a constituent in HMA.

Asphalt binders are categorized into "grades" based on their rheological properties. Performance Grade (PG) is the most commonly used system and it has several advantages over the other systems. Three major tests for PG asphalt binders, based on the Strategic Highway Research Program (SHRP), are the Dynamic Shear Rheometer (DSR) test, the Bending Beam Rheometer (BBR) test, and the Direct Tension Tester (DTT). These tests are essential for quality control and quality assurance of asphalt binders used in HMA. The DSR is used to characterize the shear viscous and elastic behavior of asphalt binders at medium and high temperatures. The results of the DSR test on asphalt binder ensure that the HMA pavement will resist against permanent deformation (rutting) at high temperature and fatigue cracking at medium temperature. The BBR and DTT provide a measure of low temperature stiffness and relaxation properties of asphalt binders. These parameters give an indication of an asphalt binder's ability to resist low temperature cracking. The DTT is used in combination with the BBR to determine an asphalt binder's low temperature performance grading (Aspahlt-Institute, 2003).

1.2 Problem Statement

The procedure of quality control (grade verification) of PG asphalt binders involves testing with expensive laboratory devices. This procedure is time consuming and it needs expert technicians. There is a need for a rapid, simple and non-destructive test to determine the physical properties of asphalt binders. Ultrasound testing provides a viable alternative to physical property tests for characterization of asphalt binders. By developing a correlation between the results of ultrasound testing and physical testing of mechanical properties, savings in time and money is possible.

1.3 Objective

The objective of this study is to find the best ultrasound technique to eventually be used as a substitute for grade verification tests. This objective will be achieved in two stages. The first stage will explore different ultrasound measurement configurations to identify the best method that can distinguish between two or more PG asphalt binders. In the second stage the ultrasound measurements with selected method(s) from the first stage and physical property tests will be performed on an array of PG asphalt binders in order to develop correlations. These tests and measurements are done at a range of temperatures higher that room temperature. The statistical method of Discriminant Function Analysis is used to predict the grades of asphalt binders when ultrasound measurements of the asphalt binder samples are available.The potential economic impact of the proposed method is presented in Appendix E of this dissertation.

2. CHAPTER 2: GENERAL BACKGROUND

2.1 Basic Principles of Ultrasonic Testing

Ultrasonic Testing (UT) uses high frequency sound energy to conduct examinations and make measurements. It can be used for, but not limited to, flaw detection/evaluation, dimensional measurements, and material characterization. A typical Ultrasound Testing inspection system consists of a pulser-receiver, transducer(s), and a display unit. A pulser-receiver is an electronic device that can produce high voltage electrical pulse, which causes the transducer to generate a high frequency ultrasonic energy. The sound energy is transmitted through the material in the form of waves (McMaster, Non Destructive Testing Handbook, 1959).

Sound waves propagate due to the vibrations or oscillatory motions of particles within a material. An ultrasonic wave may be visualized as an infinite number of oscillating masses or particles connected by means of elastic springs. Each individual particle is influenced by the motion of its nearest neighbor, and both inertial and elastic restoring forces act upon each particle.

The sound wave requires a physical elastic medium to travel (NDT, 2012). When a particle of a material is displaced from its position by any stress, the inertial forces will restore the particle to its original position; they are not moving away from the stress but are vibrating around their equilibrium positions. Waves generated by a mechanical stress, such as a transducer, become pressure waves, which transfer their energy to the material moving from particle to particle.

The sound frequency range is wide from sub-sonic to high frequency as demonstrated in Figure 2-1. Ultrasonic Non Destructive Testing (UNDT) utilizes the

range of frequencies from approximately 20 KHz to over 100 MHz, with most work being performed between 500 KHz and 20 MHz. Both longitudinal and shear, as well as surface wave modes of vibration are commonly used. Many material analysis applications will benefit from using the highest frequency that the test piece will support. The reason is that the resolution of the measurement is better at a higher versus lower frequency (NDT, 2012). Sound pulses are normally generated and received by piezoelectric transducers that have been acoustically coupled to the test material such as with water or oil.

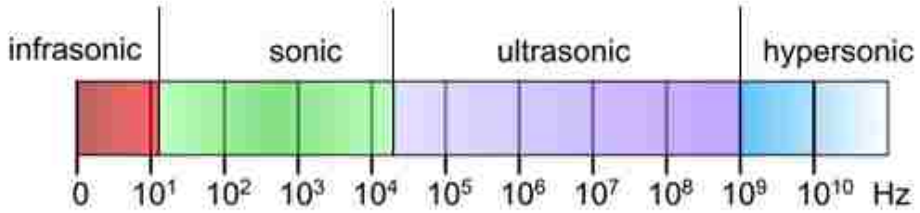

Figure 2-1Acoustic Spectrum (Hyperphysics, 2011)

Descriptive information about wave theory and ultrasonic testing are presented in chapter 3 of this dissertation.

2.2 Application of Ultrasound in Pavement Materials

Ultrasound has been used for the inspection of Portland Cement Concrete (PCC) for many years. Its use in the inspection of asphaltic concrete is limited to mainly laboratory based experimental studies, which have shown promising results (Sztukiewicz, R., 1991; Dunning M., 1996). The coupling of ultrasonic testing with laboratory-based performance testing of HMA would provide a vital link to rapid quality control testing and quality assurance verification. Following are some of the previous researches on application of ultrasound measurement in asphalt pavement materials.

MichaelDunning (1996)evaluated the application of ultrasound testing, to detect aggregate gradation differences in asphalt concrete pavements. Empirical data had previously been used to suggest that the coarser the gradation, the less incidence's of rutting. It was his thesis that the more coarse the gradation, the higher the velocity of a sound wave through the asphalt concrete. This being the case, the velocity measure can be used in a design or field quality control procedure as a correlation to a performance test to choose a coarse gradation that has non-rutting field performance properties. Tests were performed on actual production quality control samples of various gradation types to demonstrate that the ultrasound velocities detect gradation (Dunning M. , 1996). Figures 2-2 through 2-4 demonstrate that with further refinements, it would be possible to develop quality control techniques, which would enable a rapid acceptance of materials.

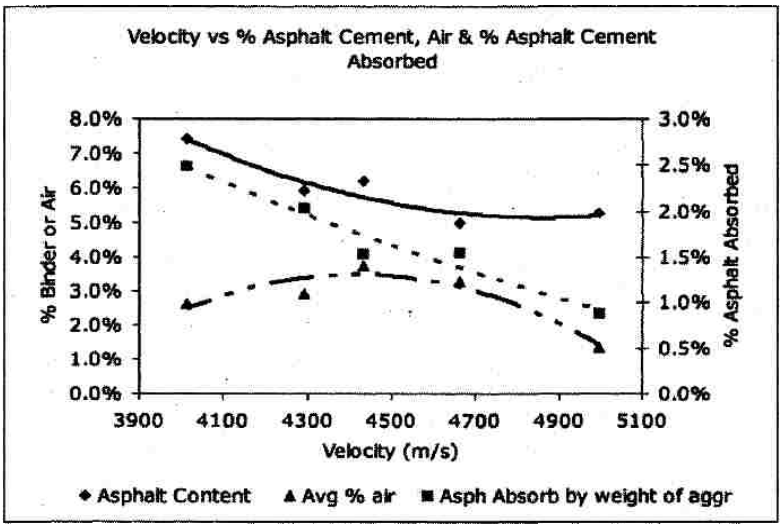

Figure 2-2Velocity versus % Binder, % Air content and % Asphalt Absorbed (Dunning M. , 1996)

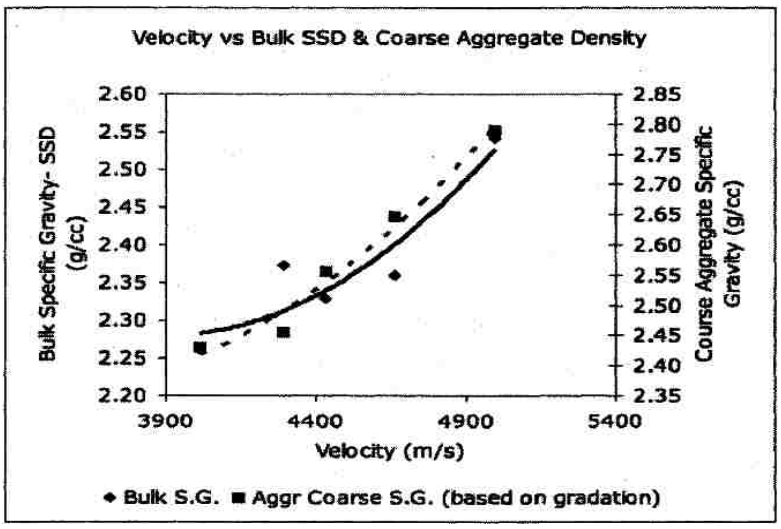

Figure 2-3Velocity versus Bulk Specific Gravity (Dunning M., 1996)

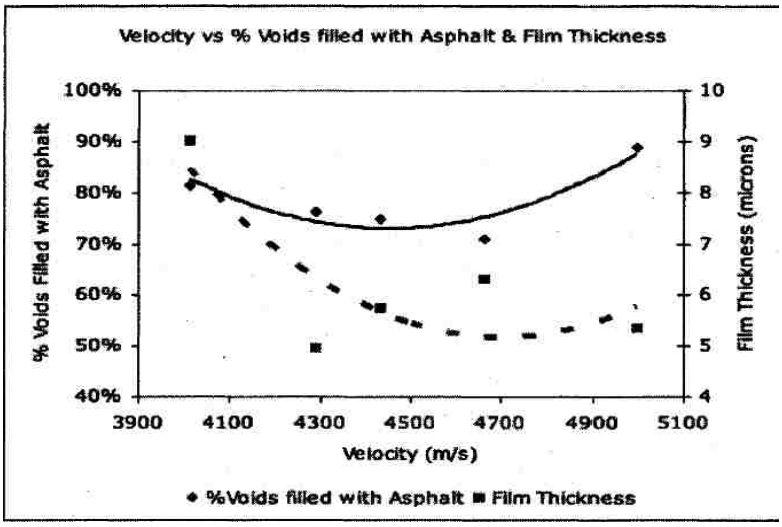

Figure 2-4Velocity versus % Voids Filled and Film Thickness (Dunning M. , 1996)

Michael Dunning (2006) used non-destructive testing with the non-contact ultrasound in order to reduce the testing time. Four different asphalt concrete mix designs were fabricated from four different aggregate sources with varied gradation and asphalt cement. The comparison of the same sets were discerned with use of two signal properties, Integrated Response (IR) against the tested material property of specific gravity and a performance value of the Asphalt Pavement Analyzer (APA) rut test. The research was performed in three phases. The first phase was to determine the type of

ultrasound system, the sensitivity of the ultrasound system, and its parameters. The second phase was to see if the ultrasound measurement of attenuation and material sound wave velocity could correlate to the HMA material property of specific gravity and the HMA performance rut depth value using APA. The third phase was to see if the procedure would work in two other designs to demonstrate that the process was reliable. It was demonstrated (Figures 2-5 through 2-7) that the IR and the material velocity does relate to the bulk specific gravity average of all data sets within the gradation type or with the use of individual HMA replicate sample sets (Dunning M. , 2006).

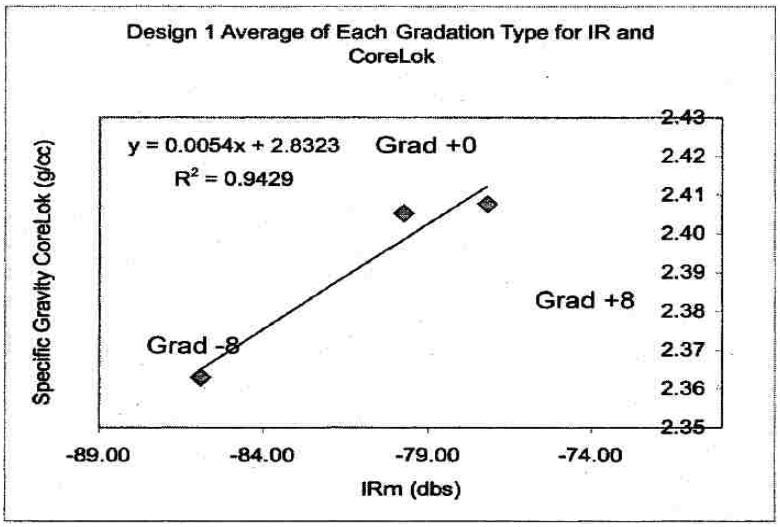

Figure 2-5Average Gradation Type for Integrated Response and Specific Gravity (Dunning M., 2006)

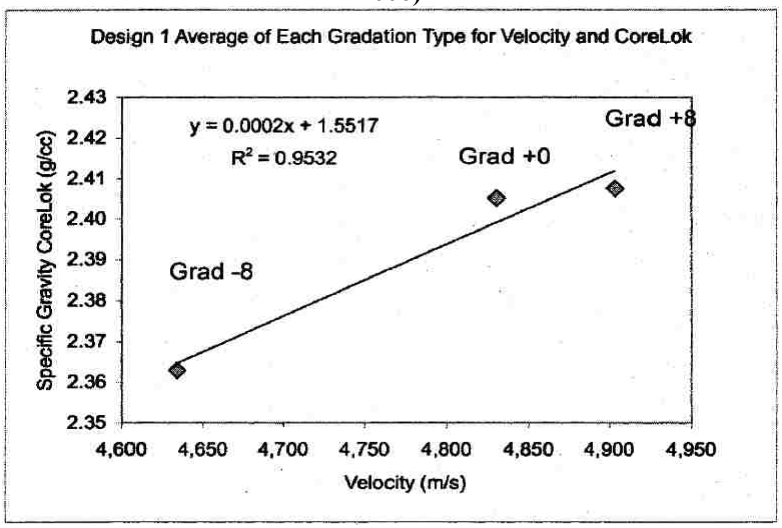

Figure 2-6Average Gradation Type for Velocity and Specific Gravity (Dunning M. , 2006)

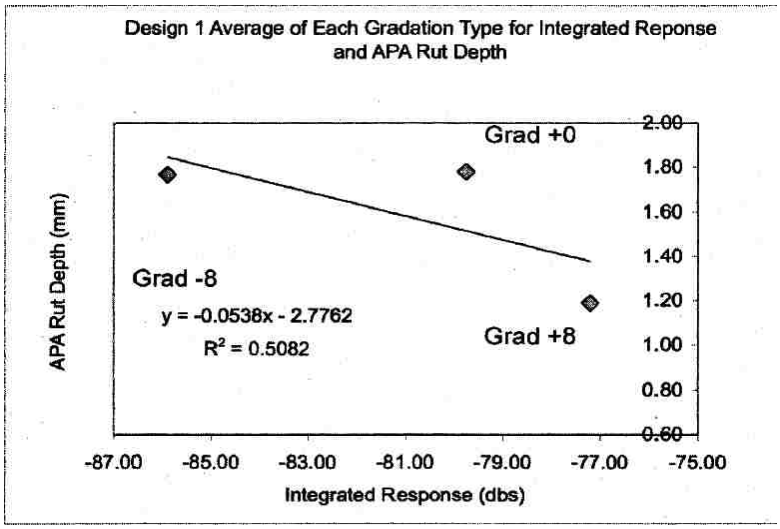

Figure 2-7Average Gradation Type for Integrated Response and the APA Rut Depth (Dunning M. , 2006)

The use of non-contact ultrasound was explored by AnandKrishnan (2005)in order to find correlations between physical properties (viscosity and penetration) of asphalt binder with ultrasound measurements of material velocity and Integrated Response (IR). Two viscosity grade asphalt binder from two sources were picked and tested. Rolling Thin Film Oven (RFTO) aged samples were also tested. Final results indicated that IR correlation showed a peak at 30 degree Celsius which needs further researchincludong chemical analysis at various temperatures. This research is unable to prove the correlation conclusively but some trends are noticed (Figures 2-8 through 2-10) . Further research would help in identifying setup conditions and reduce the errors generated (Krishnan, 2005).

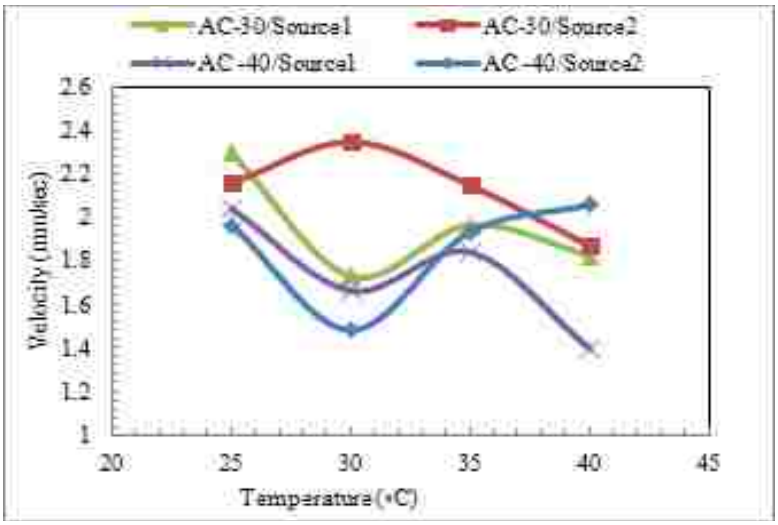

Figure 2-8Velocity at Different Temperatures for Different Original Asphalt Binders (Krishnan, 2005)

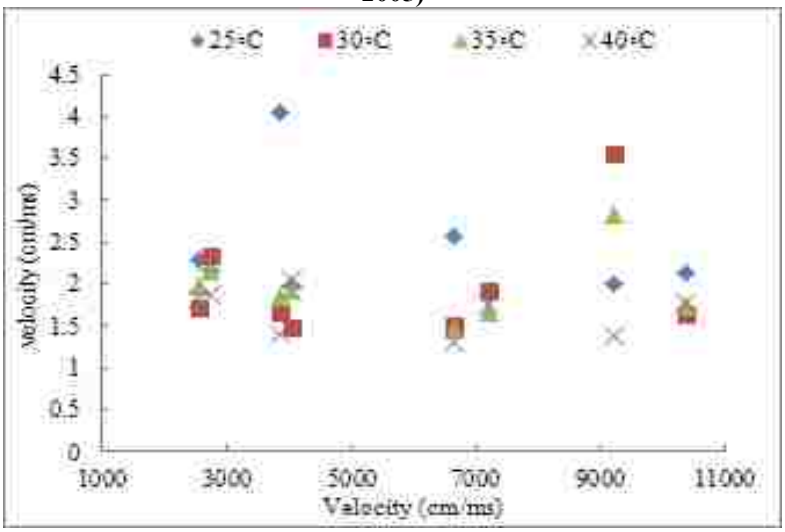

Figure 2-9Viscosity at 60◦C vs. Velocity for Original and Aged Samples (Krishnan, 2005)

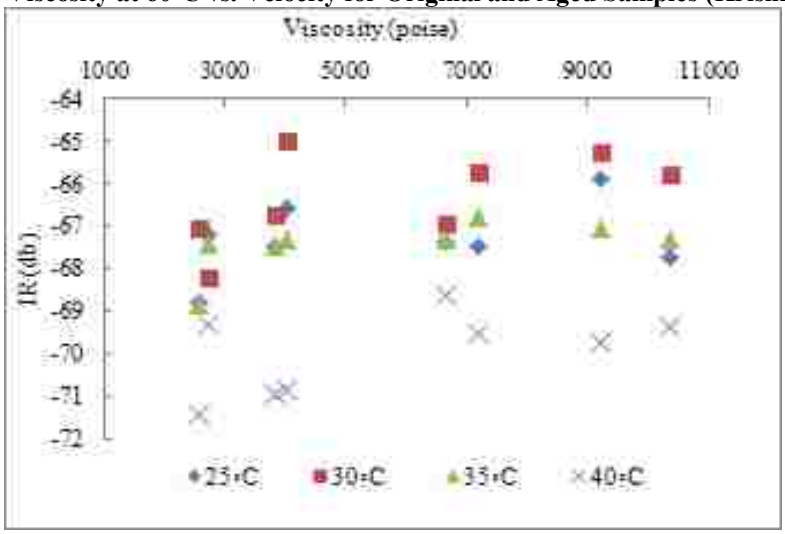

Figure 2-10Viscosity at 60◦C vs. Integrated Response (Krishnan, 2005)

R.Lakes (2004) applied this technique for viscoelastic materials with the use of a piezoelectric ultrasonic oscillator, which is based on a device that uses two piezoelectric crystals, and the material cemented together. The properties of the material are inferred from electrical measurements upon the sensor crystal and from the dimensions and masses of the specimen and crystals (Lakes, 2004).

Spectral Analysis of Surface Waves (SASW) method was used by H. Alexander (1992) to evaluate dispersive characteristics of surface waves to determine the variation of the shear wave velocity with depth (Alexander, 1992). The SASW testing is applied from the surface allowing for less costly measurements than with traditional borehole methods (Figure 2-11). Once the shear wave velocity profilesare determined, the shear and Young's modulus of the material can be calculated.The shear wave velocity profiles are determined from the experimental dispersion curves (surface wave velocity versus wavelength) obtained from SASW measurements through a process called forward modeling.

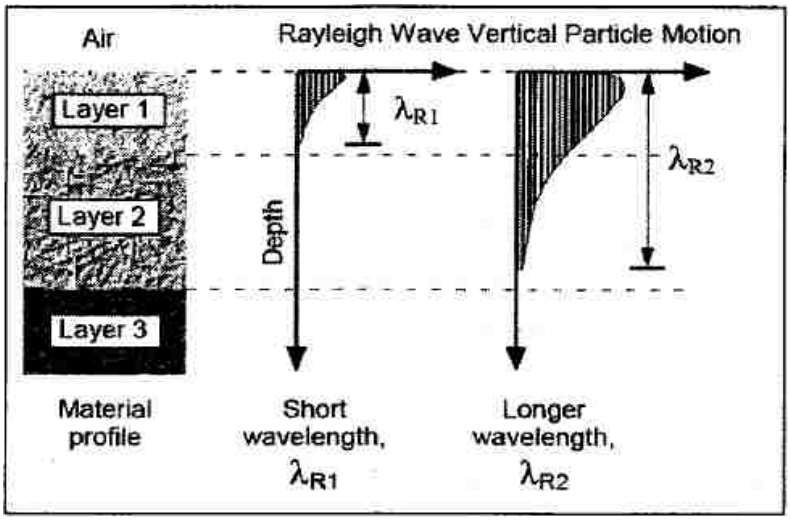

Figure 2-11SASW Surface Wave Profile (Alexander, 1992)

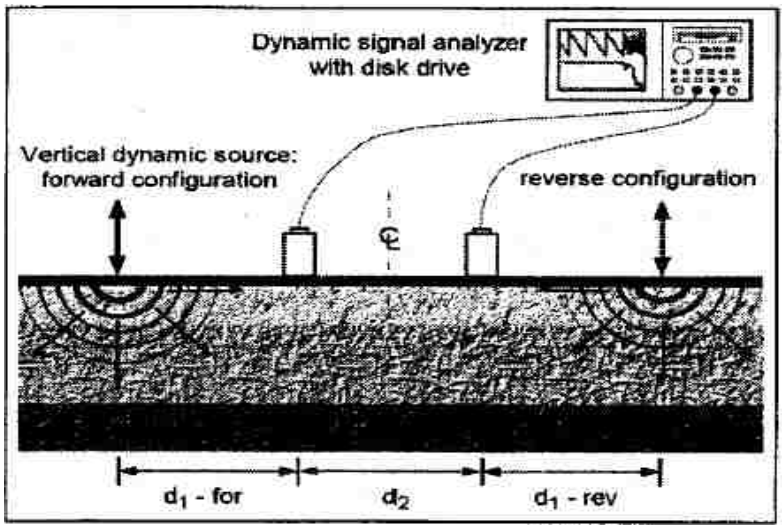

Figure 2-12SASW Transducer Position and Analyzer Setup (Alexander, 1992)

Two receiversare placed on the surface, and a hammer is used to generate the wave energy. Other sources can be used such as solenoid-operated impactors, large drop weights, and bulldozers. Short receiver spacing is used to sample the shallow layers while long receiver spacing is used in sampling the deep materials (Figure 2-12). Two profiles, a forward profile and a reverse profile, are typically obtained in SASW measurements where the accessible surface is struck by a hammer on two opposite sides of the receivers. A signal analyzer is used to collect and transform the receiver outputs to the frequency domain.

In a study by J. Sztukiewicz(1991) two ultrasound techniques were employed, shallow transmission and pulse-echo, for the testing of asphalt concrete (Sztukiewicz, 1991). In both cases, the accuracy of the longitudinal wave was measured with an accuracy of 0.1μs. The transmission method was used on laboratory-fabricated samples with contact transducers on either side of the samples while the thickness was manually measured between the transducers. For the field application, the only feasible method was the pulse-echo. The asphalt concrete layer was about 50mm thick and the distance of the

transducers was measured manually. The author states that the longitudinal wave was used for both and resulted in different velocities. The laboratory samples were tested at 200°C with 500 kHz transducers. The author utilized the Abram's fractional grading coefficient, which is similar to the concrete aggregate fineness modulus, to characterize the mineral mix aggregate grading. It was found that the condition of the pavement could be defined with ultrasound, which correlated directly with weather and traffic patterns.

3. CHAPTER 3: INTRODUCTIONTO WAVE THEORY AND ULTRASONIC TESTING

The research for this study utilizes equipment and transducers that use the Chirp wave. The purpose of this section is to allow the reader to get a better understanding of what this wave is and why it is used. The following are definitions of some key concepts in wave theory;

3.1 Traveling Waves

Ultrasonic testing is based on the vibrations in materials, which are generally referred to as acoustics. All material substances are comprised of atoms, which are able to be forced into a vibration motion around their equilibrium positions. Acoustics is focused on particles that contain many atoms that move in unison to produce a mechanical wave. When a material is not stressed in tension or compression beyond its elastic limit, its individual particles perform elastic oscillations. When the particles of a material are displaced from their positions, internal restoration forces occur which can be measured as a response to the acoustic pressure (Lempriere, 2002).

The three different types of pressure waves generated in the ultrasonic methods that are applicable for material testing are longitudinal, shear, and surface waves. These waves travel at three different velocities with the compression waves traveling about twice as fast as the other two. The particle displacement of the compression wave is in the same direction of the wave. The shear wave is next in velocity with the particle displacement at right angles to the direction of wave travel. The Rayleigh (surface) waves travel the slowest and generate waves along the surface pushing the particle displacement

in an elliptical fashion. Waves that propagate entirely inside of materials are planar and sometimes spherical represented by simple wave equations. These waves are governed only by elasticity and inertia (NDT-ed.org).

In a material that is isotropic, the speed of a plane wave is the same in any direction. Thus a point source excites spherical waves, which can be considered as plane waves with infinitesimal distances on the perimeter of the sphere (Figure 3-1) (Lempriere, 2002).

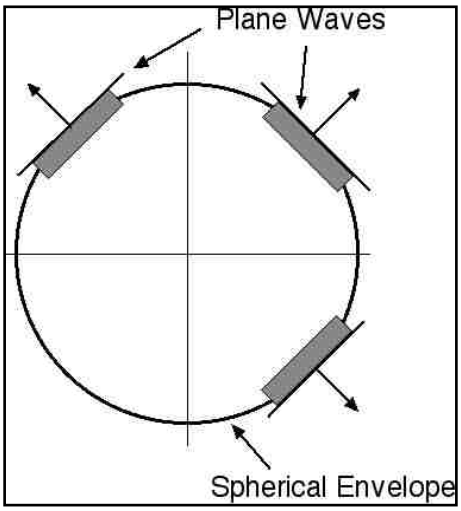

Figure 3-1Example of Plane Waves on Sphere Surface (Lempriere, 2002)

The plane wave can be represented by an envelope of spherical waves emitted from points over a plane, such as a transducer element as exampled in Figure 3-2.

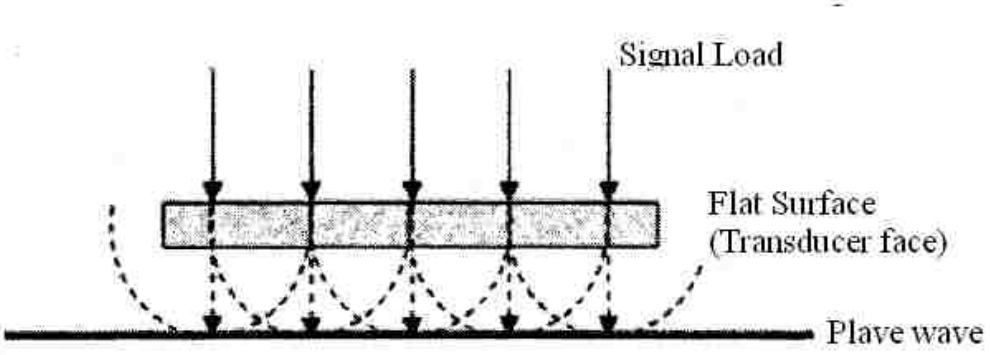

Figure 3-2Example of Plane Wave Developed by Overlapping Spheres

The acoustic waves associated with transmission through the air are longitudinal waves, which are the type of wave that is used for this research. In longitudinal waves, the oscillations occur in the longitudinal (parallel) direction to the direction of wave propagation. The velocity of longitudinal wave is dependent to specimen's geometry and wavelength (Brown, 1995). Therefore, the velocity of a set dimensional material will be different from that of infinite dimensions, which may affect the research results in that the fabricated samples have fixed dimensions.

The longitudinal wave causes the molecules to be subjected to compression and subsequent tension, creating a dense wave moving in one plane as demonstrated in Figure 3-3.It is also sometimes called density wave because their particle density fluctuates as it moves. Compression waves can be generated in liquids, as well as solids.

When the wavelength is less than one-fifth of the material lateral dimension, the velocity is often referred to as a bulk specimen longitudinal velocity.

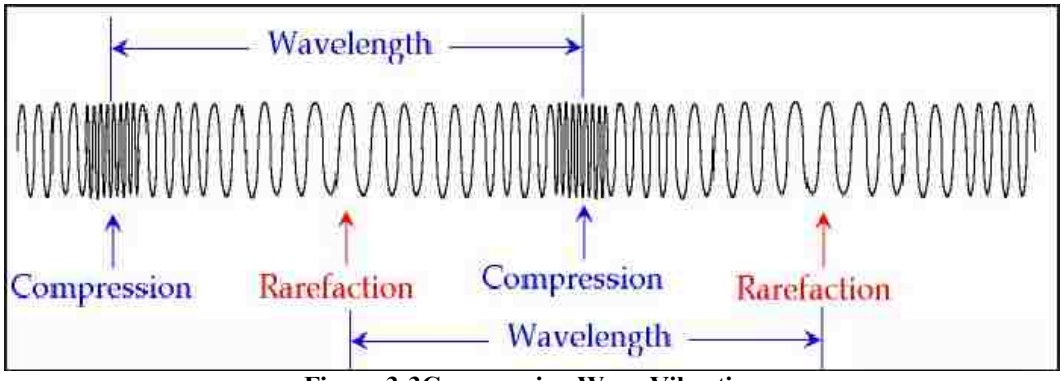

Figure 3-3Compression Wave Vibration

3.2 Periodic Motion

The elasticity and a source of energy are what is needed for periodic motion. When the elastic object is an extended body, then the periodic motion takes the form of traveling waves (Figure 3.4). To produce a vibration frequency of "*f*" Hz, the source

object must sustain periodic motion at "*f*" vibrations per second and the time between cycles is represented in Equation 1:

$$t_p = \frac{1}{f} \qquad [1]$$

where

f = frequency

t_p = time required to complete a full cycle

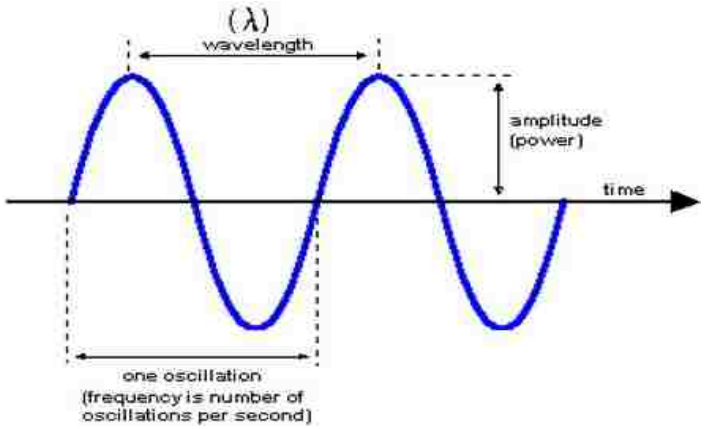

Figure 3-4Wave Properties

A single frequency-traveling wave will take the form of a sine wave. An example of this wave is demonstrated in Figure 3-5, which represents an instant of time for the relationship of the wave properties of frequency, wavelength, and propagation velocity. The displacement of the material is perpendicular to the direction of propagation of the wave. This wave cannot propagate in a gas or a liquid because there is no means for driving the motion perpendicular to the propagation of the wave(Hyperphysics, 2011).

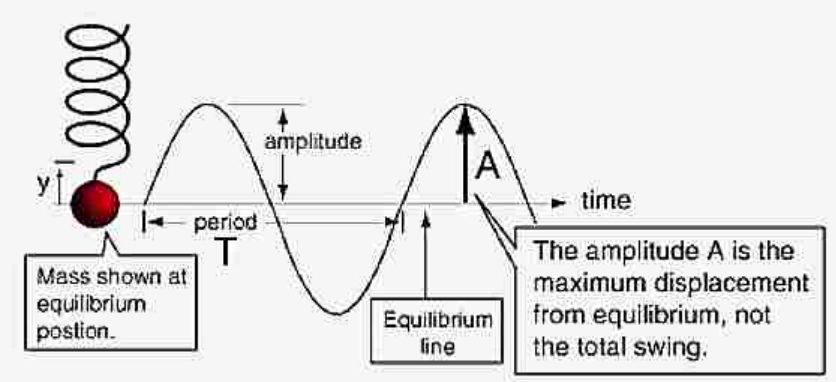

Figure 3-5 Example of a Periodic Motion (Hyperphysics, 2011)

Among the properties of waves propagating in isotropic solid materials are wavelength, frequency, and velocity. The wavelength is directly proportional to the velocity of the wave and inversely proportional to the frequency of the wave. This relationship is shown by the Equation 2:

$$\lambda = \frac{v}{f} \qquad [2]$$

where

$v = velocity$

$\lambda = \text{wavelength}$

$f = \text{frequency}$

The wavelength,λ, is the distance traveled by one cycle in an instant in time. A change in frequency will result in a change in wavelength. As an example, for a frequency of 100 KHz and a material velocity of 3,000 meters per second, the wavelength would be 0.03 meters, or 30mm. In ultrasonic testing, the shorter wavelength resulting from an increase in frequency will usually provide for the detection of smaller flaws (Hyperphysics, 2011).

The reciprocal of a wavelength is the number of cycles for a given distance while the wave number is the quantity of radians in one cycle:

$$k = \frac{2\pi}{\lambda} \quad [3]$$

where

k = wave number

λ = wavelength

The motion relationship of distance with velocity and time is the key to the wave relationship. One method of visualizing and developing equations is to use a vibrating string. A solution to the wave equation for an ideal string can take the form of a traveling wave as displayed in Equation 4:

$$y(x,t) = A\sin\frac{2\pi}{\lambda}(x - vt) \text{ or} \quad [4]$$

$$y(x,t) = A\sin\frac{2\pi}{\lambda}(x + vt)$$

where

A = amplitude

v = velocity

x = Location of wave

t = Time

3.3 Phase Velocity

The progression of a wave is the wave-speed also termed phase velocity. The material itself does not move, however, the wave-speed does depend on the material type and, with exception of isotropic materials, also on the direction of the wave propagation. The phase velocity, v_ϕ is:

$$v_\phi = \frac{\omega}{k} = f\lambda \quad [5]$$

where

ω = Angular velocity

f = Frequency

λ = Wave length

k = Wavenumber

The speed of sound in gas, liquids, and solids is predictable from their density and elastic properties namely, the modulus, *B*. In a volume, the phase velocity is the general Equation 6.

$$V = \sqrt{\frac{\text{elastic property}}{\text{inertial property}}} = \sqrt{\frac{B}{\rho}} \quad [6]$$

where

V = Velocity

B = Modulus

ρ = Density

The property of the velocity that is calculated from Equation 6 is corresponding to the modulus of the material. Shear velocity (velocity of the shear waves) is related to elastic shear modulus and longitudinal velocity (velocity of the longitudinal waves) is related to compression/tension elastic modulus.

3.4 Angular Velocity

For an object rotating about an axis, every point on the object has the same angular velocity. The tangential velocity of any point is proportional to its distance from the axis of rotation. Angular velocity has the unit of radian per second.

Equation 7 is represented by of a point following the perimeter of a circle as indicated in Figure 3-6. The location on the perimeter at a given time is given by the phase angle (Equation 8).

$$\omega = 2\pi f \quad [7]$$

where

ω = Angular ve locity

f = Frequency

$$\phi = kx - \omega t = k(x - vt) = \frac{2\pi x}{\lambda} \quad [8]$$

where

k = Wavenumbe r

x = Distance

ω = Angular ve locity

t = Time

λ = Wavelength

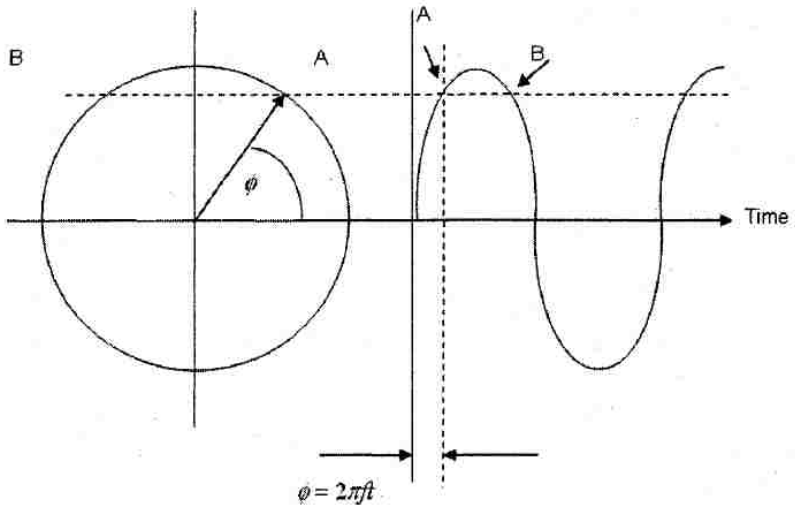

Figure 3-6 Phase Angle (Lempriere, 2002)

A steady wave oscillation with a magnitude of *a(t)* as a function of time, with an amplitude *A,* and a angular velocity of ω yields:

$$a(t) = A\sin\omega t \quad [9]$$

where

t = Time

A = Amplitude

ω = Angular Velocity

3.5 Group Waves

A group wave will use numerous waves from the same source but at different frequencies and/or velocities at the same instance by taking advantage of the constructive influence of the combined wave patterns (Lempriere, 2002). When different waves overlap, the portions that are in phase at one instant added to produce large peaks, which are named constructive interference. If the waves are equal in positive and negative, they cancel which results in no amplitude, named destructive interface.

The constructive and destructive effects result in one waveform of the combined waves as demonstrated in Figure 3-7 and 3-8.

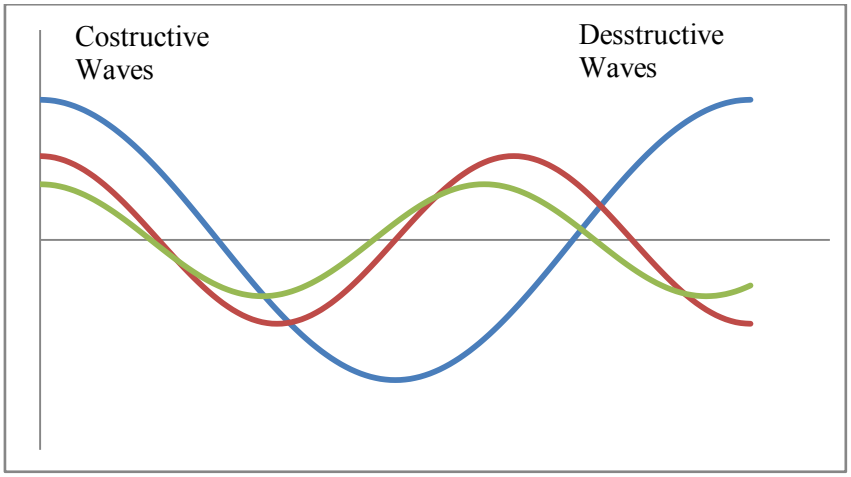

Figure 3-7 Individual Waves of the Group

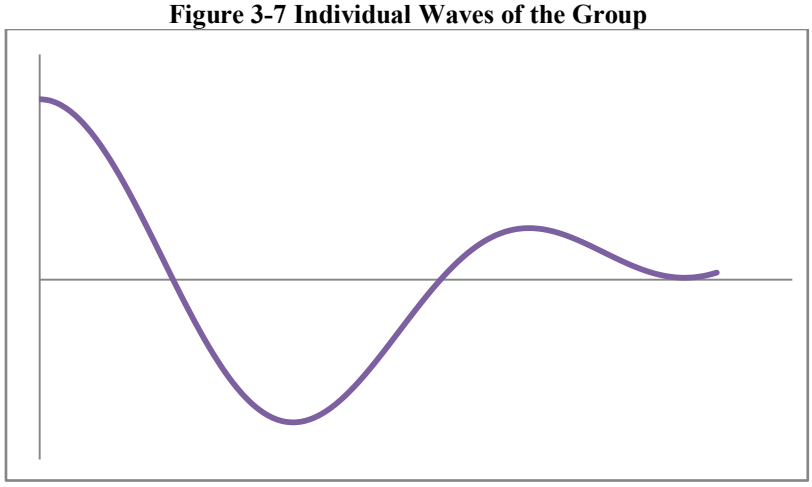

Figure 3-8 Combined Waves

The use of the group wave is the main constituent in a Chirp signal and is the main type of waveform that is used in this research. The use of a Chirp, which is a frequency swept signal, instead of a single frequency, allows for a high power, broad bandwidth signal to be used which gives excellent time resolution (Gan T.H., 2001).

3.6 Chirp Signal

The Chirp signal is related to the Doppler Effect in that the motion of the source yields a differential perceived frequency of the transmitted frequency at a given point as illustrated in Figure 3-9, which is summarized as a "Chirp" due to the similarity to a bird or bat sound.

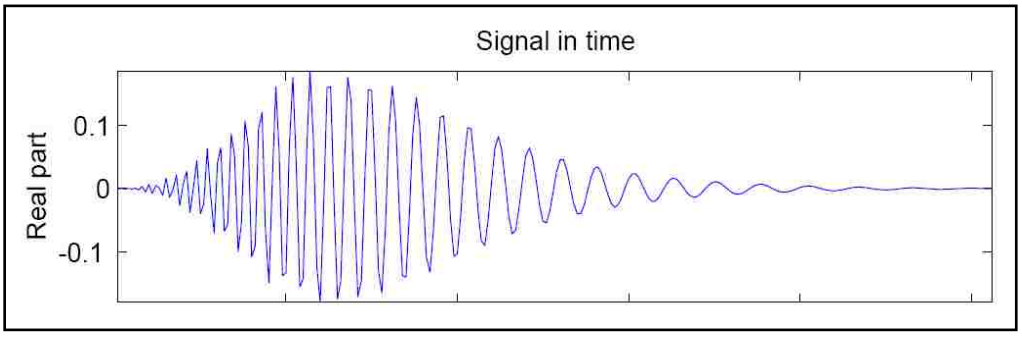

Figure 3-9Example Of Doppler Effect Relative To The Chirp Signal (Gan T.H., 2001)

The use of the Chirp is applied in this research with a pulse-compression method. With the use of pulse compression and the use of a Chirp signal, the result is an elongated waveform with the width the overall duration of the signal and the rate of the frequency sweep defining the Chirp (Gan T.H., 2001).

The wave that is generated with the Chirp signal is represented by Equation 10, and has full amplitude as displayed in Figure 3-10.

$$C(t) = \sin\left(\omega_S t + \frac{\pi B}{T} t^2\right) \qquad 0 \le t \le T \qquad [10]$$

where

ω_S = Starting angular velocity

B = Bandwidth

T = Pulse duration

t = Time

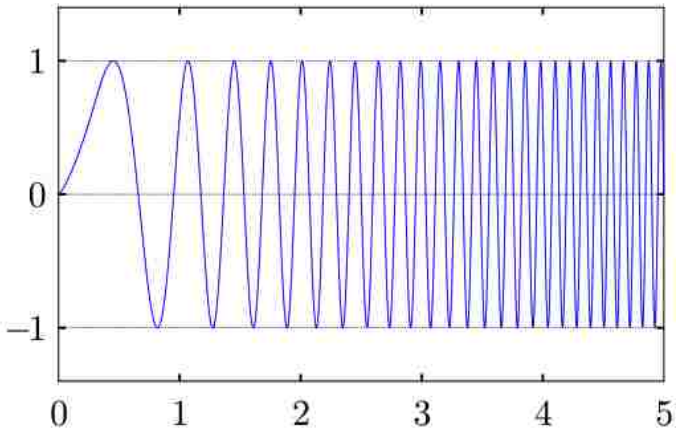

Figure 3-10Chirp Pre-Gaussian filter time domain (Gan T.H., 2001)

The Gaussian filter operator is a smoothing function that is used to smooth images and remove detail and noise. It uses a formula that represents the shape of a Gaussian (bell-shaped) hump as represented by Equation 11. The Gaussian distribution has the form as displayed in Figure 3-11.

$$G(x) = \frac{1}{\sqrt{2\pi}} e^{-\frac{x^2}{2\sigma^2}} \qquad [11]$$

where

x = Distance

σ = Standard deviation

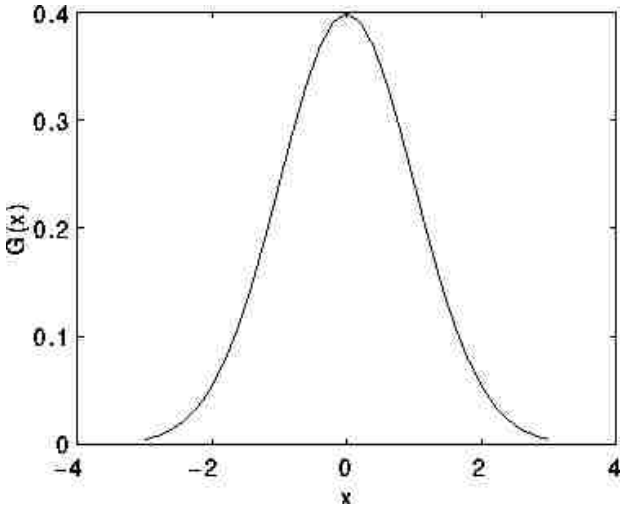

Figure 3-11Gaussian Distribution (Gan T.H., 2001)

If a Gaussian filter is not used, the Chirp would be a straight full amplitude signal displayed from the lowest to highest frequency (Figure 3-10) which results in a bumpy Fourier transformed frequency spectrum as indicated in Figure 3-12 (Gan T.H., 2001).

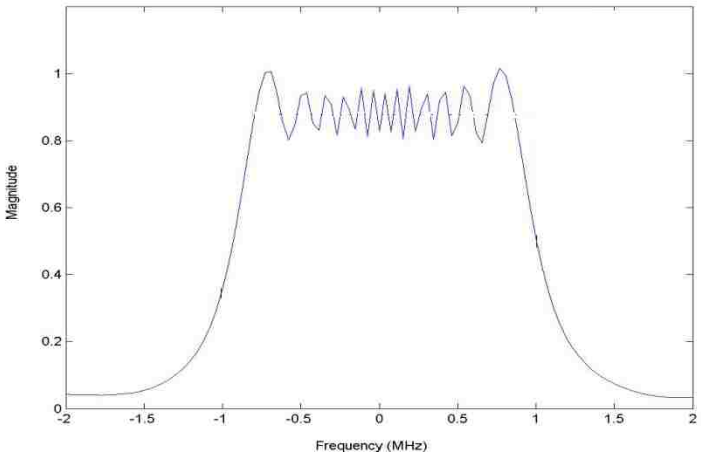

Figure 3-12Chirp Pre-Gaussian frequency domain (Gan T.H., 2001)

In order to eliminate this, a Gaussian filter is used represented by Equation 11.When the filter is applied, the frequency spectrum is more defined, and visually there is the distinctive bell shape as illustrated in Figure 3-13.The importance of this shape is to assure good sensitivity for the application of non-contact transducers.

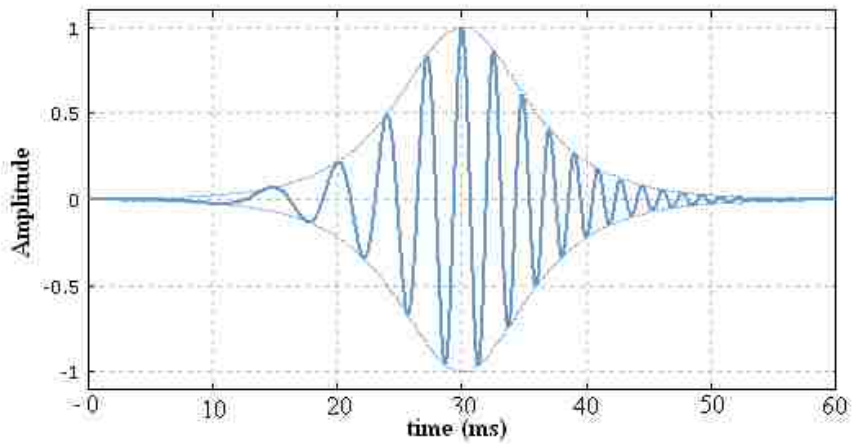

Figure 3-13Filtered Chirp (Gan T.H., 2001)

3.7 Sound Pressure

Sound waves consist of pressure waves (longitudinal) and one of the ways to quantify the sound is to state the amount of pressure variation relative to atmospheric pressure caused by the sound as described in Equation 12 (Hyperphysics, 2011):

$$I(dB) = 10\log_{10}\left[\frac{I}{I_0}\right] = 20\log_{10}\left[\frac{P}{P_0}\right] \qquad [12]$$

where

I = Intensity

P = amplitude of the pressure wave

The factor of 20 is from the factor of 10 for conversion from bels to decibels and a factor of 2 is introduced because in acoustics, a signal characterized by its power is the square of its magnitude.

Sound intensity, *I,* is defined as the sound power per unit area with the basic units of watts/m^2 or watts/cm^2. Many sound intensity measurements are made relative to a standard threshold of hearing (I_0):

$$I_0 = 10^{-12}\,\frac{watts}{m^2}$$

This decibel level of measurement is generally referenced to a standard threshold of hearing at 1000 Hz for the human ear as stated above or in terms of sound pressure:

$$P_0 = 2x10^{-5}\frac{N}{m^2}$$

This value has wide acceptance as a nominal standard threshold and corresponds to zero decibels. It represents a pressure change of less than one billionth of standard atmospheric pressure.

The sound intensity will obey the inverse square law as long as there are no reflections or reverberations. A plot as indicated in Figure 3-14 represents this intensity drop.

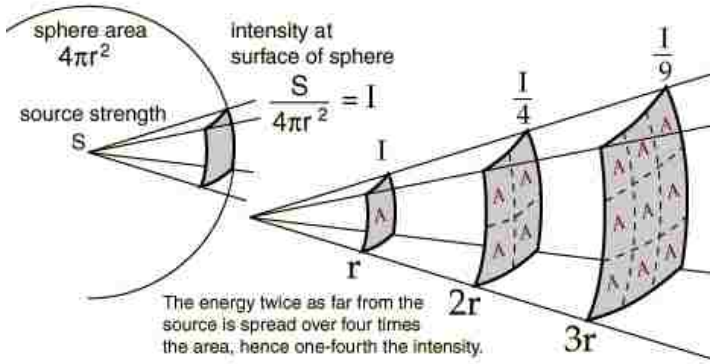

Figure 3-14Inverse Square Example (Hyperphysics, 2011)

The power carried by a plane wave is proportional to the square of the amplitude. The energy transferred to a material from a pressure wave is represented by the change in decibels by Equation 13.

$$\Delta I(dB) = 20\log_{10}\left(\frac{V_2}{V_1}\right) \quad [13]$$

where

V_1 and V_2 are the measured voltage amplitudes

A plane wave will not change until it encounters a different material property that affects the elastic response for the wave. The change in amplitude is called attenuation or gain. This will result in a change in the waveform and affects the wave spectral content.

The attenuation is a negative value, however, if the signal is amplified, the logarithm is positive which is then called gain.

The amplitude of a constant sine wave is the peak reached in each cycle. When there are many superimposed waves at different frequencies such as a group wave, the amplitude is defined as the peak. However, it is better to determine the character of the wave through the amplitudes of the individual waves, which are called the spectrum. The amplitudes of the stress and velocity in a wave are related by the acoustic impedance (Lempriere, 2002).

3.8 Attenuation

Attenuation often serves as a measurement tool that leads to the formation of theories to explain physical or chemical characteristics, which decreases the ultrasonic intensity as shown in Figure 3-15.Ultrasonic attenuation is the decay rate of mechanical energy as it propagates through material. A decaying plane wave is expressed in Equation 14.

$$A = A_o e^{-\alpha x} \qquad [14]$$

where

A = reduced amplitude at some location

A_0 = amplitude of the wave

x = travel distance

e = napiers constant = 2.71828

(Dividing by 0.1151 will convert to dB/length)

Attenuation can be determined by evaluating the multiple back-wall reflections seen in a typical display such as Figure 3-15. The number of decibels between two adjacent signals is measured and this value is divided by the time interval between them. This calculation produces an attention coefficient in decibels per unit time, U_t. This value can be converted to nepers/length by Equation 15.

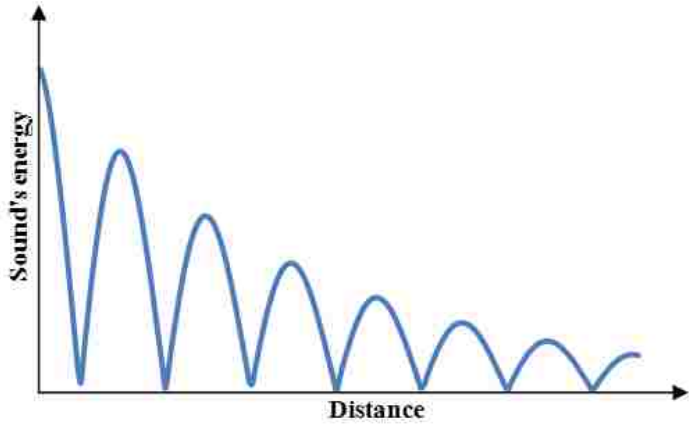

Figure 3-15A-scan Display Example of Attenuation of a Signal

$$\alpha = \frac{0.1151}{v} U_t \qquad [15]$$

where

α = attenuation coefficient (nepers/length)

v = velocity of sound (m/s)

U_t = decibels per second

3.9 Internal Friction

Attenuation is the combined effect of scattering and absorption, which is due to the internal friction Q. This converts kinetic energy into heat from non-elastic material responses or defects. Internal Friction is the ratio of change of amplitude to the initial amplitude in a cycle as expressed in Equation 16.

$$Q = \frac{-1}{\pi\left(\frac{\Delta A}{A}\right)} = \frac{-1}{2\pi\left(\frac{\Delta E}{E}\right)} \quad [16]$$

where

A = Amplitude

E = Energy

The factor 2 in the denominator is due to the energy being the square of the amplitude. A frequency-dependent *Q,* is represented by Equation 17.

$$A = A_o e^{\frac{-\omega x}{2Qc}} \quad [17]$$

where

$$\alpha = \frac{\omega}{2Qc} = \text{attenuation coefficient} = \frac{0.1151}{v} U_t$$

ω = Angular velocity

Q = Internal friction

v = Velocity of sound

U_t = dbs per sec

Attenuation over a given distance x for a single wave is then expressed as Equation 18.

$$dB = \frac{-8.686\omega x}{2Qc} = -8.686\alpha x \quad [18]$$

where

α = Attenuation coefficient

x = Distance

The above equation is expressed for a single wave to calculate the attenuation, and the phase spectra, which are then used to calculate the phase velocity(Zhao, 2004). This is the transmission velocity of a sinusoidal wave at a given frequency in a material. The change of a waveform for a plane wave of this type of ultrasound due to the dispersion through the material and attenuation can be described mathematically as:

$$s(t) = \sum_{i=1}^{n} A_i e^{-x_i x} \cos 2\pi f_i \left(t - \frac{x}{v_i} \right) \quad [19]$$

where

A_i = amplitude

x_i = attenuation coefficient

t = time

v_i = phase velocity

f_i = frequency

n = is the number of components,

x_i and v_i are frequency dependant

As an example, to simulate the process of waveform evolution of the pulse described by Equation 19, an initial pulse $s_1(t)$ is first generated at $x = 0$, as shown in Equation 20.

With the use of a Chirp signal and due to the numerous sine waves, Fourier theory is introduced at this point, which is any complex periodic waveform that can be decomposed into a set of sinusoids with different amplitudes, frequencies and phases. The process of doing this is called Fourier analysis, and the result is a set of amplitudes, phases, and frequencies for each of the sinusoids in the Chirp waveform. Adding these sinusoids together again will reproduce exactly the original waveform. A plot of the frequency or phase of a sinusoid against amplitude is called a spectrum θ.

The Gaussian wave is used for the pulse represented by the following:

$$s_1(t) = \frac{\exp\left(\frac{-t^2}{4B} \right)}{\sqrt{4\pi B}} \cos(2\pi f_c t) \quad [20]$$

where

f_c = center frequency

B is the bandwidth

Or expressed as:

$$s_1(t) = \sum_{i=1}^{n} A_i \cos(2\pi f_i t - \theta_i)$$

Ai is same as Equation 19, but was obtained by calculating a Fourier transform of the Gaussian pulse and θ_i is phase spectrum.

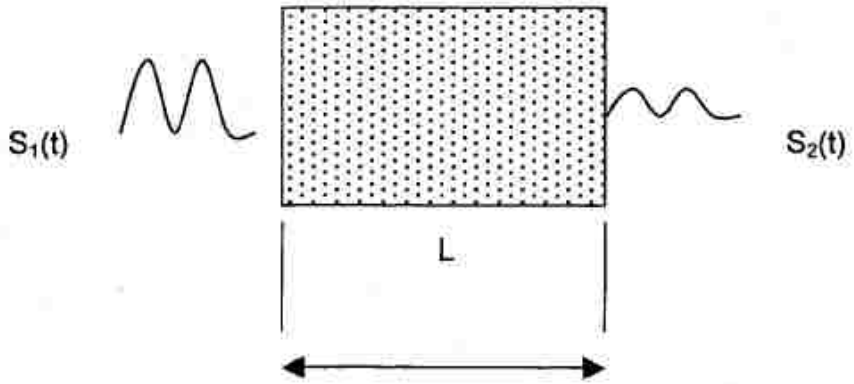

Figure 3-16 Ultrasound Pulse Transmission

Assuming the length of the propagation path to be *L,* (Figure 3-16), the pulse signal $s_1(t)$ evolves into the pulse signal $s_2(t)$:

$$s_2(t) = \sum_{i=1}^{n} A_i e^{-\alpha_i L} \cos\left[2\pi f_i\left(t_i - \frac{L}{v_i}\right) - \theta_i\right] \qquad [21]$$

where

$$v_i = v_0 + f\left(\frac{dv}{df}\right)$$

$$\alpha_i = \alpha_0 + f\left(\frac{d\alpha}{df}\right) = \text{attenuation coefficient}$$

Figure 3-17 shows the transition of a pulsed signal reflection to frequency and time domain amplitude.

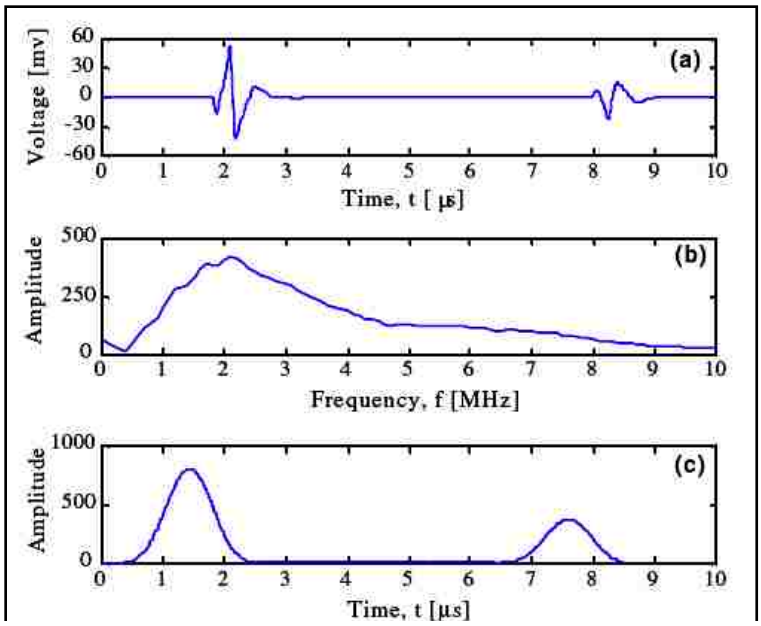

Figure 3-17Example of a) Pulsed Signal with Reflection, b) Amplitude of the Signal, c) Fourier Transformed Signal

3.10 Acoustic Impedance

Sound travels through materials under the influence of sound pressure. Because molecules or atoms of a solid are bound to one another, the excess pressure results in a wave propagating through the solid (NDT-ed.org).Acoustic impedance is a ratio of acoustic pressure to flow and is somewhat similar to electric impedance. An analogy is the comparison with electrical resistance, which is often explained with the flow of water. However, impedance is used instead of resistance because it is more complex than resistance. In electricity with direct current, resistance is used. However, with high frequency alternating current, impedance is used because more than the resistance in the wire is involved. When using hydraulic resistance, it would be the ratio of the pressure difference between the ends of a pipe to the flow in the pipe.Thus electrical resistance is the ratio of the voltage applied to the electrical current it produces. The specific acoustic

impedance is a ratio of acoustic pressure to specific flow, or flow per unit area, or flow velocity.

The acoustic impedance Z of a material is defined as the product of density $\rho$and acoustic velocity V of that material.

$$Z = \rho V \qquad [22]$$

where

Z = acoustic impedance

ρ = density

V = velocity of the material

$$\text{Unit} = \frac{\text{g}}{\text{cm}^2 - \text{sec}}$$

Acoustic impedance is used for the determination of acoustic transmission and reflection at the boundary of two materials having different acoustic impedances, which in turn generates the Integrated Response value. The reflected energy is that percentage not absorbed by the material and reflected back to the transducer, while the transmission energy is what percentage is passing through the material. Both are expressed in decibels.

3.11 Reflection Coefficient

Change in the acoustic impedance at the interface boundaries affects the amount of acoustic energy that is reflected and transmitted. The values of the reflected and transmitted energy are the fractional amounts of the total energy incident on the interface. Note that the fractional amount of transmitted sound energy plus the fractional amount of reflected sound energy equals one.

Ultrasonic waves are reflected at boundaries where there is a difference in acoustic impedances (Z) of the materials on each side of the boundary. This difference in Z is commonly referred to as the impedance mismatch. The greater the impedance mismatch,

the greater the percentage of energy that will be reflected at the interface or boundary between one medium and another.

The fraction of the incident wave intensity that is reflected can be derived because particle velocity and local particle pressures must be continuous across the boundary (Figure 3-18). When the acoustic impedances of the materials on both sides of the boundary are known, the fraction of the incident wave intensity that is reflected can be calculated with the Equation 23. The value produced is known as the reflection coefficient. Multiplying the reflection coefficient by 100 yields the amount of energy reflected as a percentage of the original energy.

$$R = \left[\frac{Z_2 - Z_1}{Z_2 + Z_1}\right]^2 \qquad [23]$$

where

R = reflection coefficient

Z_1 = acoustic impedances of material 1

Z_2 = acoustic impedances of material 2

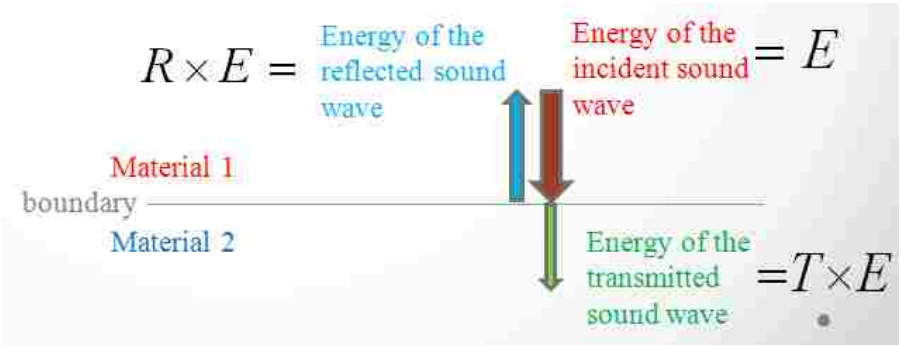

Figure 3-18 Reflected and Transmitted Energy of Sound Wave

Since the amount of reflected energy plus the transmitted energy must equal the total amount of incident energy, the transmission coefficient is calculated by simply subtracting the reflection coefficient from one.

$$T = 1 - R = 1 - \left[\frac{Z_2 - Z_1}{Z_2 + Z_1}\right]^2 = \frac{Z_1 Z_2}{(Z_1 + Z_2)^2} \quad [24]$$

where

$T = \text{transmiss ion coefficien t}$

$R = \text{reflection coefficien t}$

$Z_1 = \text{acoustic impedances of material 1}$

$Z_2 = \text{acoustic impedances of material 2}$

The reflection and transmission coefficients are often expressed in decibels (dB) to allow for large changes in signal strength to be more easily compared. To convert the intensity or power of the wave to dB units, one should take the log of the reflection or transmission coefficient and multiply this value times 10. However, 20 is the multiplier used here since the power of sound is not measured directly in ultrasonic testing. The transducers produce a voltage that is approximately proportional to the sound pressure. The power carried by a traveling wave is proportional to the square of the pressure amplitude. Therefore, to estimate the signal amplitude change, the log of the reflection or transmission coefficient is multiplied by 20.

3.12 Integrated Response

The Integrated Response (fundamental response) is one of the measured values used in this research, which is directly related to the reflection coefficient of the material(Bhardwaj, 2004). The Integrated Response (IR) is the calculated attenuation as measured, in decibels, of the tested material using a Chirp signal.

The basic equation for how the IR is determined in the pulser-receiver is using the amplitude spectra of the two signals; the initial, and the exiting. The signal is converted to a decibel value, which is the unit of the Integrated Response, which is a function of the sound pressure.

If the material is homogeneous, the measurement of IR related to the reflection coefficient is expressed as:

$$IR = 20\log R \qquad [25]$$

where

IR = integrated response

R = reflection coefficient

Since the reflection coefficient in always less than or equal to one (not negative), the amount of IR is always negative.

3.13 Ultrasonic Sources

Mechanical vibrations for measurement, analysis, or test purposes are generated by electromechanical transducers, i.e., elements having the ability to transform electrical into mechanical energy, and viceversa. For ultrasonic inspection at frequencies above 200 kHz, piezoelectrictransducers are used. These employ materials which generate electric chargeswhen mechanically stressed, and conversely, become stressed when electricallyexcited. Transducer elements suitably mounted for inspection work are commonlycalled search units, crystals, or probes(NDT-ed.org).

The piezoelectric (pz) effect creates a mechanical stress in a pz material when an electric field is applied as a voltage across it or it creates a voltage when a mechanical stress is applied. The piezoelectric effect is a crystal, which acquires a charge when compressed, twisted, or distorted. The transducer will contain a resonant material, a coupling or wear-face, and a case which includes a reflector as illustrated in Figure 3-19. The conversion of electrical pulses to mechanical vibrations and the conversion of returned mechanical vibrations back into electrical energy is the basis for ultrasonic testing (Figure 3-20).

Figure 3-19Section of a Piezoelectric Transducer (www.NDT-ed.org)

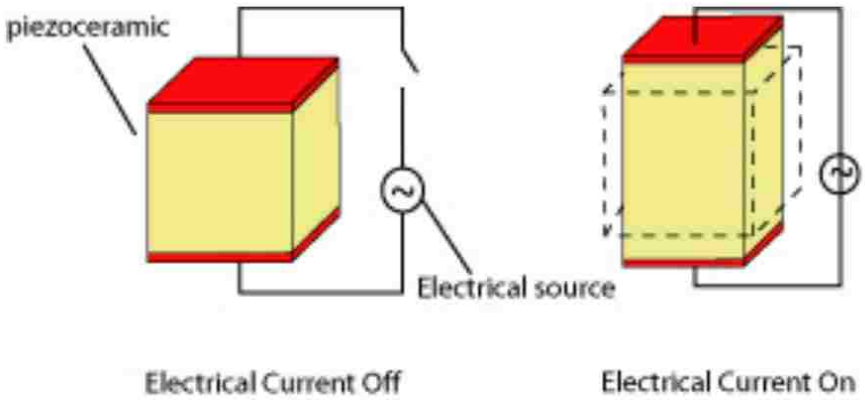

Figure 3-20PiezoceramicExcitation (www.NDT-ed.org)

Contact transducers, non-contact transducers and immersion transducers are three major types of transducers used in the industry and research fields. Following is the description of each type of transducer.

3.13.1 Contact Transducers

The Contact Transducer is thus named due to it is having physical contact with the material to be tested.They have elements protected in a rugged casing to withstand sliding contact with a variety of materials. These transducers have an ergonomic design so that they are easy to grip and move along a surface. They often have replaceable wear plates

to lengthen their useful life. Coupling materials of gel, grease, oils, or commercial materials are used to remove the air gap between the transducer and the component being inspected.

3.13.2 Non-contact Transducers

A non-contact transducer is used without touching the material to be tested. Unlike the contact transducer, which transmits the signal directly into the material, the non-contact transducer signal passes first through air displayed in Figure 3-21.

In the materials industry, one of the early applications of non-contact ultrasound was the testing of Styrofoam blocks by utilizing a 25kHz frequency (Bhardwaj, M. 2001). A precursor to high frequency non-contact transducers was the 1982 development of piezoelectric dry coupling longitudinal and shears wave transducers up to 25MHz frequency. Dry coupling transducers feature a solid compliant and acoustically transparent transitional layer in front of the piezoelectric materials. These devices, which eliminate the use of liquid couplant, do require contact with the material. An important by-product of dry coupling devices was the development of air-gas propagation transducers, which utilize less than very low acoustic impedance matching layer of a non-rubber material on the piezoelectric material. These commercially available transducers have been successfully produced in a frequency range of 100 kHz to 5MHz. These devices quickly found applications in aircraft/aerospace industries for imaging and for defect detection in fibrous, low, and high-density polymers, and composites.

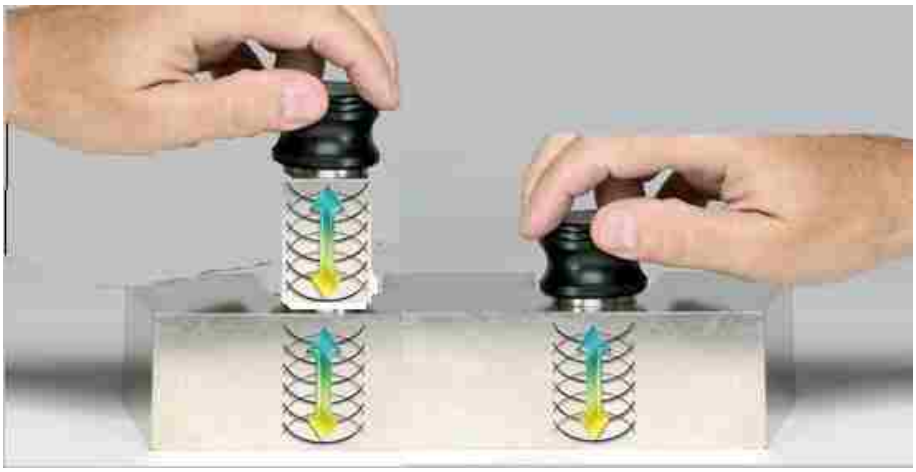

Figure 3-21Example of Contact and Non-contact Method

3.13.3 Immersion Transducers

Immersion transducers do not contact the component. These transducers are designed to operate in a liquid (usually water) environment and all connections are watertight. Immersion transducers usually have an impedance matching layer that helps to get more sound energy into the water and, in turn, into the component being inspected (Figure 3-20). Immersion ultrasonic tests utilize high-frequency mechanical vibrations to probe test objects. These vibrations are coupledto test objects by immersing the crystal (which provides the searching and receiving signals) and the test object in water or other suitable liquid couplant (Figure 3-22).Immersed ultrasonic inspection may, in a limited way, utilize the basic electronicequipment employed in contact pulse-reflection ultrasonic testing(NDT-ed.org).

Higher test frequencies offeradvantages in immersion ultrasonic testing. Low frequency or longer wavelengthspermit ultrasonic penetration to greater depth in the material, but this deeperpenetration may cause the loss of near-surface resolution and small flaw detection.To compensate for the loss of near-surface resolution, the part

should be scannedfrom both surfaces(McMaster, Non Destructive Testing Handbook, 1959).

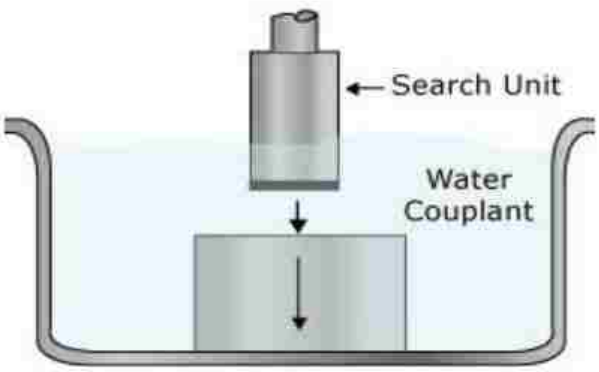

Figure 3-22 Immersion Ultrasonic Method (NDT-ed.org)

3.13.4 Radiated Fields of Ultrasonic Transducers

The sound that emanates from a piezoelectric transducer does not originate from a point, but instead originates from most of the surface of the piezoelectric element. Round transducers are often referred to as piston source transducers because the sound field resembles a cylindrical mass in front of the transducer (Figure 3-23). The sound field from a typical piezoelectric transducer is shown below. The intensity of the sound is indicated by color, with lighter colors indicating higher intensity(NDT-ed.org).

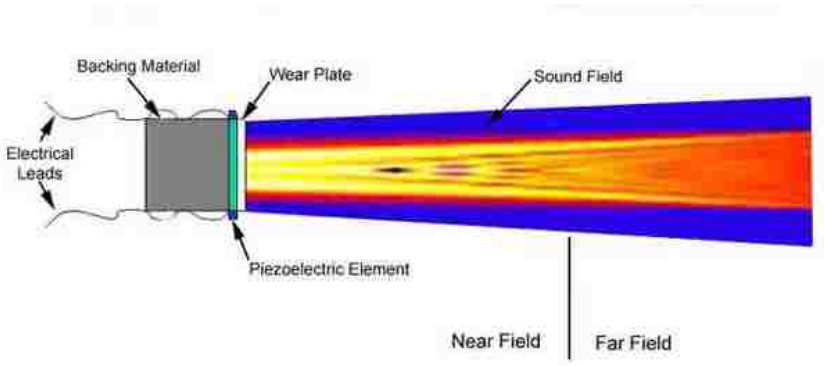

Figure 3-23 Cylindrical Beam of Sound Wave from a Transducer (NDT-ed.org)

Since the ultrasound originates from a number of points along the transducer face, the ultrasound intensity along the beam is affected by constructive and destructive wave interference as discussed in a previous page on wave interference. These are sometimes also referred to as diffraction effects. This wave interference leads to extensive fluctuations in the sound intensity near the source and is known as the “near field”. Because of acoustic variations within a near field, it can be extremely difficult to accurately evaluate flaws in materials when they are positioned within this area.

The pressure waves combine to form a relatively uniform front at the end of the near field. The area beyond the near field where the ultrasonic beam is more uniform is called the far field. In the far field, the beam spreads out in a pattern originating from the center of the transducer. The transition between the near field and the far field occurs at a distance, N, and is sometimes referred to as the "natural focus" of a flat (or unfocused) transducer (Figure 3-23). The near/far field distance, N, is caused by amplitude variations that characterize the near field change to smoothly declining amplitude at this point. The area just beyond the near field is where the sound wave is well behaved and at its maximum strength. Therefore, optimal detection results will be obtained after this point.

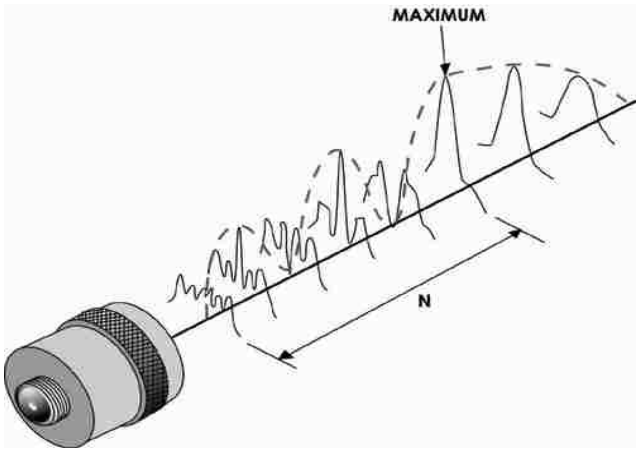

Figure 3-24 Location of Transition between the Near Field and the Far Field (NDT-ed.org)

However, at some point the pressure waves combine to form a relatively uniform front. The area where the ultrasonic beam is more uniform and spreads out in a pattern originating from the center of the transducer is called the far field. Knowing where the far field starts is important since optimal detection occurs when flaws are located at the start of the far field. The transition point between the near field and the far field (sometimes referred to as the "natural focus" of an unfocused transducer) can be calculated if the frequency and diameter of the transducer and the speed of sound in the material are known.For a piston source transducer of diameter (D), frequency (f), and velocity (V) in a liquid or solid medium, Equation 26 calculates the near/far field transition point(NDT-ed.org).

$$N = \frac{D^2 f}{4V} \qquad [26]$$

where

N = near/far field distance

f = frequency

D = transducer's diameter

V = ultrasoun velocity

3.14 Ultrasound Testing/Measurement Methods

Pulse/receive and pulse/echo and are two major configurations for ultrasound testing and measurement.

In pulse/receive method one transducer emits the ultrasound wave and another transducer receives the wave passed through the testing material (Figure 3-25). In the diagram of amplitude-time (Figure 3-17) for a pulse/receive measurement there is only one hump corresponding to the wave received by the receiver transducer (Figure 3-26).In the graphical user interface (GUI) of the ultrasound system the time and IR corresponding to the received pulse are given (Figure 3-26).

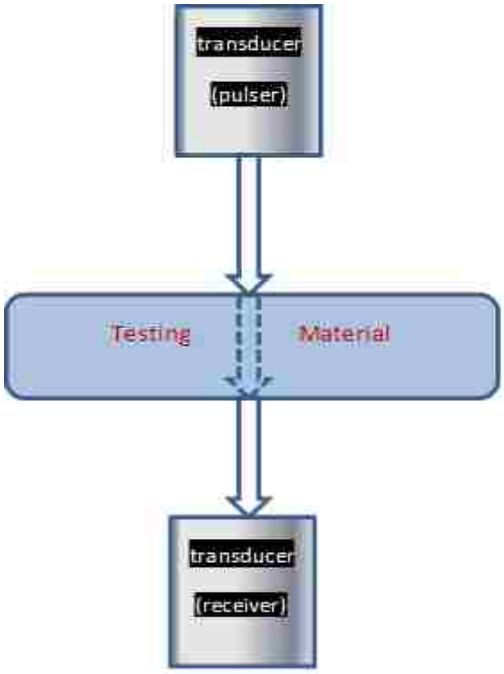

Figure 3-25 Pulse/receive Ultrasound

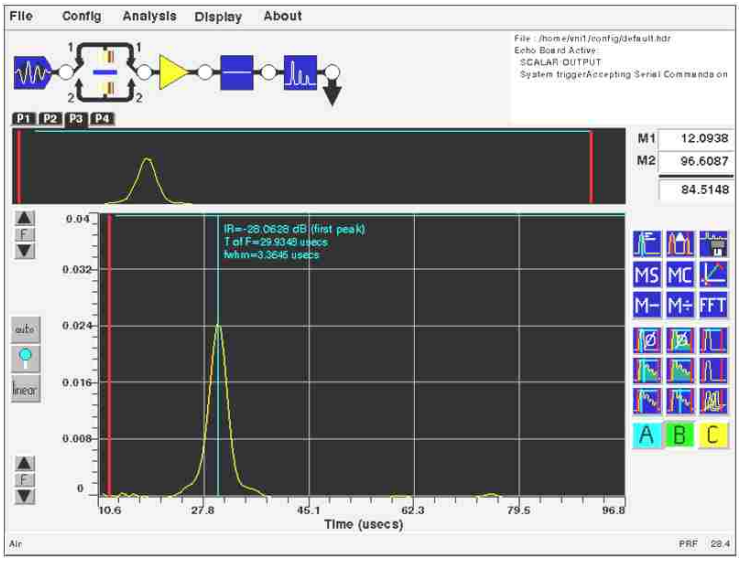

Figure 3-26Amplitude-Time for Pulse/receive Ultrasound

Knowing the thickness of the material sample, the distance between two transducers, and pulse velocity of the ambient medium (water or air), pulse velocity of the material is obtained using Equation 27.

$$V_m = \frac{d}{\frac{l-d}{V_a} - t} \qquad [27]$$

where

V_m = pulse velocity of material

d = thickness of the material sample

l = distance between two transducers

V_a = pulse velocity of ambient medium

t = time of pulse

IR of the material is obtain knowing the IR of the regular pulse/receive test (given in the GUI) and IR of the pulse when there is no sample between the transducer(Figure 3-27) (Equation 28).

$$IR_m = IR_c - IR_a \quad [28]$$

where

IR_m = integrated response of the material

IR_c = integrated response of the pulse when test material presents

IR_c = integrated response of the pulse when test material does not present

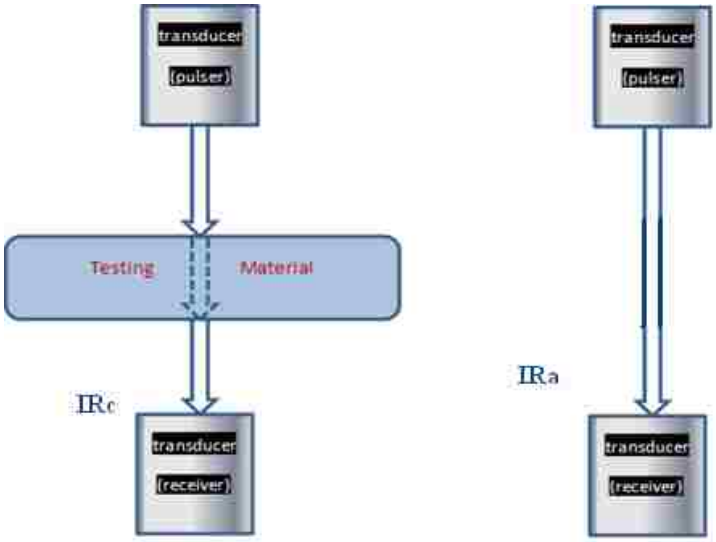

Figure 3-27 Integrated Response of the Material from Pulse/reprieve Test

In pulse/echo method, one transducer emits the ultrasound wave and the same transducer receives the reflected wave from the near or far surface of the testing materials (Figure 3-28). In the diagram of amplitude-time (Figure 3-17) for a pulse/echo measurement there are two humps corresponding to each receives (Figure 3-29). In the graphical user interface (GUI) of the ultrasound system, the time and IR corresponding to each reflection are given (Figure 3-29). Knowing the thickness of the material sample, pulse velocity of the material is obtained using Equation 29.

$$V_m = \frac{2d}{t_2 - t_1} \quad [29]$$

where

V_m = pulse velocity of material

d = thickness of the material sample

t_1 = time of reflection from surface

t_2 = time of reflection from bottom

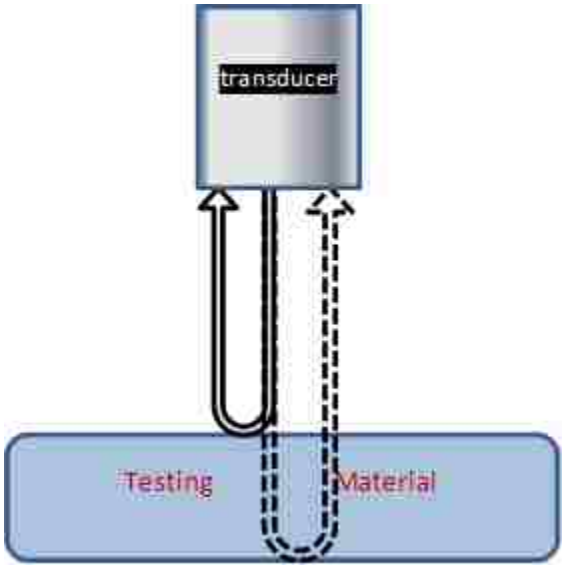

Figure 3-28Pulse/echo Ultrasound

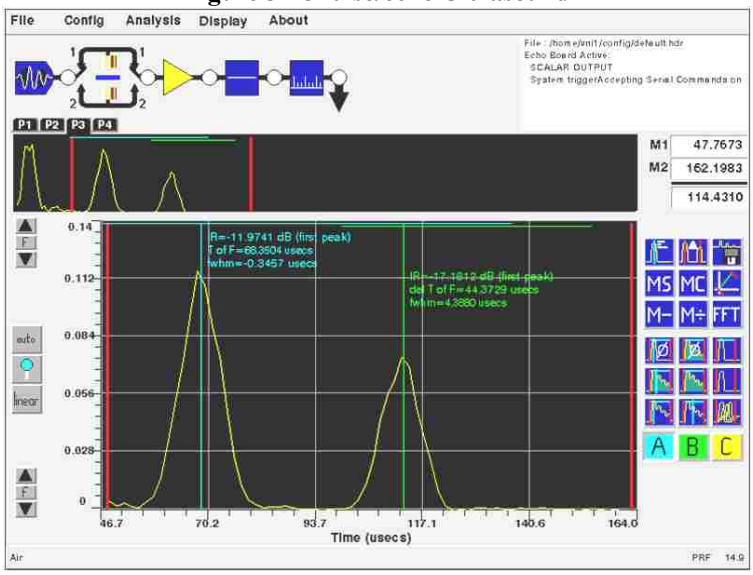

Figure 3-29 Amplitude-Time for Pulse/echo Ultrasound

Integrated response of the reflection from surface of the sample is called IR_1 and from bottom of the sample is called IR_2. Each IR corresponds to the reflection or transmission coefficient that the pulse has been through before it receives by the transducer (Figure 3-30). Equations 30 and 31 show the magnitude of each IR.

$$IR_1 = 20\log R_{I/II} \quad [30]$$

where

IR_1 = integrated response of the reflection from surface of the testing material

$R_{I/II}$ = reflection coefficient at the inteface that sound wave passes to material II *from* material I

$$IR_2 = 20\log T_{II/I} \quad [31]$$

where

IR_2 = integrated response of the reflection from bottom of the testing material

$T_{II/II}$ = transmission coefficient at the inteface that sound wave passes through material I from material II

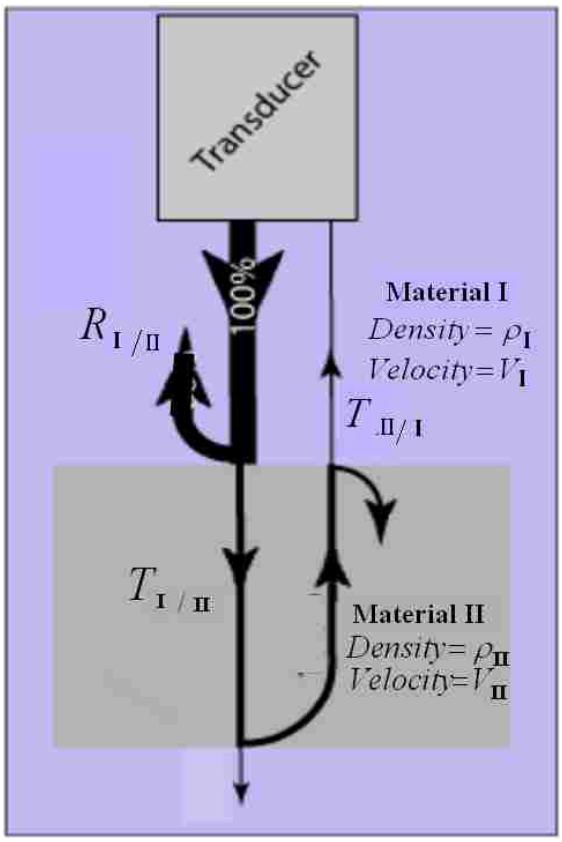

Figure 3-30 Reflection and Transmission of the Sound Wave at the Interface of Two Materials (Pulse/echo Measurement)

4. CHAPTER 4 :INTRODUCTION TO PERFORMANCE GRADE ASPHALT BINDER

4.1 Asphalt Binder Grades

Grading of asphalt binders has been introduced by different methods over the years. The main objective of these grading systems is to classify the binders based on their rheological properties, assuming that these properties relate to the field loading condition and binder performance. Penetration grading, viscosity grading, viscosity of aged residue grading and SUPERPAVE performance grading are four major methods of grading asphalt binders (Papagiannakis A.T., 2007).

Performance grading is the most commonly used system and it has several advantages over the other three systems. It was developed considering the influence of rate of loading on the binder properties. The second and the greatest advantage of SUPERPAVE performance grade is that the laboratory tests are conducted at temperatures that represent the geographical location in which the binder will be used. The penetration and viscosity grading systems are based on tests at fixed temperatures that may not represent the field temperature.

4.2 Performance Grade

Performance grade asphalt binder is noted by two numbers. The first number is the average 7-day high pavement temperature and the second number is the minimum pavement temperature in degree Celsius. For example, PG 76-22 is the asphalt binder which is used in the climate area with average 7-day maximum pavement temperature lower than or equal to 76°C and minimum pavement temperature higher than or equal to -22°C. With 6°C intervals the high temperature varies from 46°C up to 82°C and low

temperature varies from -46◦C to -10◦C. Figure 4-1 shows the major performance grade asphalt binders used.

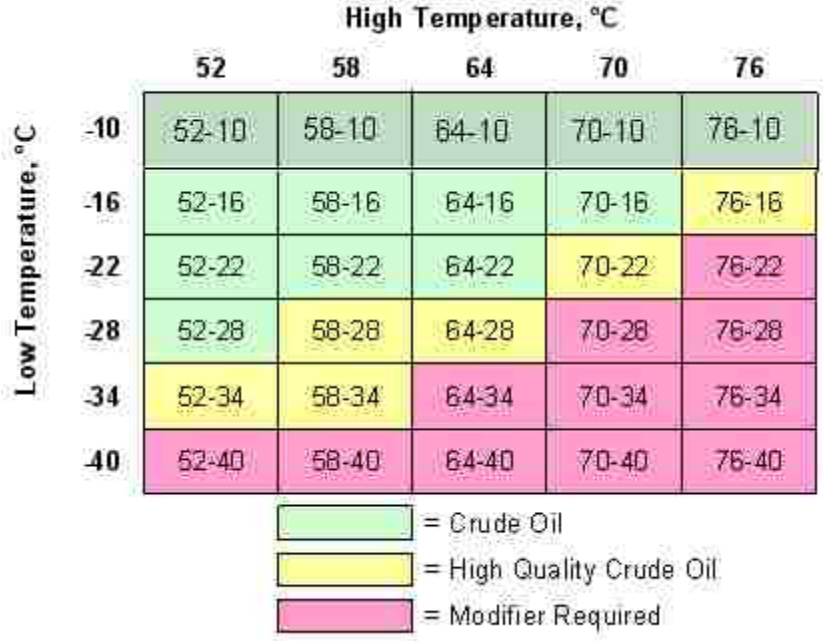

Figure 4-1 Performance Grade Asphalt Binder (Interactive, 2012)

The performance of the asphalt binder as part of HMA under different climate situations is tested during the procedure of quality control of asphalt binder. Three major key resistance properties are examined by mechanical tests. Those are permanent deformation resistance, fatigue cracking resistance and low-temperature cracking resistance. Permanent deformation or rutting occurs at high temperatures as the asphalt softens and the mix loses its elasticity and fatigue cracking is due to high volume of load applications and aging of the asphalt. Low-temperature cracking occurs as asphalt becomes brittle and the pavement shrinks in cold weather (Atkins, 2003). Table 4-1 shows the specifications of performance grade asphalt binder according to ASTM D 6373 (ASTM, 2007).

Table 4-1Performance Graded Asphalt Binder Specification

Performance Grade	PG 46	PG 52	PG 58	PG 64
	–34 –40 –46	–10 –16 – 22 –28 –34 –40 –46	–16 –22 –28 –34 –40	–10 –16 –22 –28 –34– 40
Average 7-day maximum Pavement Design Temperature, °C	<46	<52	<58	<64
Minimum Pavement Design Temperature,° C[A]	> –34 > –40 > –46	> –10 > –16 > –22 > –28 > –34 > –40 > –46	> –16 > –22 > –28 > –34 > –40	> –10 > –16 > –22 > –28 > –34 > –40
				Original Binder
Flash Point Temp., D92; min °C				230
Viscosity, D4402:[B] max. 3 Pa·s, Test Temp., °C				135
Dynamic Shear, D7175:[C] G*/sinδ, min. 1.00 kPa 25 mm Plate, 1 mm Gap Test Temp. at 10 rad/s, °C	46	52	58	64
				Rolling Thin Film Oven (Test Method D2872)
Mass Loss, max. percent				1.00
Dynamic Shear, D7175: G*/sinδ, min. 2.20 kPa 25 mm Plate, 1 mm Gap Test Temp. at 10 rad/s,°C	46	52	58	64
				Pressure Aging Vessel Residue (Practice D6521)
PAV Aging Temperature, °C[D]	90	90	100	100
Dynamic Shear, D7175: G*·sinδ, max 5000 kPa 8 mm Plate, 2 mm Gap Test Temp. at 10 rad/s, °C	10 7 4	25 22 19 16 13 10 7	25 22 19 16 13	31 28 25 22 19 16
Creep Stiffness, D6648:[E] S, max 300 MPa, m-value; min. 0.300 Test Temp at 60 s, °C	–24 –30 –36	0 – 6 –12 –18 –24 –30 –36	– 6 –12 –18 –24 –30	0 – 6 –12 –18 –24 –30
Direct Tension, D6723:[E] Failure Strain, min. 1.0 % Test Temp. at 1.0 mm/min., °C	–24 –30 –36	0 – 6 –12 –18 –24 –30 –36	– 6 –12 –18 –24 –30	0 – 6 –12 –18 –24 –30

Performance Grade	PG 70	PG 76	PG 82
	–10 –16 –22– 28 –34 –40	–10 –16 –22 –28 –34	–10 –16 –22 –28 –34
Average 7-day maximum Pavement Design Temperature, °C	<70	<76	<82
Minimum Pavement Design Temperature,° C[A]	> –10 > –16 > –22 > –28 > –34 > –40	> –10 > –16 > –22 > –28 > –34	> –10 > –16 > –22 > –28 > –34
Flash Point Temp., D92; min °C			
Viscosity, D4402:[B] max. 3 Pa·s, Test Temp., °C			
Dynamic Shear, D7175:[C] G*/sinδ, min. 1.00 kPa 25 mm Plate, 1 mm Gap Test Temp. at 10 rad/s, °C	70	76	82
Mass Loss, max. percent			
Dynamic Shear, D7175: G*/sinδ, min. 2.20 kPa 25 mm Plate, 1 mm Gap Test Temp. at 10 rad/s,°C	70	76	82
PAV Aging Temperature, °C[D]	100	100	100
Dynamic Shear, D7175: G*·sinδ, max 5000 kPa 8 mm Plate, 2 mm Gap Test Temp. at 10 rad/s, °C	34 31 28 25 22 19	37 34 31 28 25	40 37 34 31 28
Creep Stiffness, D6648:[E] S, max 300 MPa, m-value; min. 0.300 Test Temp at 60 s, °C	0 – 6 –12 –18 –24 –30	0 –6 –12 –18 –24	0 – 6 –12 –18 –24
Direct Tension, D6723:[E] Failure Strain, min. 1.0 % Test Temp. at 1.0 mm/min., °C	0 –6 –12 –18 –24 –30	0 – 6 –12 –18 –24	0 – 6 –12 –18 –24

4.3 Aging of the AsphaltBinder

Aging is the change in the binder structure and composition due to exposure to oxygen and severe temperature. This change makes the asphalt binder harder and more brittle.

Two stages of aging occurrs in asphalt binder in the asphalt mix. Short term aging is the aging of asphalt during the construction of the HMA and it is simulated in the laboratory using the Rolling Thin Film Oven (RTFO) according to ASTM D 2872 (AASHTO T240) procedure. In this test, bottles with small amount of asphalt are placed in a rack in an oven at the temperature similar to that used in asphalt mixing in the plant (typically 162°C). A thin film of asphalt forms inside the bottle as the rack rotates around its center (Figure 4-2). This film of asphalt is subjected to hot air flow as the bottle rotates (Papagiannakis A.T., 2007).

Figure 4-2Rolling Thin Film Oven (RTFO)

Aging of asphalt also occurs during the service life of the pavement due to oxidation which is called long term aging. This process is simulated in the laboratory by the

Pressure Aging Vessel (PAV) according to ASTM D6521. In a PAV machine a thin film of asphalt binder is subjected to oxygen at high pressure and high temperature for a relatively long time (Figure 4-3). Aging in the field is more severe for thin films and asphalt mixtures with connected voids (Papagiannakis A.T., 2007).

Figure 4-3Pressure Aging Vessel (PAV)

4.4 SUPERPAVE Performance Tests of Asphalt Binders

Three mechanical tests are done to study the behavior of asphalt binder under different loading and temperature conditions .The Dynamic Shear Rheometer (DSR) is used to characterize the viscous and elastic behavior of asphaltbinders at medium and high temperatures. The basic DSR test uses a thin asphalt binder sample sandwiched between two circular plates. The lower plate is fixed while the upper plate oscillates back and forth across the sample at 10 rad/sec (1.59 Hz) to create a shearing action (Figure 4-4). DSR test is conducted at high temperature on un-aged and RTFO aged samples (first temperature of the grade) and at medium temperature on PAV aged samples.

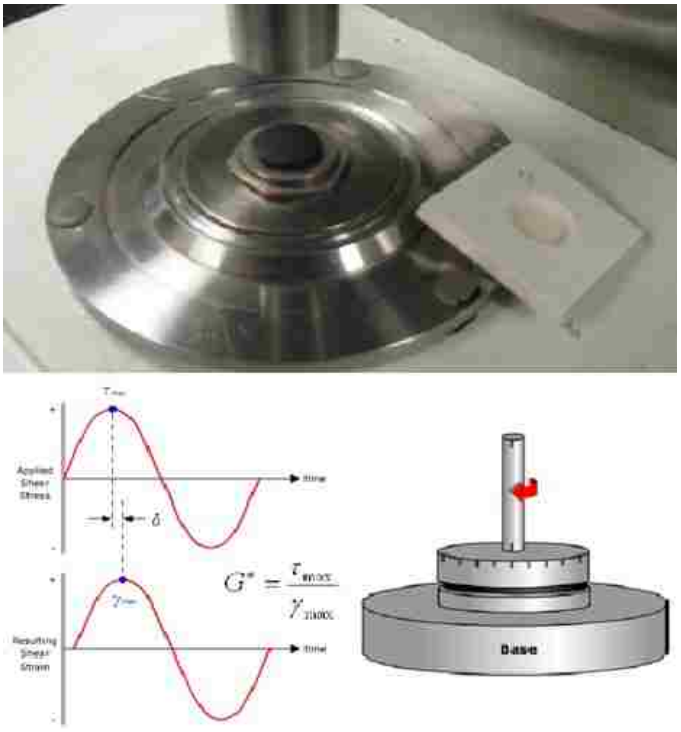

Figure 4-4Dynamic Shear Rheometer, Stress/strain Variation, Test Configuration (Interactive, 2012)

The DSR measures a specimen's complex shear modulus (G*) and phase angle (δ). The complex shear modulus can be considered the sample's total resistance to deformation when repeatedly sheared, while the phase angle is the lag between the applied shear stress and the resulting shear strain. The larger the phase angle, the more viscous the material (Figure 4-5) (Interactive, 2012)

In order to resist rutting, an asphalt binder should be stiff (it should not deform too much) and it should be elastic (it should be able to return to its original shape after load deformation). Therefore, the complex shear modulus elastic portion, G*/sinδ should be large. When rutting is of greatest concern (during an HMA pavement's early and mid-life), a minimum value for the elastic component of the complex shear modulus is specified.

In order to resist fatigue cracking, an asphalt binder should be elastic (able to dissipate energy by rebounding and not cracking) but not too stiff (excessively stiff substances will crack rather than deform-then-rebound). Therefore, the complex shear modulus viscous portion, G*sinδ, should be a minimum. When fatigue cracking is of greatest concern (late in an HMA pavement's life), a maximum value for the viscous component of the complex shear modulus is specified (Interactive, 2012).

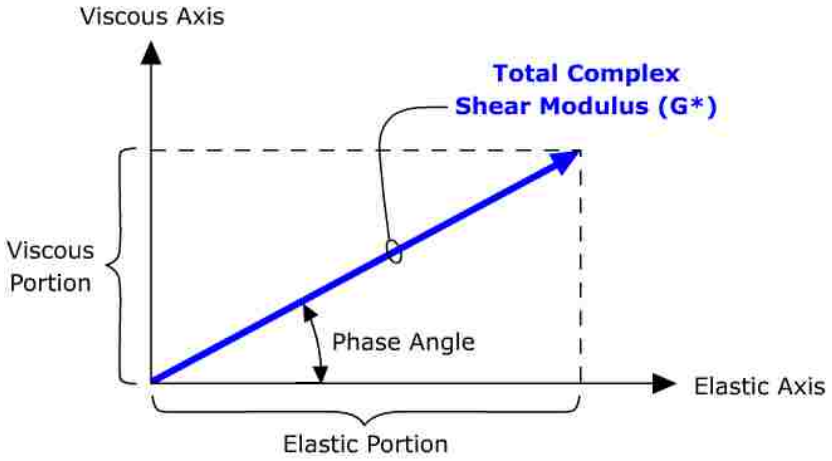

Figure 4-5Complex Shear Modulus (Interactive, 2012)

The Bending Beam Rheometer (BBR) test and Direct Tensile Tester (DTT) provide a measure of low temperature stiffness and relaxation properties of asphaltbinders. These parameters give an indication of an asphalt binder's ability to resist low temperature cracking (Interactive, 2012).

The basic BBR test uses a small asphalt beam that is simply supported (Figure 4-6) and immersed in a cold liquid bath. A load is applied to the center of the beam and its deflection is measured against time. Stiffness is calculated based on measured deflection and standard beam properties and a measure of how the asphalt binder relaxes the load induced stresses is also recorded. Stiffness and the slope of the graph of variation of

stiffness with time, both in log scale, are measured 60 seconds after stating the load application. In order to resist low-temperature cracking, an asphalt binder should have a low stiffness and high rate of stress relaxation. BBR tests are conducted on PAV aged asphalt binder samples (Interactive, 2012).

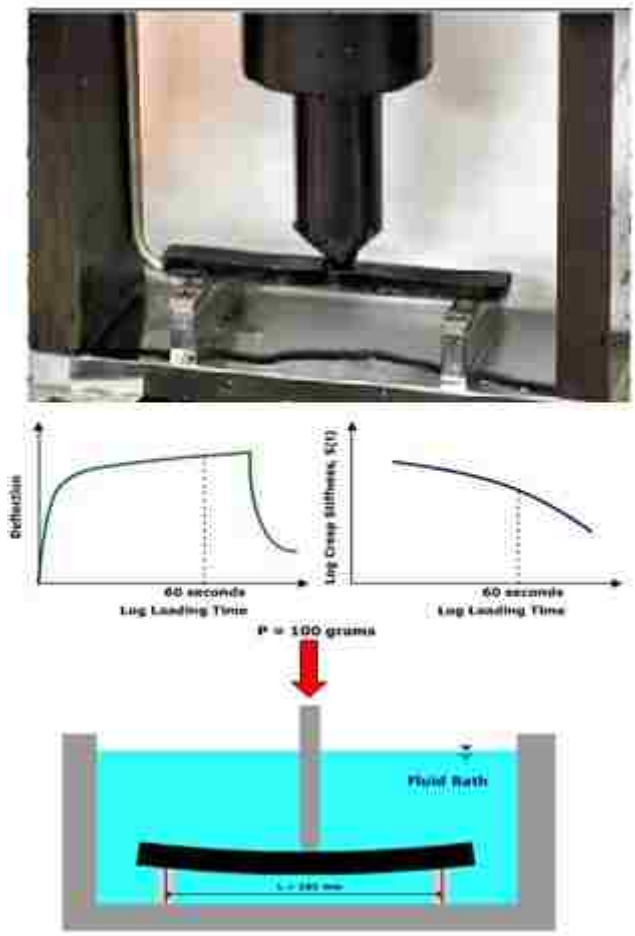

Figure 4-6Bending Beam Rheomoter, Stress/strain Variation, Testing Configuration (Interactive, 2012)

The basic DTT test measures the stress and strain at failure of a specimen of asphalt binder pulled apart at a constant rate of elongation (Figure 4-7). Test temperatures are such that the failure will be from brittle or brittle-ductile fracture. The test is of little use

at temperatures where the specimen fails by ductile failure (stretches without breaking). DTT tests are conducted on PAV aged asphalt binder samples (Interactive, 2012).

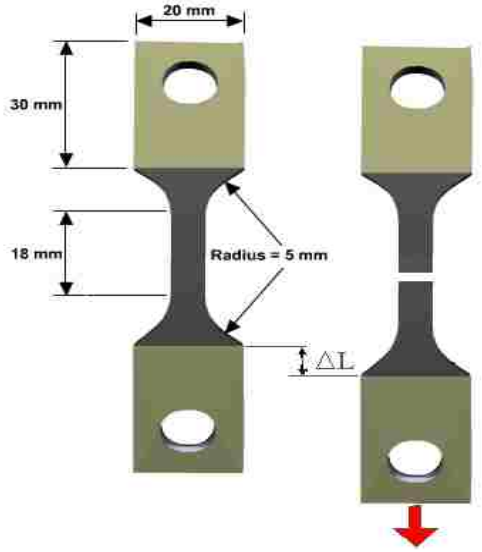

Figure 4-7 Direct Tensile Tester, Testing Configuration (Interactive, 2012)

Some agencies including the Nevada Department of Transportation (NDOT) have replaced the DTT test by the ductility test. The ductility test measures asphalt binder ductility by stretching a standard-sized briquette of asphalt binder at a constant strain rate (1cm/min or 5 cm/min) (Figure 4-8, 4-9) to its breaking point. The stretched distance in centimeters at breaking is then reported as ductility (Interactive, 2012).

Figure 4-8Ductility Test

Figure 4-9 Ductility Tests Samples

The standard ductility test is performed at 25˚C, but when it is used as a direct tension test to characterize the low temperature performance of asphalt binder the test

temperature is 4°C. Table 4-1 shows the specifications of performance grade asphalt binder used in Nevada for ductility test at 4°C.

Table 4-2 Low Temperature Ductility for Performance Grade Asphalt Binder (NDOT)

Grade		Minimum Ductility (cm)	
		Original State	RTFO State
64 - *	Polymer Modified	50	25
	Non-polymer	10	5
76 - *	Polymer Modified	20	10
	Non-polymer	5	2.5

4.5 Modified Asphalt Binders

Modifiers have been added to asphalt cements to improve rheological properties of asphalts (Theterm “asphalt cement” refers to anunmodified material, while the term“binder” includes both modified andunmodified materials). These modifiers can enhance the resistance of the asphalt pavements to permanent deformation, fatigue and low temperature cracking, stripping, and oxidation. In order to meet the SUPERPAVE specifications, especially for temperature grades over 70°C and under -28°C, modifiers are necessary for most asphalt binders. Extreme climate conditions can have a negative effect on HMA pavement performance. Cracking can occur in cold temperatures when asphalt cement is too stiff, and rutting or other deformation can occur in hot temperatures when asphalt cement is too fluid. An ideal temperature range exists for each asphalt cement, in which it displays the right combination of viscous and elastic properties for good pavement performance, as illustrated in Figure 4-10 (IllinoisDOT, 2005).

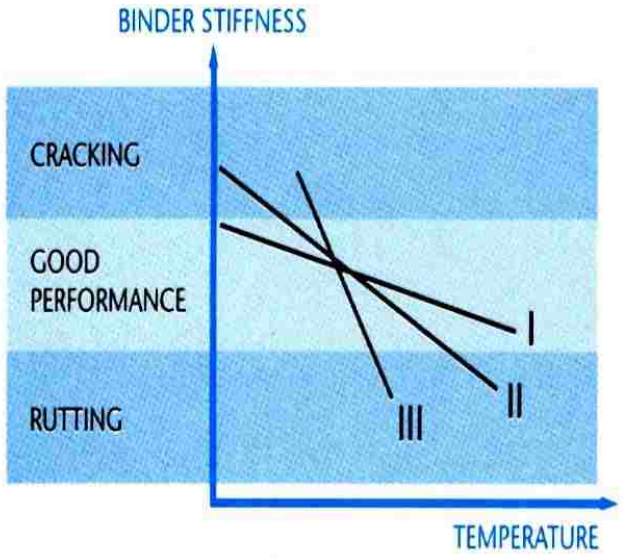

Figure 4-10 Ideal Temperature Ranges for Good HMA Pavement Performance (IllinoisDOT, 2005)

4.5.1 Polymer Modified Asphalt Binder

Polymers can be added, which modify thenatural viscoelastic behavior of theasphalt cement; thus, affecting the idealtemperature range. There are two mainclasses of polymers used for this purpose:elastomers, which enhance strength athigh temperatures, as well as elasticity atlow temperatures; and plastomers, whichenhance strength but not elasticity. Threetypes of elastomeric copolymer modifiersare currently used:styrene-butadiene diblock (SB), styrenebutadienetriblock (SBS); and styrenebutadienerubber (SBR).

As an example of how polymer-modifierscan be useful, consider the three binders

(I, II, and III) in Figure 4-10. Binder III has a narrow ideal temperaturerange that would be suitable for use ina moderate climate with consistent year-roundtemperatures, but not suitablefor a climate featuring extreme seasonaltemperature variations. In order forBinder III to perform well in such aclimate, polymer-modifiers could be addedthat would change its behavior to bemore like that of Binder I or Binder II.Both of those

materials display wider idealtemperature ranges that are better suitedfor highly variable temperatures. With allelse being equal, an HMA pavementcontaining Binder I would be expected toperform the best under those conditions (IllinoisDOT, 2005).

In addition to improving pavement performanceat locations with extremehot-cold temperature variations, there areother potential benefits of using polymermodifiedbinders in HMA construction.Polymer-modified binders typically aremore viscous than unmodifiedbinders, and tend to show improvedadhesive bonding to aggregate particles. These properties result in athicker binder coating on the aggregateparticles that does a better job of holdingthe particles together. Thicker bindercoatings usually take longer to becomebrittle from oxidation, so the durability ofthe pavement can be improved. Thebetter adhesion helps to minimize drain-downat the time of construction, and alsohelps to reduce the tendency of thepavement to ravel once it has aged.

Areas which experience frequent heavytruck traffic and/or slow-moving trucktraffic may benefit from the use ofpolymer-modified HMA mixtures. Thehigher viscosity and improved adhesionprovided by the polymers help resistrutting under extremely heavy loads, whileincreased elasticity improves the fatigueresistance from repeated cycles of heavytruck loading over the lifetime of thepavement.

4.5.2 Rubberized Modified Asphalt Binder

Although they cost more than conventional binders, polymer modified asphalt binders have been utilized for many years by many State DOTs. The high cost associated with the modification process is mostly due to the availability of SBS material. The SBS market was hit with a shortage of Butadiene lately, which affected both supply and cost of polymer modified asphalt binders. It is important to have some alternative

modifiers.Ground Tire Rubber (GTR), which contains styrenebutadienerubber (SBR), is a cheap and "available from recycling" product that can be used as a modifier of asphalt binder.

Rubberized asphalt-mixtures use this type of modified asphalt binder with improved temperature susceptibility and flexibility. This modified binder is formed by the interaction of crumb rubber with asphalt binder at elevated temperatures for a certain period of time. This type of modified binder has several advantages including: a) increase in the binder's elasticity, and b) increase in its resistance to aging due to anti-oxidants contained in tires.

Use of GTR in hot-mix asphalt increased substantially in the early 1990s due in large part to FHWA's mandate imposed in Intermodal Surface Transportation Efficiency Act (ISTEA). The primary use of crumb rubber modified asphalt binders in pavement applications include crack and joint sealants; binders for chip seals, interlayers, and hot-mix asphalts; and membranes. Crumb rubber modifiers have been used in asphalt binders used to produce quality hot-mix asphalt mixtures since the 1960s. There are several benefits including: improved resistance to surface initiated cracking, aging and oxidation resistance, fatigue, reflection cracking, and rutting resistance; increased night-time visibility due to contrast in the pavement and striping; reduced tire noise, construction time, splash and spray during rain storms; lower pavement maintenance costs and life cycle costs; better chip retention, and savings in energy and natural resources by using waste products.

5. CHAPTER 5 :METHODOLOGY AND MATERIALS

This chapter includes the procedures and results which lead to selection of the best ultrasound method and measurements configuration that can distinguish between two or more performance grade asphalt binders. It also discusses the selection of asphalt binder grades that would be tested with the selected method.

Contact and immersion ultrasound measurements have been tried with four different approaches in this research. Advantages and disadvantages of each approach were discussed. Some test results were shown. The approach(es) which succeeded to distinguish between two or more different PG asphalt binders where selected for future testing and investigation.

5.1 Approach 1: Pulse/Receive Contact Measurement with Contact Transducers

In the first approach the asphalt sample in a tin cup was placed between two transducer specified for contact test (Figure 5-1). In order to avoid sticking the transducer to the sample and also to make sure that there is no air gap between the transducer's surface and the sample, a thin layer of couplant gel was applied to the surface of the sample and bottom of the cup. The measurements were performed at room temperature.

Figure 5-1Pulse/Receive Contact Measurement Configuration

Due to two major issues, this Approach did not deliver reliable results. First, the sound wave traveled not only in the asphalt sample but also in the tin cup, and subtracting the effect of the tin (which has a relatively high acoustic impedance mismatch with asphalt) was almost impossible. Second, the sample was relatively small and the thickness of the couplant gel, which was extremely difficult to have control on, had a major effect on the time of flight of the sound wave.

5.2 Approach 2: Pulse/Receive Immersion Test with Contact Transducers

Two major issues involved in the first Approach were tried to be eliminated in the second Approach. Therefore, instead of the tin cup a brass ring was used to cast the asphalt sample and instead of the gel, water was used as the couplant. As it was presented in Chapter 4, when water fills the gap between transducer and the testing material, the method of ultrasound testing or measurement is immersion.

5.2.1 Design

In this Approach, an asphalt sample was cast in a brass ring with diameter of 2.5 in (6.1 cm) and a thickness of 1 in (2.5 cm) (Figure 5-2).

Figure 5-2Asphalt Sample

A top-open box with dimensions of 4×4×12 in (10×10×30 cm) was fabricated for this Approach, as shown in Figure 5-3.

Figure 5-3Top-open Box for Approach 2

Contact transducers were placed on each side of the box, and the sample was placed at the center bottom of the box (Figure 5-4). The test box was filled with deionized water at room temperature .The sound wave emitted from one transducer passed through the asphalt sample and was received by the other transducer, as illustrated in Figure 5-5 . Given the distance between face of the two transducers and the speed of sound in water, by measuring the time of flight of the sound wave from one transducer to the other, one can calculate the sample's velocity.

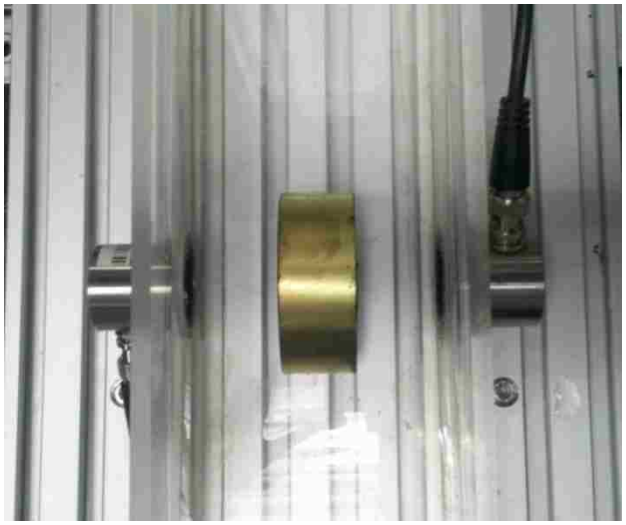

Figure 5-4Bird's Eye View of the Sample Placed between the Two Transducers

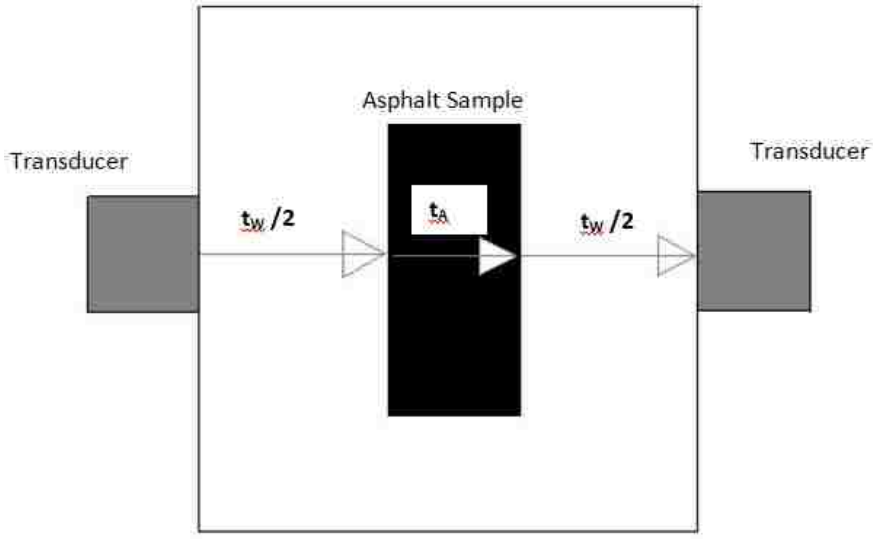

Figure 5-5Illustration of the Sound Wave Traveling through the Sample

5.2.2 Measured Parameters

Material velocity and IR according to Equation 27 and 28 has been measured and calculated, respectively. Testing materials were three PG asphalt binders, PG 64-10, PG 70-10 and PG 76-16, all taken from one source. Three identical samples from each grade were cast and ultrasound parameters were measured three times at room temperature. Table 5-1 shows the results of these measurements.

Table 5-1 Velocity and IR Measured in Approach 2

Sample no.	Measurement	64-10		70-10		76-16	
		V_m (m/s)	IR_m (dB)	V_m (m/s)	IR_m (dB)	V_m (m/s)	IR_m (dB)
1	1	1808.6	0.724	1869.3	1.345	1900.4	1.040
	2	1810.1	0.808	1869.8	1.346	1880.8	0.894
	3	1810.8	0.874	1870.0	1.367	1880.3	0.856
2	1	1808.6	0.724	1849.2	0.474	1829.8	1.643
	2	1810.1	0.808	1848.7	0.354	1832.1	1.633
	3	1810.8	0.874	1848.5	0.301	1832.6	1.596
3	1	1808.8	1.115	1850.9	0.111	1850.6	1.725
	2	1813.2	0.861	1851.0	-0.075	1849.2	1.749
	3	1814.7	0.656	1851.0	-0.126	1848.1	1.731

5.2.3 One-way ANOVA on Data from Approach 2

To examine whether the average of each measurement for each PG asphalt binder is significantly different or not, one-way ANOVA was performed on the data set. Table 5-2 is the summary of statistical analysis and Figure 5-6 illustrates the box plot of the results.

Table 5-2One-way ANOVA on Data from Approach 2

		Between PG 64-10 & PG 70-10	Between PG 64-10 & PG 76-16	Between PG 70-10 & PG 76-16
Velocity	p-value	0.000	0.000	0.957
	Significantly different?	YES	YES	NO
IR	p-value	0.235	0.000	0.003
	Significantly different?	NO	YES	YES

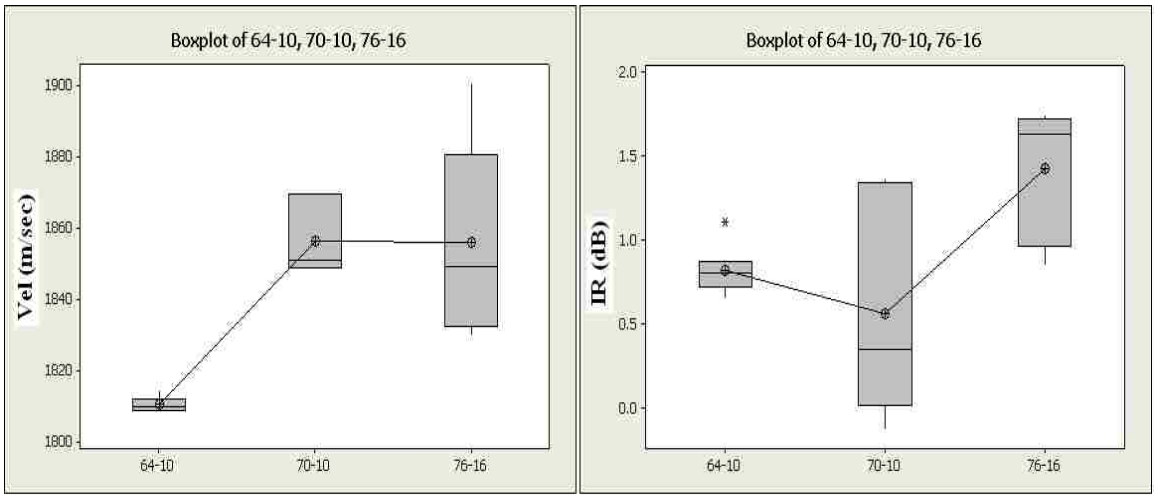

Figure 5-6 Boxplot of the Results from Approach 2

5.3 Approach 3: Pulse/Echo Immersion Test with Contact Transducer

5.3.1 Design

As it was stated in Section 4.2, in order to verify the high grade temperature of performance grade asphalt binders, the DSR test is conducted at that temperature. For example, G*/sinδ of the PG 64-10 should be higher than 1 kPa when the test is conducted at 64◦C.

This concept encouraged the researchers to conduct the ultrasound measurement at temperatures higher than room temperature. Having no control on the temperature of the water in the test box and sagging of the surface of the asphalt sample at high temperature were the main problems which made ultrasound measurement impossible with the configuration of Approach 2.

However, conducting a pulse/echo test on the asphalt sample in a tin cup that is seated at the bottom of a water bath with temperature control (Figure 5-7) could be an excellent idea for elevated temperature measurements.

Figure 5-7Ultrasound Measurement Configuration in Approach 2

5.3.2 Measurements

Ultrasound measurements were conducted on asphalt binder samples at four elevated temperature of 30°C, 40°C, 50°C and 60°C as well as room temperature. Tin cups with diameter of 68.9 ±0.02 mm and depth of 42.5±0.02 mm were used to hold the asphalt samples (Figure 5-8). Same grades of asphalt binders as previous approach were selected and three samples were made from each. Since the main testing is done on aged samples during the grade verification of performance grade asphalt binders, RTFO and PAV aged samples were also prepared and tested. Pulse velocity, IR_1 and IR_2 of the asphalt binders according to Equations 29 through 31 were measured. Figures 5-9 through 5-11 show the variation of velocity, IR_1 and IR_2 with temperature in measurements of the Approach 3.

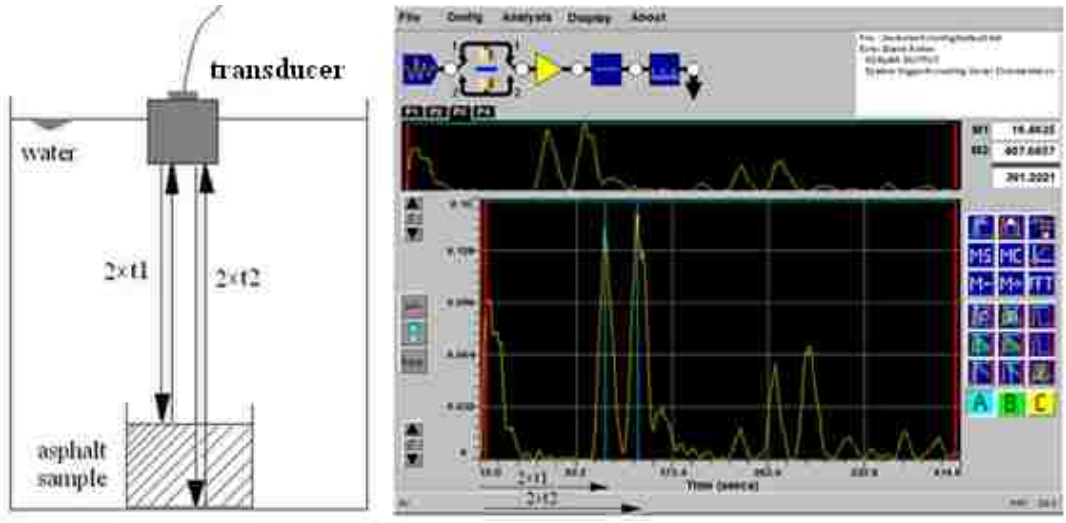

Figure 5-8Configuration and the Time of Flight for a Pulse/echo Immersion Ultrasound Measurement

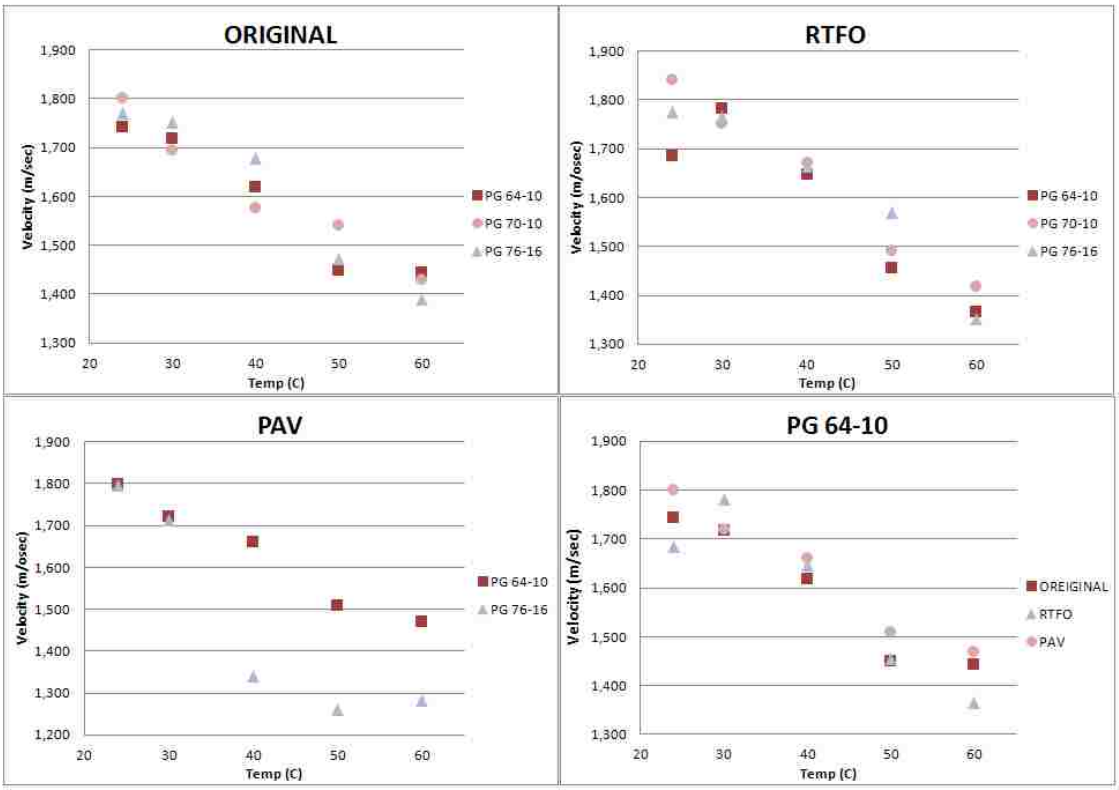

Figure 5-9Variation of Velocity with Temperature for Original and Aged Samples

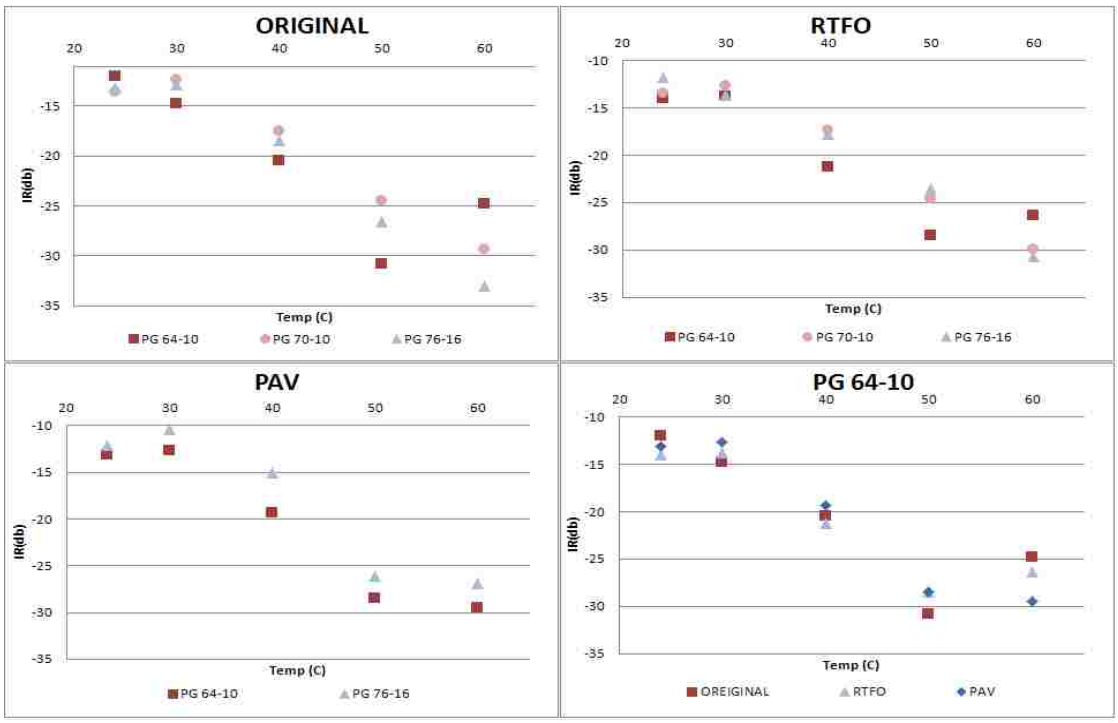

Figure 5-10Variation of IR for Reflection from the Surface (IR_1) with Temperature

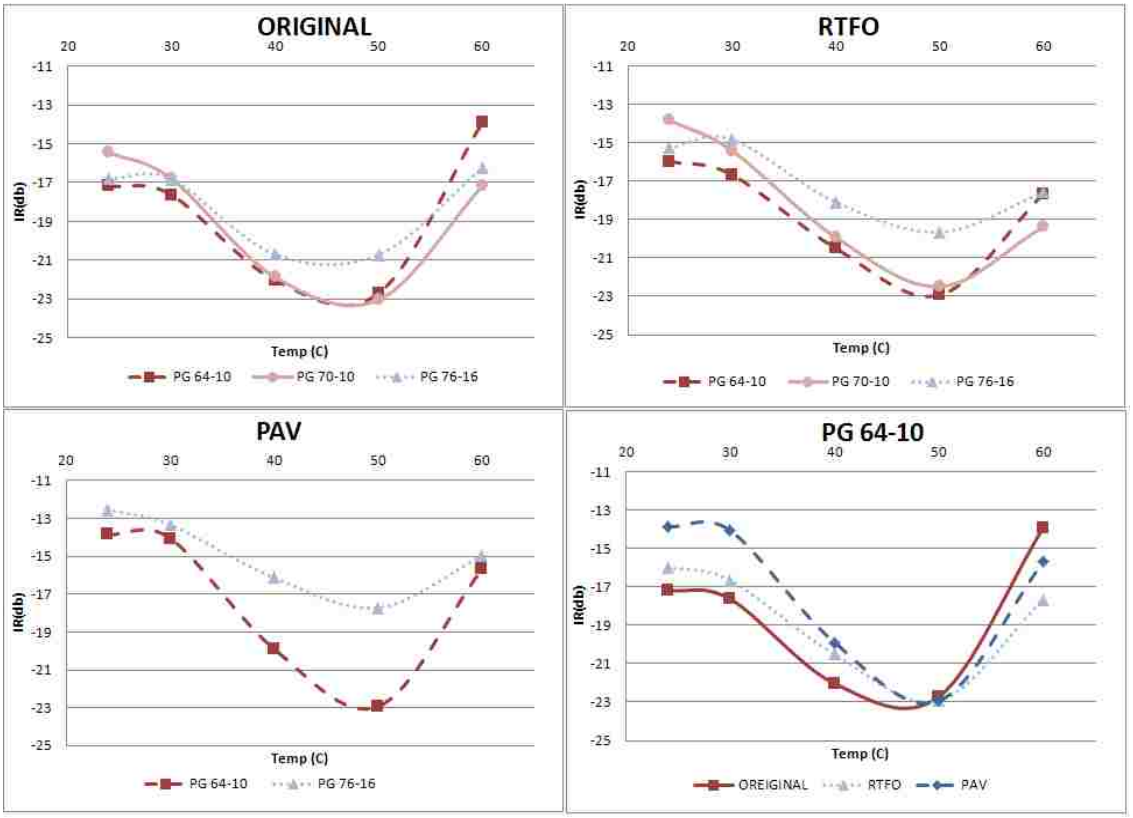

Figure 5-11Variation of IR for Reflection from the Bottom (IR_2) with Temperature

5.3.3 One-way ANOVA on Data from Approach 3

Analysis of variance for original asphalt binder does not show that ultrasound measurement can distinguish between three asphalt binders.

Table 5-3One-way ANOVA on Data from Approach 3

		PG 64-10 and PG 70-10					PG 64-10 and PG 76-16				
		24 C	30 C	40 C	50 C	60 C	24 C	30 C	40 C	50 C	60 C
Velocity	p-value	0.005	0.512	0.406	0.011	0.042	0.253	0.018	0.000	0.808	0.059
	Significantly different?	YES	NO	NO	YES	YES	NO	YES	YES	NO	NO
IR1	p-value	0.003	0.000	0.001	0.002	0.002	0.000	0.000	0.000	0.008	0.000
	Significantly different?	YES	YES	YES	YES	YES	YES	YES	YES	YES	YES
IR2	p-value	0.101	0.001	0.301	0.545	0.700	0.000	0.000	0.001	0.050	0.002
	Significantly different?	NO	YES	NO	NO	NO	YES	YES	YES	YES	YES

		PG 70-10 and PG 76-16				
		24 C	30 C	40 C	50 C	60 C
Velocity	p-value	0.910	0.033	0.000	0.001	0.340
	Significantly different?	NO	YES	YES	YES	NO
IR1	p-value	0.157	0.000	0.038	0.084	0.012
	Significantly different?	NO	YES	YES	NO	YES
IR2	p-value	0.059	0.876	0.000	0.002	0.434
	Significantly different?	NO	NO	YES	YES	NO

5.4 Approach 4: Pulse/Echo Immersion Test with High Frequency Immersion Transducer

Approaches 2 and 3 were involved immersion ultrasound measurement. However, the transducers used were specified for ultrasound contact measurements. Also, the recommended frequency of contact transducers was fairly low (250 kHz). According to literature, high frequency measurement is more reliable for characterizing the behavior of

viscoelastic materials (Bhardwaj, 2004). This encouraged the researchers to use high frequency (≥ 1 MHz) transducers specified for immersion measurements.

Another advantage of the immersion transducers is that the connection cord connects to the back of the transducer (Figure 5-12) (unlike the contact transducer which connects to the side). This helps when the operator wants to change the depth of the penetration of the transducer in to the water.

Figure 5-12 Immersion Transducer in Pulse/echo test

Only two performance grade asphalt binders were used in this Approach (PG 64-22 and PG76-22 and original state only). Similar parameters that were measured in the Approach 3 were also measured here at the same temperatures. Figure 5-13 shows the variation of velocity, IR_1 and IR_2 with temperature. Sample size (thickness) changed in this approach due to the better response that could be obtained from a thinner sample. This is discussed in Section 5.7.

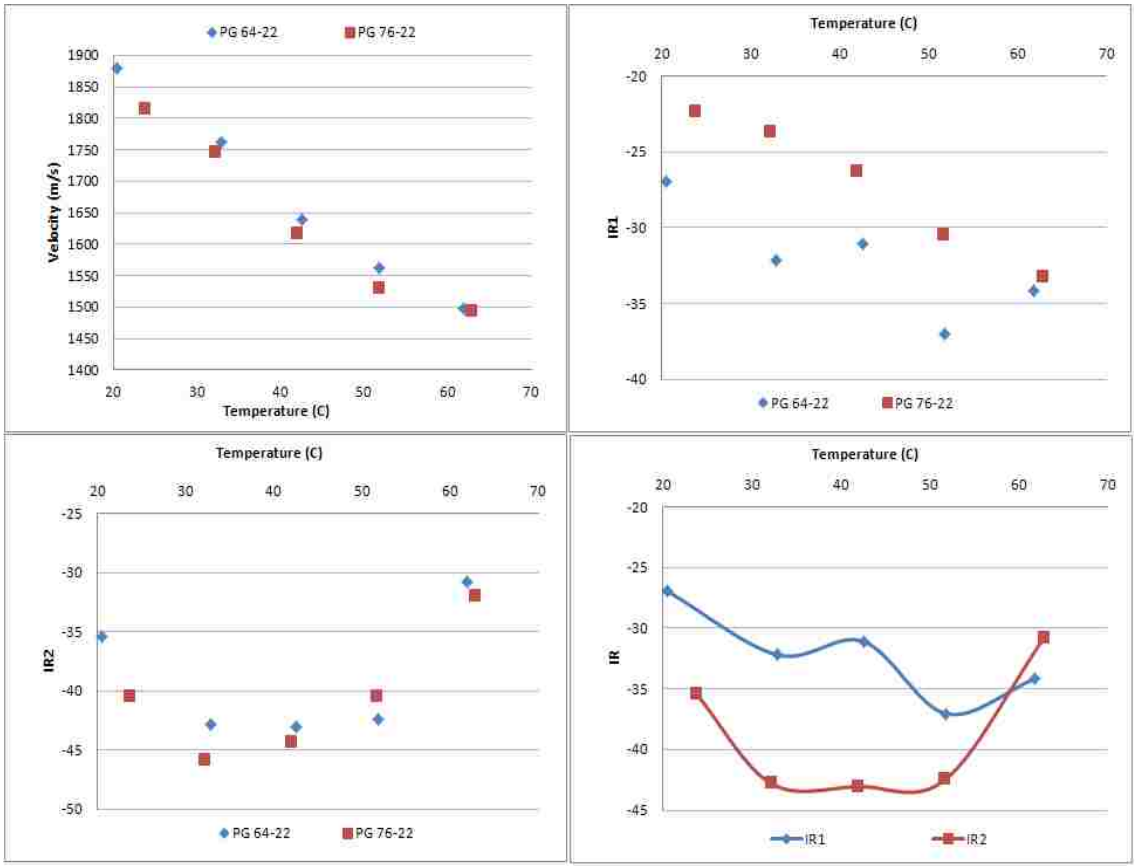

Figure 5-13 Variation of Velocity and IR with Temperature

5.4.1 One-way ANOVA on data from Approach 4

Analysis of variance for this measurements shows better results than the Approach 3 (using contact transducer).

Table 5-4One-way ANOVA on Data from Approach 4

		24 C	30 C	40 C	50 C	60 C
Velocity	p-value	0.000	0.010	0.000	0.000	0.542
	Significantly different?	YES	YES	YES	YES	NO
IR1	p-value	0.000	0.000	0.000	0.000	0.553
	Significantly different?	YES	YES	YES	YES	NO
IR2	p-value	0.000	0.000	0.000	0.000	0.007
	Significantly different?	YES	YES	YES	YES	YES

5.5 Selection of the Best Method

All measurements showed decrease in velocity and IR from reflection from surface with increase in temperature. Variation of the velocity with temperature using the immersion transducer is very close to a linear relationship. Integrated response from reflection from bottom of sample showed a minimum point for all asphalt binders, which needs further investigation to find its reason. Pulse/receive measurement at room temperature can distinguish between two grades asphalt binders that are 2 increments away from each other (PG64-10 and PG76-16). Pulse/echo measurement using contact transducer at room temperature cannot distinguish between asphalt binders. Increasing the temperature of samples does not help to relieve the difference between measurements. However, pulse/echo measurement using immersion transducer showed better results. The Approach 4 relieved better results compared to 2 and 3 and it is selected for main measurements of this research.

5.6 Selection of the Optimum Sample Thickness

Immersion transducer used in the Approach 4 was a high frequency (around 1 MHz) transducer. This resulted in a week response from the bottom of the samples when 1.5 inches deep cups were used to hold the asphalt sample (Figure 5-14). A shallower cup was needed to get a better response (maximum energy gain) from the surface as well as the bottom of the sample. Cups with different depths were made and tested to find the optimum depth (sample thickness).

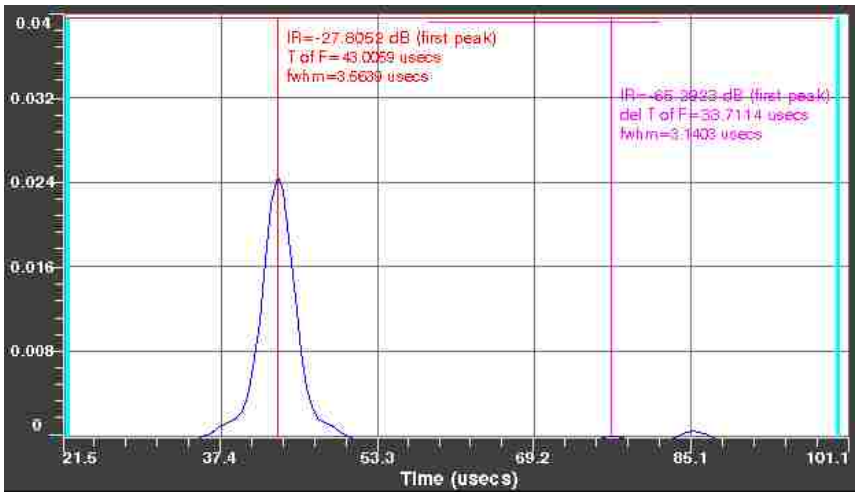

Figure 5-14 Week Response (Short Hump) from the Bottom of the Sample

Four tin cups with different depths, ¾ “, 1”, 1¼“, and 1½”, were made and filled with asphalt binder to the top (Figure 5-15). Samples were tested for the ultrasound response from the surface and bottom at room temperature.

Figure 5-15 Samples with Different Thicknesses Tested to Obtained the Minimum Thickness

Results revealed that a thickness between ¾ “and 1” would give the best response from the surface and bottom of the sample. Tin cups with depth of 0.8 inch (20.3 mm) were selected and used for the main body of the research.

5.7 Asphalt Binder Grade Selection

In the selection of the asphalt binder the researchers started with the grades used in Nevada. PG76-22 and PG64-28 are two main grades that are used in Southern and Northern Nevada, respectively. Both grades are modified due to the high and low temperature grades. Two types of modifiers common in Nevada are SBS polymer and crumb tire rubber. Asphalt binders modified with the SBS have "NV" at the end of the grade name and asphalt binders modified with the crumb tire rubber have "TR" at the end of the grade name. PG64-28NV, PG64-28TR, PG76-22NV, and PG76-22NV, all from one source, were the first four grades obtained for this research. Having both SBS modified and tire rubber modified might result in observing the differences in ultrasound responses. PG76-22 produced by a different source was also used. To avoid confusion, from now on this grade is noted as PG 76-22E. Next selected grade was PG64-22 which is also produced and used in the middle part of Nevada. This grade is usually not modified but some suppliers may produce modified PG64-22.

Other selected grades are used in California. PG64-10, PG76-10, and PG64-16 are used on the South Coast, Central Coast and Northern Coast of California, respectively. None of these grades are modified. PG64-10 and PG64-16 as well as PG64-22 are suitable grades to make comparisons with PG64-28. PG76-10 is a suitable grade to make comparisons with PG76-22. Table 5-5 summarizes all nine selected grades and the reason for their selection.

Table 5-5Selected Grades for the Main Research

Selected Grade	Reason of Selection
PG64-28NV	Used in Northern Nevada
PG64-28TR	Compare with PG64-28NV respect to ultrasound response
PG76-22NV	Used in Southern Nevada
PG76-22TR	Compare with PG76-22NV respect to ultrasound response
PG64-22	Compare with PG64-28 respect to ultrasound response
PG76-22E	Compare different sources
PG64-10	Compare with PG64-28 respect to ultrasound response
PG76-10	Compare with PG76-22 respect to ultrasound response
PG64-16	Compare with PG64-28 respect to ultrasound response

All these grades were ordered from the sources by the researches and were tested according to the descriptions in Chapter 6.

5.8 Samples

Asphalt binder sample for the ultrasound measurements were cast in the tin cups. Dimensions of the cups according to Section 5.7 were depth = 20.3mm and diameter = 60mm. Asphalt binder was heated in the oven to the temperature close to mixing temperature of asphalt concrete (around 163 ˚C) and then poured in to the cup.

Thickness of the material has a major effect on the results of velocity measurement in ultrasound. For example, in asphalt binder samples in cups with depth of 20.3mm and diameter of approximately 60mm, 1 mm difference in the assumed thickness of the material may lead to 5% error in the calculated velocity of the material. Therefore, the cups should be filled with the asphalt binder in a way that there is maximum confidence in the thickness of the asphalt binder. To assure that, the first method used was filling the cup to its inside marked line. The mark was made through an accurate measurement with a caliper. The defect of this method occurred when the ultrasound measurements were performed at high temperature. Due to the softness of the asphalt binder at high temperature (higher that 45-50 ˚C) and high surface tension between asphalt and tin, a

concave surface was formed on asphalt sample (Figure 5-16). This had unwanted effects on the measured parameters.

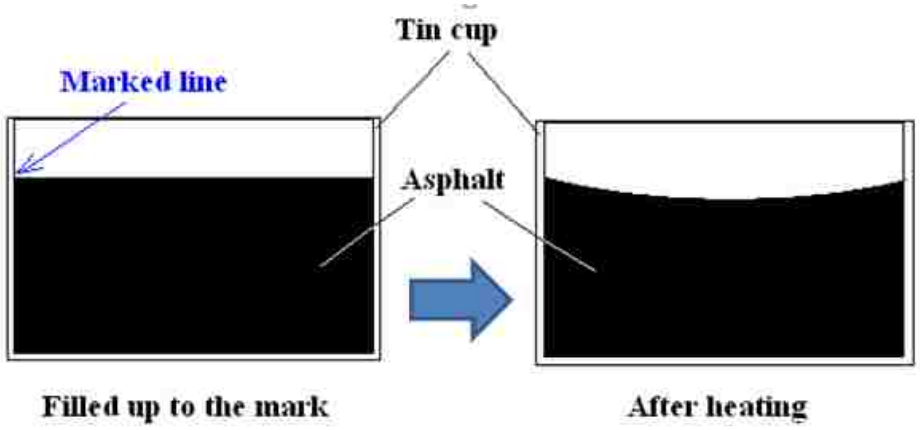

Figure 5-16Concave Surface Due to Heating

The second method was to fill the cup with the asphalt binder to the top. Therefore, the thickness of the asphalt binder is equal to the depth of the cup. For the early measurement (in approaches of the methodology section) the method that was used was making a temporary aluminum collar at the top of the cup and then flush trimming the extra from top of the cup with a hot knife (Figure 6-17). This method was untidy and the final surface of the sample was not smooth enough. Unsmooth surface had unwanted effects on the measured parameters, especially on IR_1 (Integrated Response of the sound wave reflection from the surface of the material).

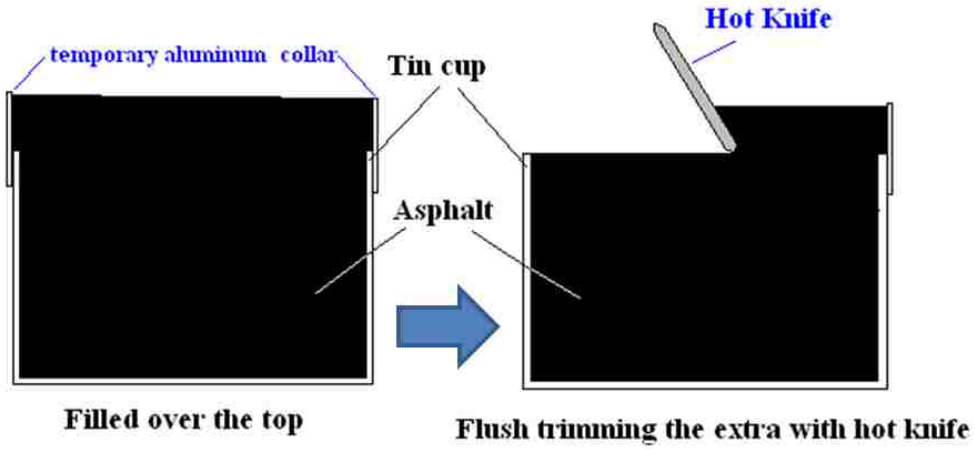

Figure 5-17 Flush Trimming Method

After a discussion with asphalt lab technicians, the method of measured mass was tried. At the time of pouring the asphalt into the cup, asphalt is hot and liquid with a lower density (higher volume) compared to room temperature. So the mass of the asphalt that makes a full cup (volume of asphalt is exactly equal to the volume that the cup can hold) has higher volume than the cup can hold. Thanks to the surface tension between asphalt binder's molecules this amount of mass does not over flow from top of the cup at high temperature of pouring (Figure 5-18). In a trial and error process the amount of asphalt that would fill to the top the cup was obtained. This amount for a cup with inside diameter of 60mm and depth of 20.3 mm was equal to 63 grams.

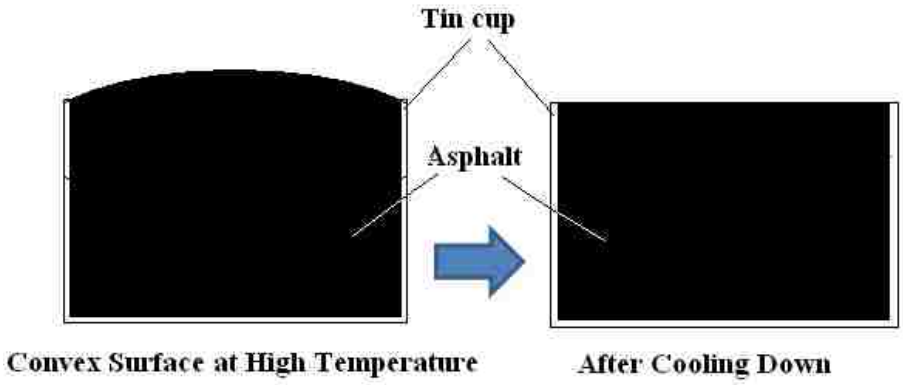

Figure 5-18 Using Surface Tension to Fill a Full Cup

From each asphalt binder grade, 5 replicates were made from original as well as RTFO-aged and PAV-aged asphalt binder. Total of 135 samples were fabricated and ultrasound parameters were measured at five different temperatures.

5.9 Bubbles in the Hot Water

In the early measurements, deionized water was used in the water bath of the immersion ultrasound. The advantages of the deionized water were availability in the lab and also the fact that the density and velocity of the deionized water are much closed to distilled water and could be found in the literature. The only disadvantage was the bubbles that formed in the water at high temperature. Because the asphalt binder is soft at high temperature (higher that 45-50 $^{\circ}$C), when the bubbles form on the surface of the sample they make rough (unsmooth) surface (Figure 5-19). As it was mentioned before, unsmooth surface has unwanted effect on the measured parameters, especially on IR_1. To overcome this defect deionized water was replaced by distilled water. The dissolved air is removed, to some extent, in the process of making the distilled water. To make sure the amount of dissolved air is reduced to the minimum amount the distilled water in the water bath was heated up once to 70°C (maximum temperature of the measurements) over night and then cooled down in the room temperature. This process reduced the bubbles formed on the surface of the samples to almost no bubbles (Figure 5-20).

Figure 5-19 Unsmooth Surface Made by Dissolved Air Bubbles in Water

Figure 5-20 Reduction in the Amount of Bubbles after Using Distilled Water

6. CHAPTER 6 :DISCRIPTION OF THE DATA ACQUIRED

This chapter includes a description of the data acquired during two phases. In the first phase the mechanical testing was performed on the selected asphalt binders to a) verify their grades based on SUPERPAVE grading system and b) obtain rheological properties of asphalt binder for examining the possible correlation with ultrasound measurements data. In the second phase ultrasound measurements, according to the selected method in chapter 5, were performed on the selected asphalt binders.

6.1 Phase I; Mechanical Tests

In the first phase some of the mechanical tests, which are done to verify the grade of the asphalt binder in SUPERPAVE system, were performed on the selected asphalt binders.

6.1.1 The DSR and BBR

The DSR tests on original and RTFO-aged samples were performed and shear modulus as well as phase angle were measured. Three replicate samples, from each grade, were made and tested with the DSR. The average of three samples was calculated and used for the data analysis. If the measured parameter ($G^*/\sin\delta$) was not repeatable more replicates would be tested and the data point(s) of the range would be eliminated. Repeatability according to ASTM for original samples means the all the measurements are in the range of (average ± 6% of the average), and for RTFO-ages samples in the range of (average ± 9% of the average). DSR test was also performed on PAV-aged samples and $G^*\times\sin\delta$ was measured. In order to check for repeatability for PAV-aged samples all the measurements should be in the range of (average ± 11% of the average).

The BBR tests on PAV-aged samples were performed and stiffness as well as m-values was measured. Two replicate samples were made and tested with the BBR. The average of three samples was calculated and used for the data analysis.

Table 6-1 shows the results of the average of replicates for the DSR, BBR and ductility tests on the selected performance grade asphalt binders. As you can see all asphalt binders were "passed" in the verification for their grades.

Table 6-1Rheological Properties of Selected Asphalt Binders

	DSR (ORG)	DSR (RTFO)	DSR (PAV)	BBR (PAV)		Ductility at 4◦ C (cm)	
				S at 60 s (MPa)	m-value at 60 s		
Grade	G*/sinδ(kPa	G*/sinδ(kPa	G*×sinδ(kPa			ORG	RTFO
PG64-28NV	1.50	3.39	1571	133	0.335	78.5	41.1
PG64-28TR	1.42	2.68	1783	170	0.338	66.6	36.2
PG76-22NV	1.36	1.90	905	116	0.342	54.4	22.3
PG76-22TR	1.42	2.46	732	98	0.373	31.8	22.1
PG64-22	1.13	2.95	3589	182	0.323	18.4	5.3
PG76-22E	1.37	2.62	610	71	0.364	39.6	23.8
PG64-10	1.65	4.43	4257	55	0.418	6.5	0.4
PG64-16	1.37	3.60	4332	102	0.380	10.9	4.3
PG76-10	1.01	2.39	2148	87	0.352	0.3	0.6
Specs.	**>1.00**	**>2.20***	**<5000**	**<300**	**>0.300**	**	**

* NDOTaltered this to (>1.80) for PG 76-*
** According to Table 4-2

Descriptive data from mechanical tests is presented in Appendix A of this dissertation. In those tables the elastic portion (G') and viscous portion (G'') of the complex modulus (Figure 4-5) have also been calculated and presented. They were used in the check for possible correlation with ultrasound measured data.

6.1.2 Ductility

As it was mentioned in Chapter 4 according to NDOT specifications the low temperature ductility test is performed as a direct tension test for low temperature performance of asphalt binders. From each grade three replicate samples were made and tested for ductility. Figure 6-1 shows the average of the result of ductility test on three

replicates for the selected grades. As expected modified asphalt binders showed higher ductility at low temperature.

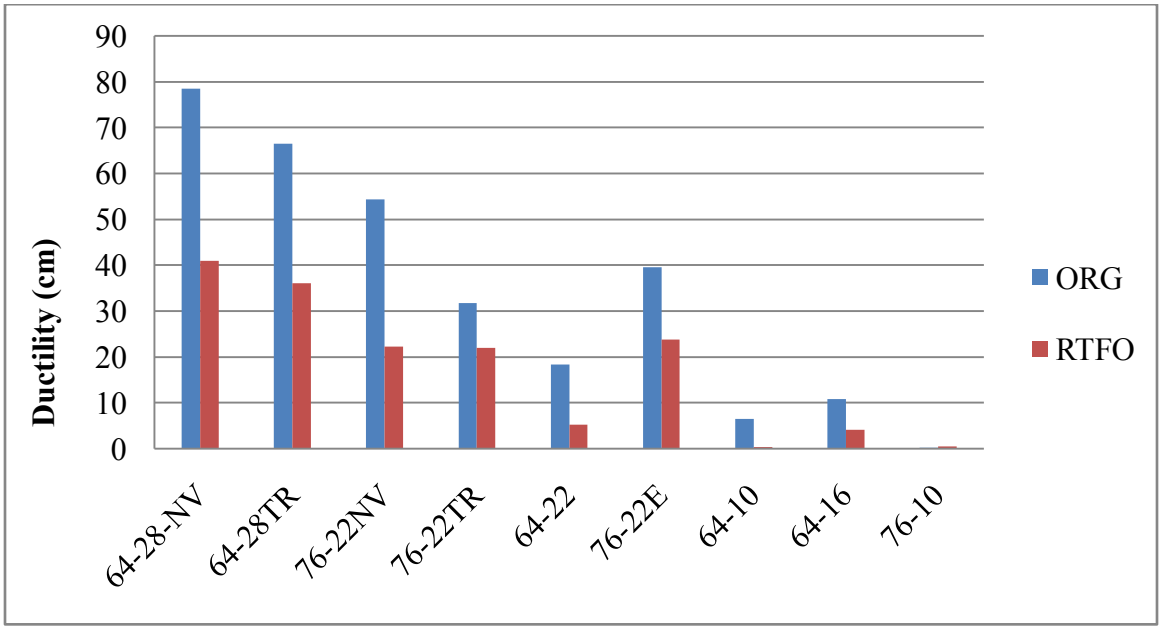

Figure 6-1 Results of the Ductility Test

Three major types of failure were observed in the ductility test. Type 1, which occurred in the modified asphalt binders, was a ductile failure after a relatively long elongation (Figure 6-2). Type 2, which occurred in PG64-22 and PG64-16, was a ductile failure after a relatively short elongation (Figure 6-3). Type 3, which occurred in PG64-10 and PG76-10, was a brittle failure after seconds of applying the strain (Figure 6-4).

Figure 6-2 Type 1 Failure in the Ductility Test

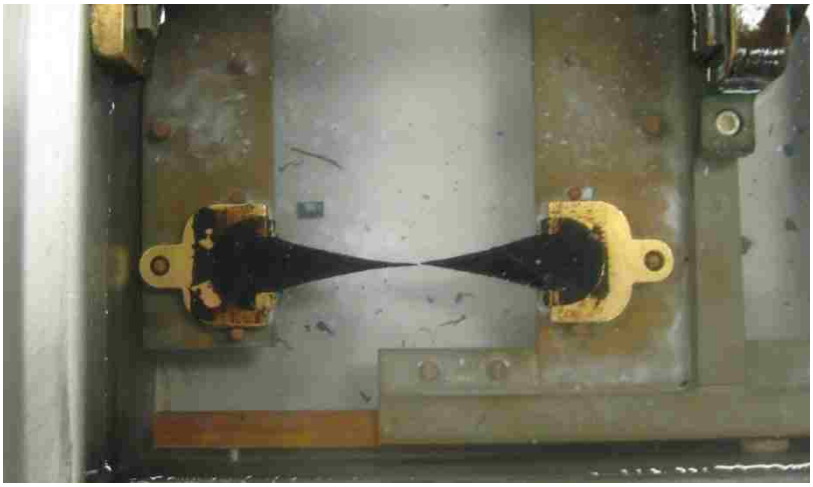

Figure 6-3 Type 2 Failure in the Ductility Test

Figure 6-4 Type 3 Failure in the Ductility Test

6.1.3 Phase II; Ultrasound Measurements

Ultrasound parameters were measured in selected asphalt binder grades in an immersion test according to the Approach 4 presented in section 5.4. As it was shown in the Approach 4, room temperature is not a reliable temperature for ambient conditions because it changes seasonally and even weekly. For the ultrasound measurements on the selected grades room temperature was eliminated and 70°C was added to the temperatures.

In the process of the recording of the ultrasound data in the Approach 4 it was observed that the Amplitude of the reflected sound wave from surface and bottom of the sample changed between grades and also between temperatures. This encouraged the researchers to record these two Amplitudes as well as velocity and IR. It could be a suitable parameter to distinguish between different grades. Amplitude of the surface reflection and bottom reflection were noted as A_1 and A_2, respectively.

6.1.4 Extra Asphalt Binder Grades

To expand the data base of the ultrasound measurement researchers decided to collect more asphalt binder grades. Four more PG asphalt binders were obtained from NDOT Material Division Lab in Las Vegas. These are left over from their performance grade verification tests. Table 6-2 shows the results of the grade verification on the mentioned asphalt binders.

Table 6-2 Rheological Properties of Added Asphalt Binders

	DSR (ORG)	DSR (RTFO)	DSR (PAV)	BBR (PAV)	
				S at 60 s (Mpa)	m-value at 60 s
Grade	G*/sinδ(kPa)	G*/sinδ(kPa)	G*×sinδ(kPa)		
PG58-28	1.08	2.67	3890	237	0.323
PG70-28	1.97	3.95	1770	180	0.326
PG 76-28	1.15	2.91	1800	205	0.310
PG 58-34	1.24	2.55	2210	211	0.321
Specs.	**>1.00**	**>2.20***	**<5000**	**<300**	**>0.300**

Since a little amount of these asphalt binders was left, 3 replicate samples only from the original binder could be made out of them for ultrasound measurements.

6.1.5 Measured Parameters

Time of flight and IR corresponding to each received pulse by the transducer are given in the GUI of the ultrasound system (Figure 3-29). These four parameters (Tof_1, IR_1, Tof_2, and IR_2) were measured 10 times for each sample and recorded using the GUI.

The average of 10 measurements was calculated later. Amplitudes for each received wave, however, were observed and recorded manually. Using Equation 29, velocity of the asphalt sample was calculated and recorded.

According to Equation 30, the IR_1 (integrated response from the surface of the sample) is a function of reflection coefficient of the sound wave when it reflects at the interface of water and asphalt. Reflection coefficient itself is a function of acoustic impedance of water and asphalt, according to Equation 23. And finally, according to Equation 22, acoustic impedance of each material is the production of its density and velocity. Combining the three equations will result in Equation 32;

$$IR_1 = 20\log R_{W/A} = 20\log\left[\frac{Z_A - Z_W}{Z_A + Z_W}\right]^2 = 20\log\left[\frac{\rho_A V_A - \rho_W V_W}{\rho_A V_A + \rho_W V_W}\right]^2 \quad [32]$$

This equation is used when the variation of IR_1 with temperature is discussed in Chapter 7. Figure 6-5 illustrates the pulse waves involved in the immersion ultrasound used for this research.

According to Equation 31, the IR_2 (integrated response from the bottom of the sample) is a function of transmission coefficient of the sound wave when it passes through the interface of water and asphalt.Transmission coefficient itself is a function of acoustic impedance of water and asphalt, according to Equation 24. And finally according to Equation 22, acoustic impendence of each material is the production of its density and velocity. Combining the three equations will result in Equation 33;

$$IR_2 = 20\log T_{A/W} = 20\log\left(\left[\frac{4Z_A Z_W}{(Z_A + Z_W)^2}\right]^2\left[\frac{Z_T - Z_A}{Z_T + Z_A}\right]^2\right) \quad [33]$$

where

Z_T = acoustic impedances of tin

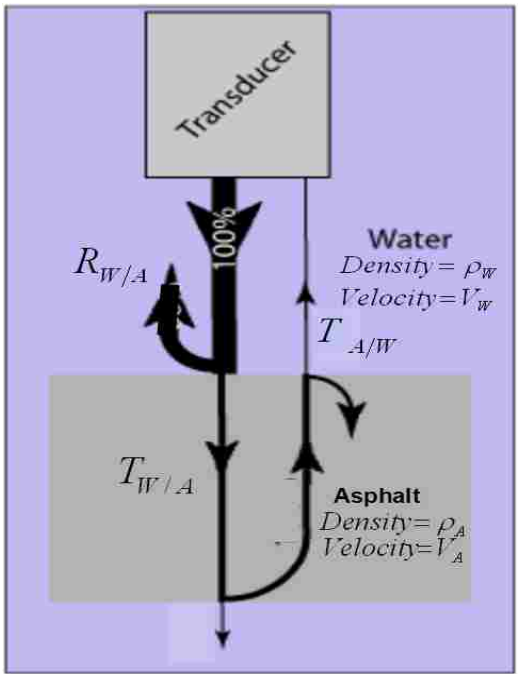

Figure 6-5 Pulse Waves Involved in the Immersion Ultrasound

Values of the measured parameters in this phase are presented in tables in Appendix B of this dissertation.

7. CHAPTER 7 :ANALYSIS OF RESULTS AND DISCUSSIONS

This chapter includes the analysis of the data presented in Chapter 6. The analysis is divided into three major categories. In the first category the variation of the ultrasound measurements with temperature was discussed. In the second category correlations between the results of the ultrasound measurements (ultrasound properties) and the results of the mechanical tests (rheological properties) on the asphalt binder were developed. In the third category the Discriminant Faction Analysis was used to predict the performance grade of the asphalt binders using the data of ultrasound measurements.

7.1 Variation of the Ultrasound Parameters with Temperature

Variation of the Velocity, IR_1 and IR_2 with changes in testing temperature is studied in this section.

7.1.1 Variation of Ultrasound Velocity with Temperature

General Trend

Molecules at higher temperatures have more energy, thus they can vibrate faster. Since the molecules vibrate faster, sound waves can travel more quickly. So, the speed of sound wave in solids and liquids increases with increase in temperature of the material body. Speed of sound in solids is generally higher than liquids because the molecules are closer together and more tightly bonded in solids. Asphalt binder is a material that transforms from solid state to liquid state in a relatively short range of temperature. At 30°C which is close to room temperature asphalt binder is solid with high velocity. When temperature increases, its state changes from solid to semi-solid and liquid which shows a lower ultrasound velocity.

Graphs of variation of ultrasound velocity with temperature for the selected grades are presented in Appendix C of this dissertation. Following is the discussion on the plot for only one grade.

Figure 7-1 shows the variation of ultrasound velocity versus temperature for original, RTFO-aged, and PAV-aged PG76-22NV. All the data points presented in this chapter are the average of five samples. Ultrasound velocity decreases with increasing temperature, as expected.

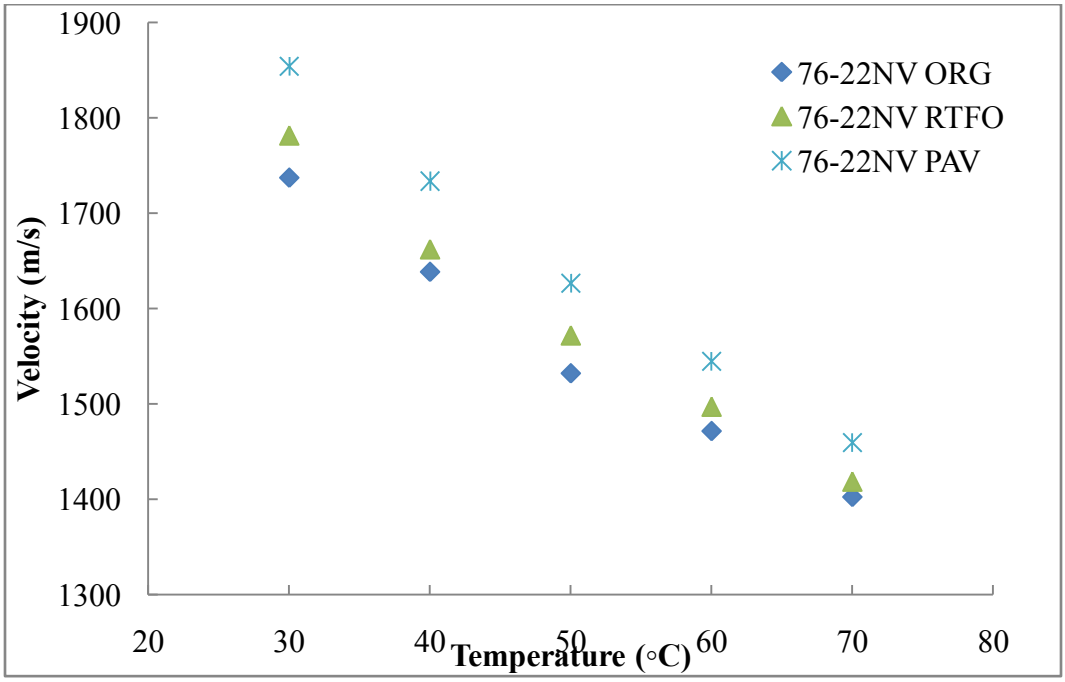

Figure 7-1Variation of Velocity with Temperature for PG76-22NV

Aged versus Un-aged Asphalt Binder

It was also observed that the aged asphalt binder has higher velocity compared un-aged. This confirms the fact that during the aging process the lighter, oily constituents of asphalt binder either evaporate or oxidize to the heavier, solid constituent like resins and asphaltenes. This change in velocity is more severe in transition from "RTFO to PAV" than "original to RTFO", because of the longer aging time the higher pressure involved.

Regression

Variation of ultrasound velocity with temperature was fitted in a regression curve (Figure 7-2). Among the possible functions to examine, logarithmic function showed the best fit for variation of Velocity with temperature for all grades.

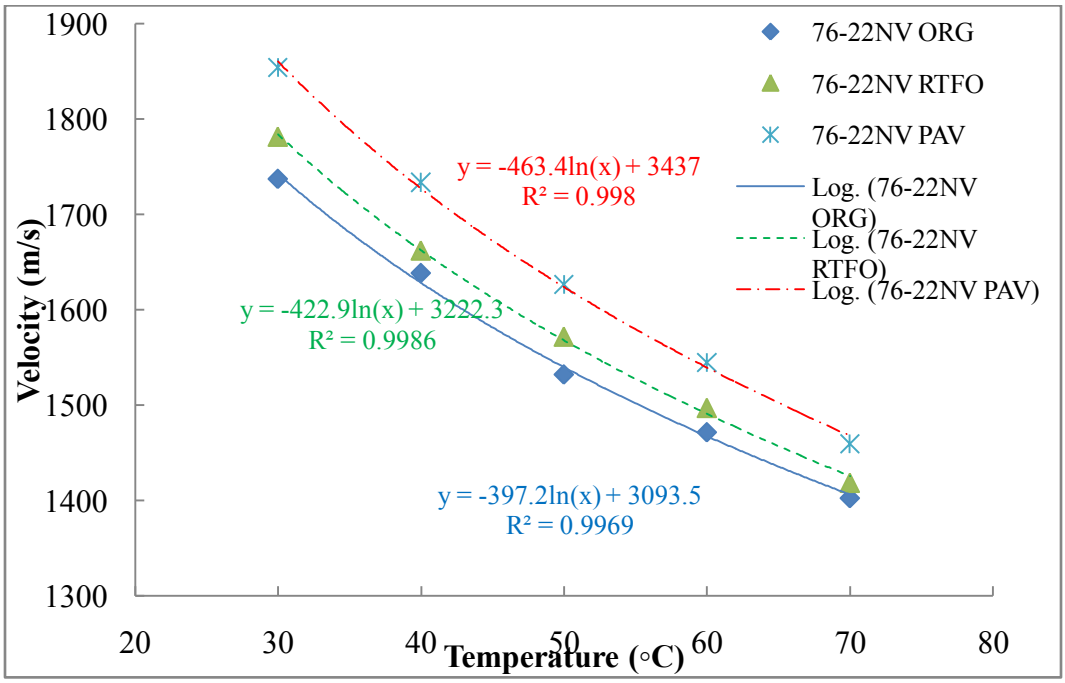

Figure 7-2 Regression Curve for Variation of Velocity with Temperature

Distinguish between Different Grades

To compare different asphalt binders with the same high temperature grades Figures 7-3 and 7-4 are shown. In these Figures variation of velocity with temperature for original asphalt binders is presented. As you can see modified asphalt binders have lower velocity than unmodified asphalt binders. The reason why the modifiers reduce the velocity of the asphalt binder is discussed in section 7.2. Another observation in these plots is that velocity measurements can distinguish between SBS modified and tire rubber modified asphalt binders. In PG64-28 tire rubber modified shows higher velocity than polymer modified while in PG76-22 is vice versa. These differences were only observed

in original asphalt binders. Velocity of the aged samples did not show difference between polymer and tire rubber modified PG76 asphalt binders.

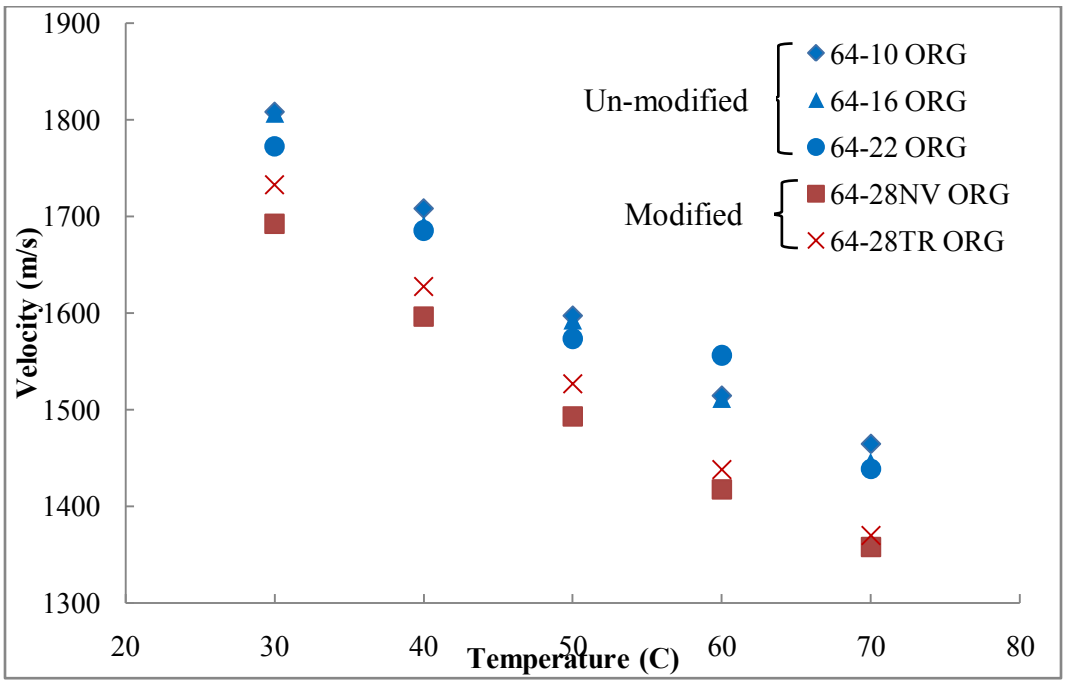

Figure 7-3 Variation of Velocity with Temperature for Original PG64-*

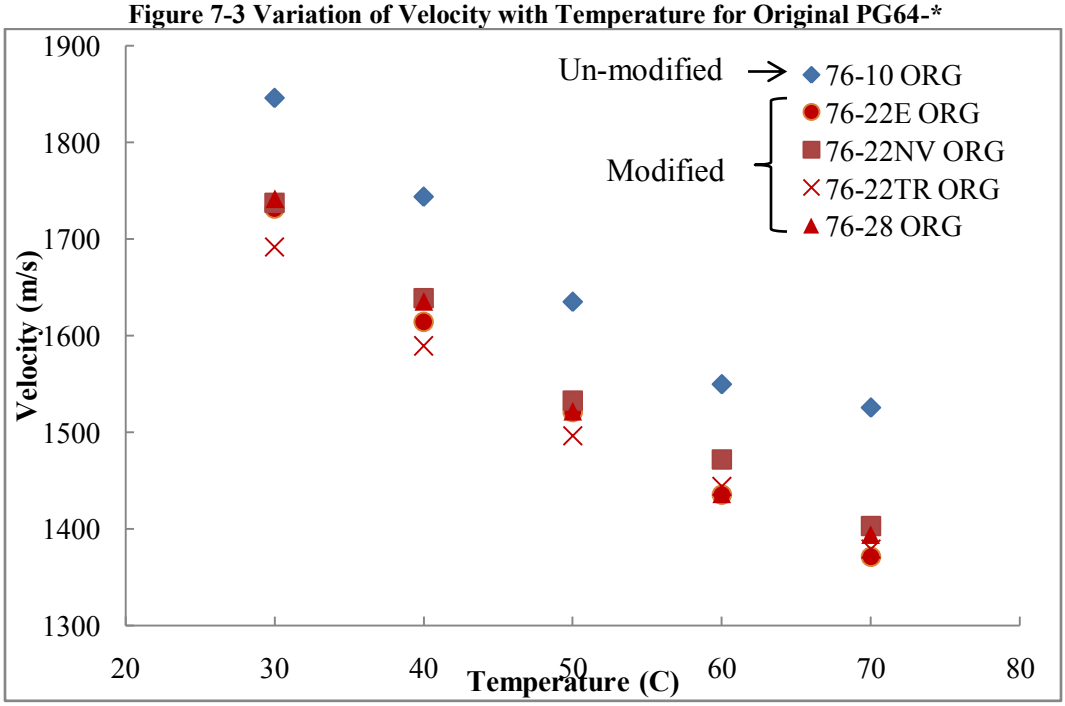

Figure 7-4Variation of Velocity with Temperature for Original PG76-*

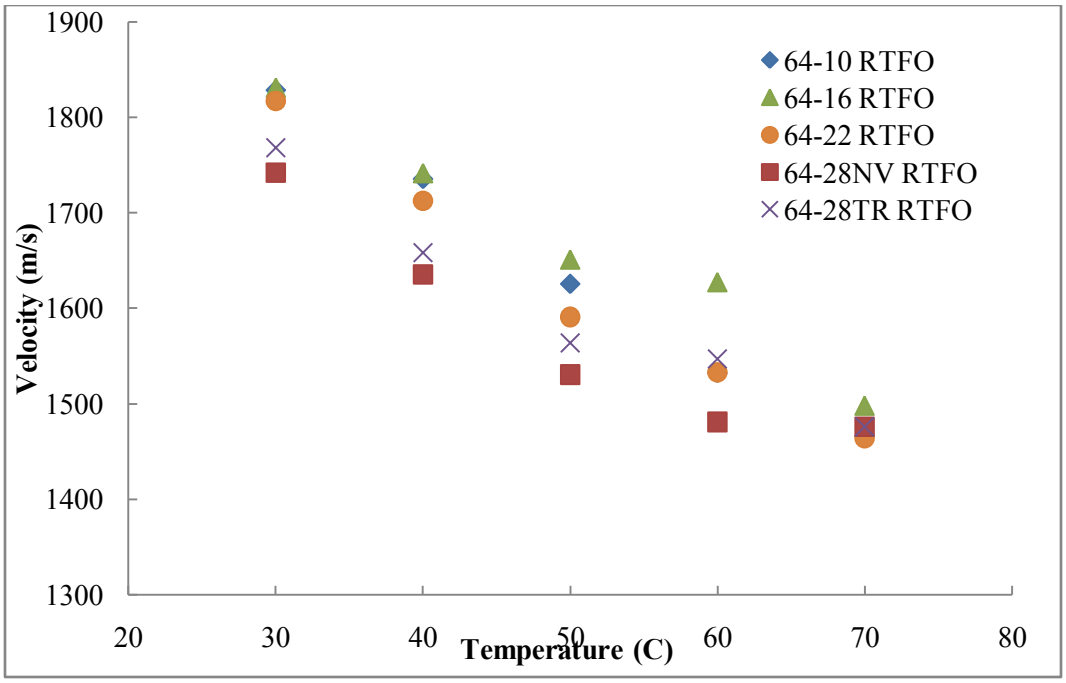

Figure 7-5Variation of Velocity with Temperature for RTFO-aged PG64-*

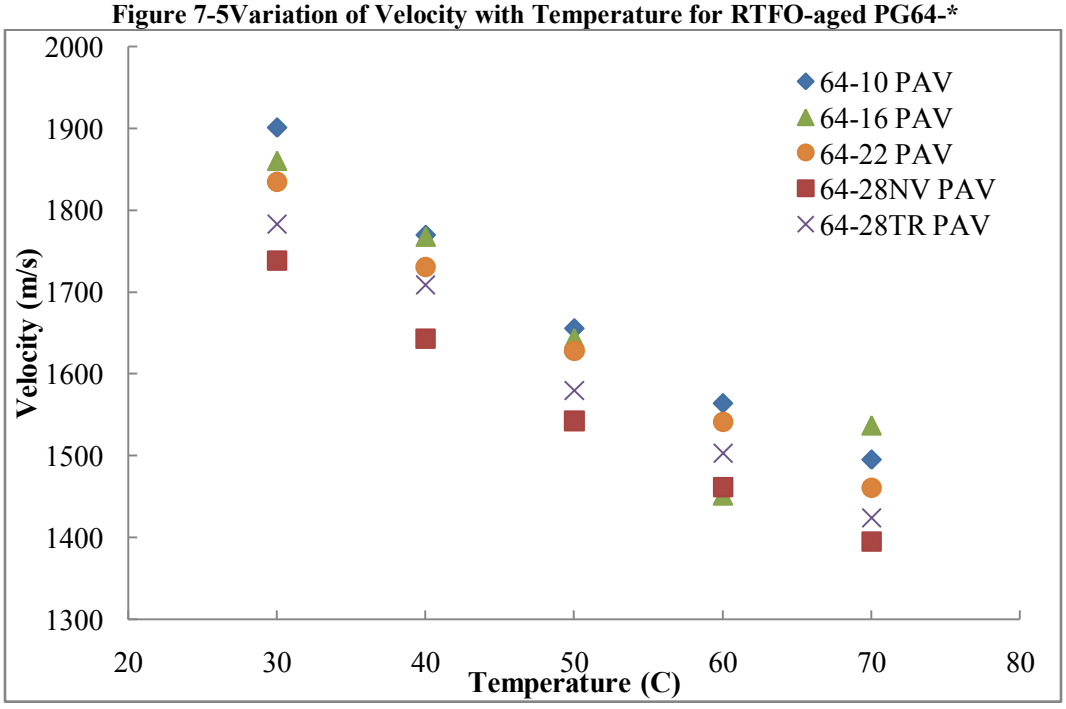

Figure 7-6 Variation of Velocity with Temperature for PAV-aged PG64-*

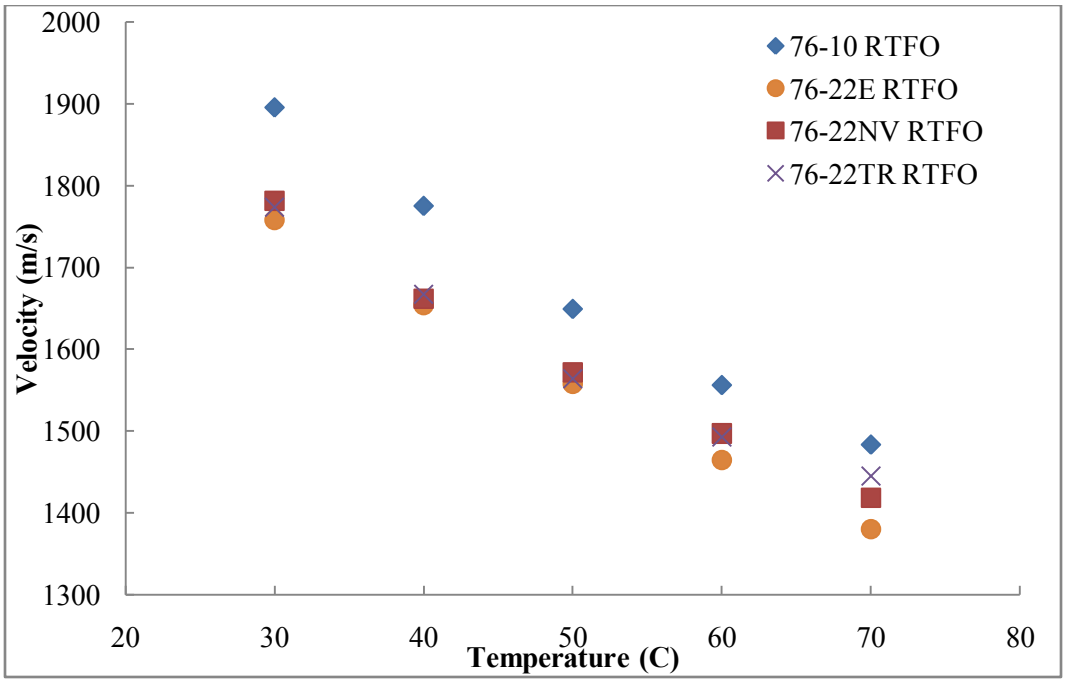

Figure 7-7Variation of Velocity with Temperature for RTFO-aged PG76-*

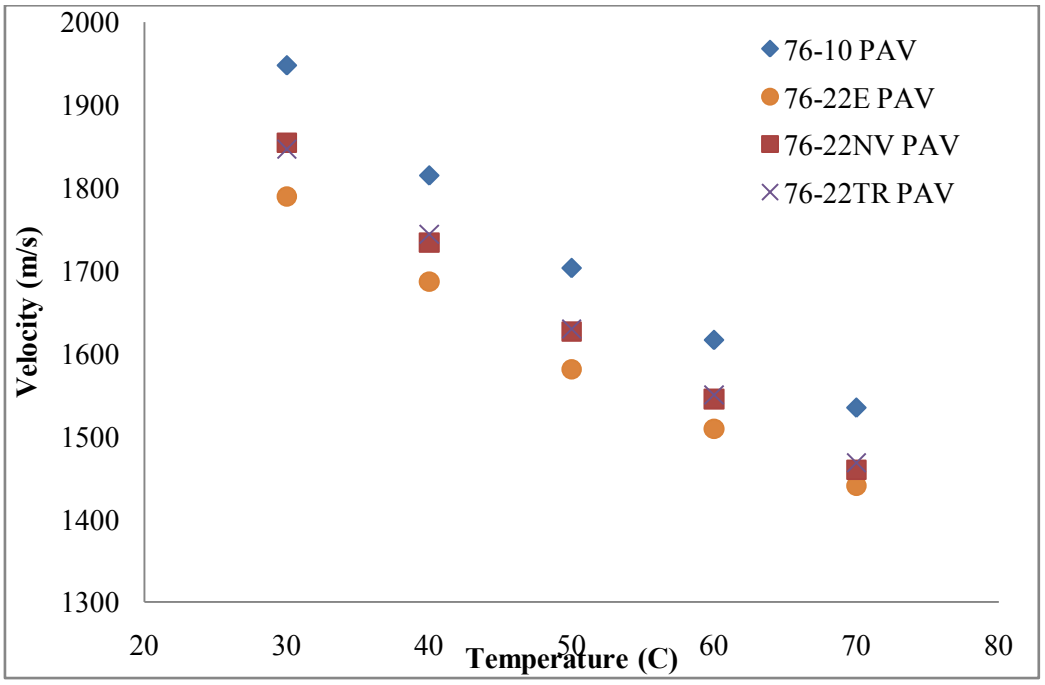

Figure 7-8 Variation of Velocity with Temperature for PAV-aged PG76-*

7.1.2 Variation of IR_1 with Temperature

The IR_1 (integrated response from the surface of the sample) is a function of density and velocity of water and asphalt. When temperature increases, density of the water

decreases and velocity increases, but rate of increase in velocity is higher than decrease in density, so the acoustic impedance increases. In asphalt, however, by increasing the temperature, density in velocity both decrease, so acoustic impedance decreases. There is a point (temperature) at which the acoustic impedance of the asphalt and water are equal. At that temperature reflection coefficient ($[(Z_A - Z_W)/(Z_A + Z_W)]^2$) is zero and integrated response goes to negative infinite ($-\infty$). This point was observed in the variation of IR_1 with temperature. Figure 7-9 shows the variation of IR1 with temperature for original, RTFO-aged, and PAV-aged PG76-22TR. Graphs of variation of IR_1 with temperature for the rest of the selected grades are presented in Appendix C of this dissertation.

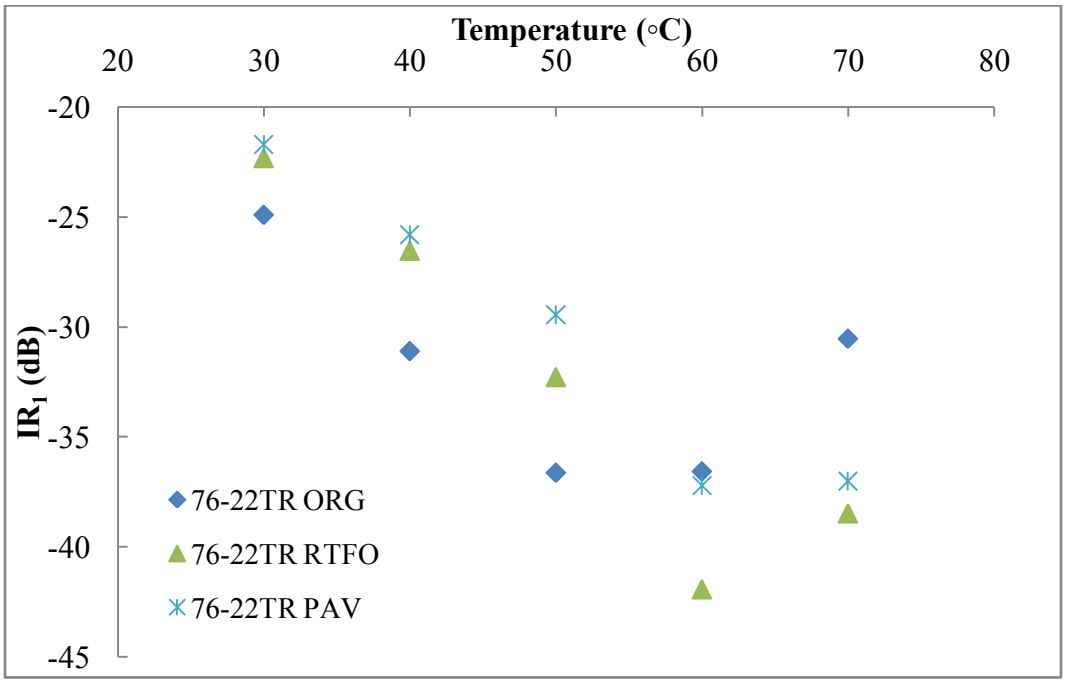

Figure 7-9 Variation of IR_1 with Temperature for PG76-22TR

As it was shown, when temperature increases, IR_1 first decreases and then increases. By fitting a logarithmic curve to the data points, the temperature at which the acoustic impedances are equal can be found (Figure 7-10). As expected the temperature at which

the acoustic impedance of the asphalt binder is equal to the one of water is higher for aged (T^*_{PAV}) than for un-aged (T^*_{ORG}) samples, due to hardening of the asphalt after aging.

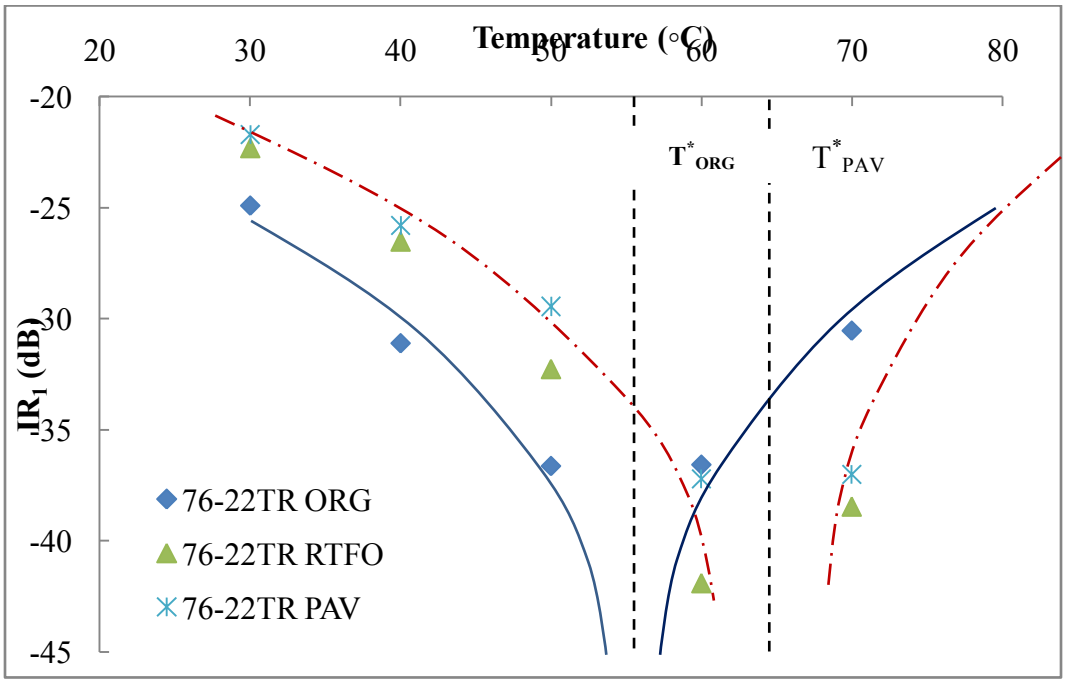

Figure 7-10 Approximate Regression for Variation of IR_1 with Temperature

7.1.3 Variation of $IR_2$with Temperature

According to Equation 33, the IR_2 (integrated response from the bottom of the sample) is a function of density and velocity of water, asphalt, and tin. Tracking the variation on IR_2 with temperature is not as easy as IR_1. However, a general trend of increasing with increase in temperature was observed. Figure 7-11 illustrates the variation of IR_2 with temperature for original, RTFO-aged, and PAV-aged PG76-22NV. Graphs of variation of IR_2 with temperature for the rest of the selected grades are presented in Appendix C of this dissertation.

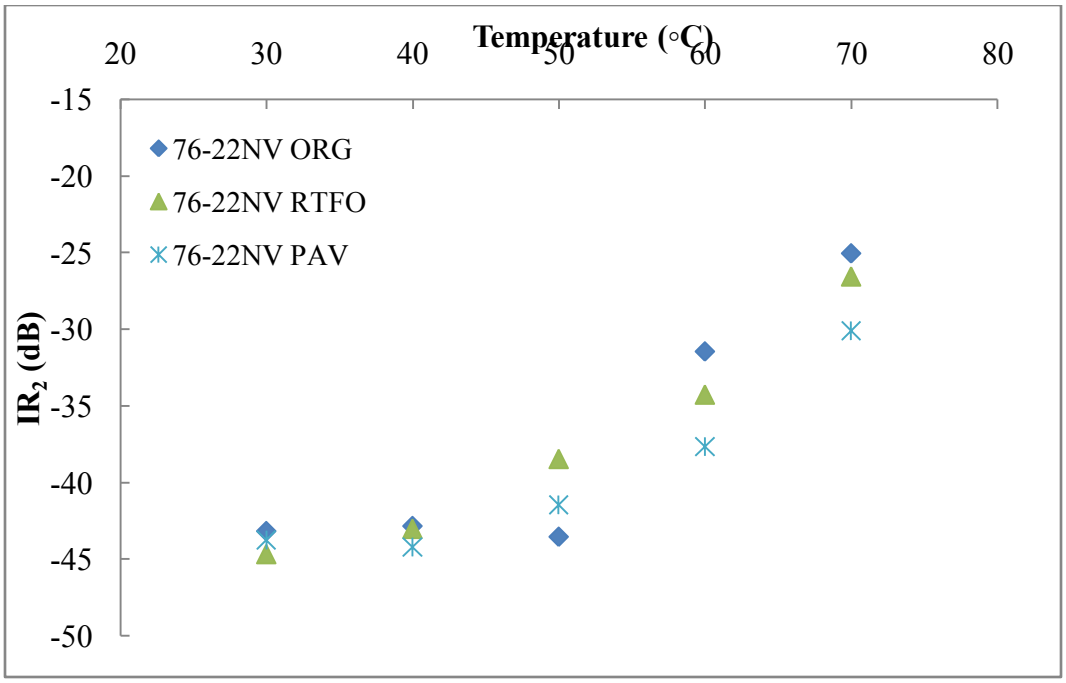

Figure 7-11 Variation of IR_2 with Temperature for 76-22NV

7.2 Correlations

In this section it is tried to form correlations between the rheological properties and ultrasound measured parameters of asphalt binders. Elastic shear modulus from dynamic shear test and stiffness from bending beam test are two mechanical/rheological properties that their variation with Velocity and IR of the ultrasound is studied.

7.2.1 Elastic Shear Modulus of Dynamic Shear

The first possible correlation is between elastic portion of the complex shear modulus and Velocity of the asphalt binders.

Figure 7-12 shows the variation of elastic portion of the complex shear modulus of original samples measured at 64◦C with the Velocity of the same grade measured at different temperatures. As the plot shows, the Velocity is lower for the asphalt binders which have higher elastic portion of the complex shear modulus. In fact, the higher elastic portion of the complex shear modulus was measured in modified asphalt binders.

The Velocity that was measured in this research is the speed of compression sound wave when in passes through the asphalt binder. This velocity has a direct relationship with compression elastic modulus. The first conclusion that could be driven from these plot is that although the used of modifiers in asphalt binders improves the shear behavior, it reduces the compression elastic modulus. There is no mechanical test performed on asphalt binder to measure the compression elastic modulus, but several researches have proofed that the use of polymer and rubber modifiers in Portland cement concrete has reduced the compression elastic modulus (Siringi, 2012) (Reis, 2005). Appendix D contains the results of these researches.

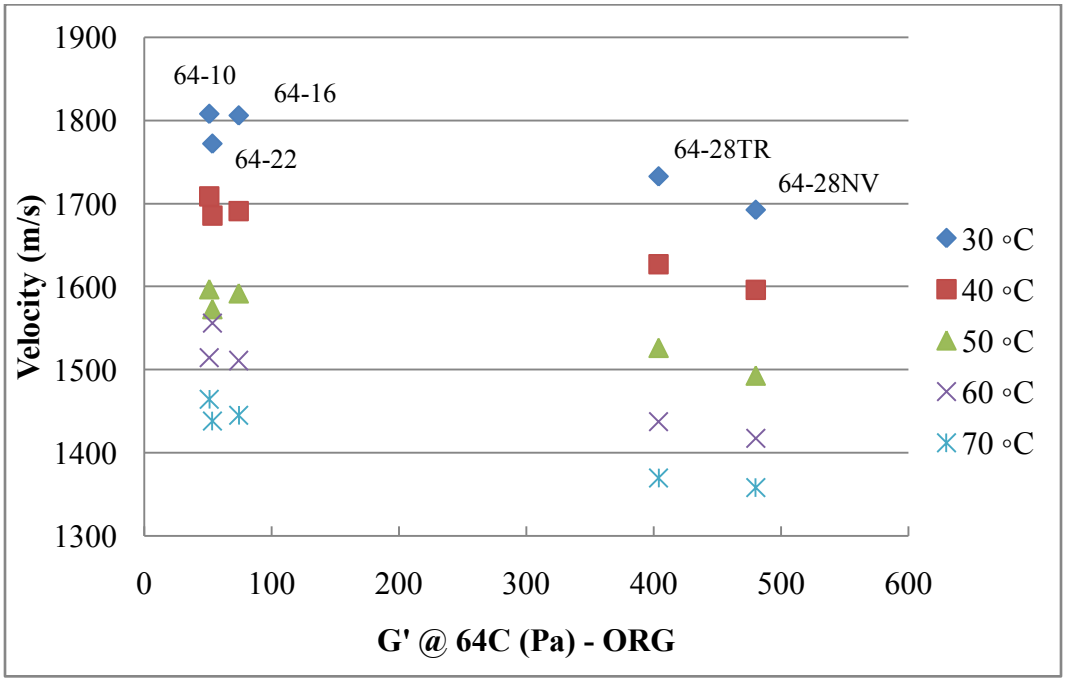

Figure 7-12 Velocity vs. Elastic Shear Modulus at 64◦C for Original

Same behavior was observed in the PG76-* and also RTFO-aged samples (Figures 7-13, 7-14, and 7-15).

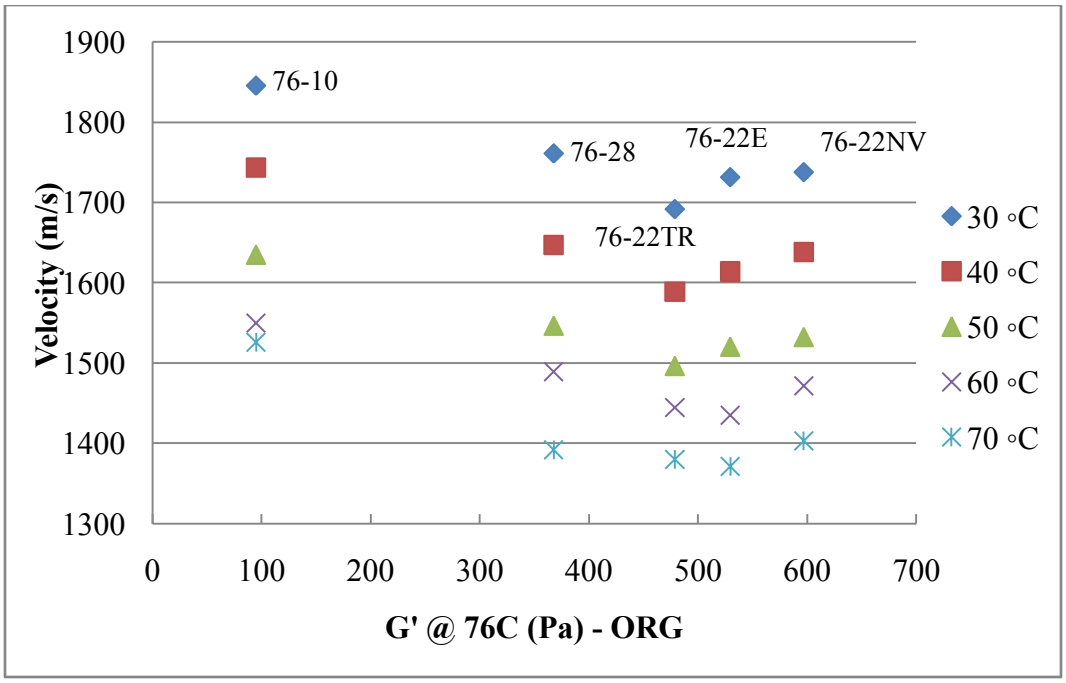

Figure 7-13Velocity vs. Elastic Shear Modulus at 76◦C for Original

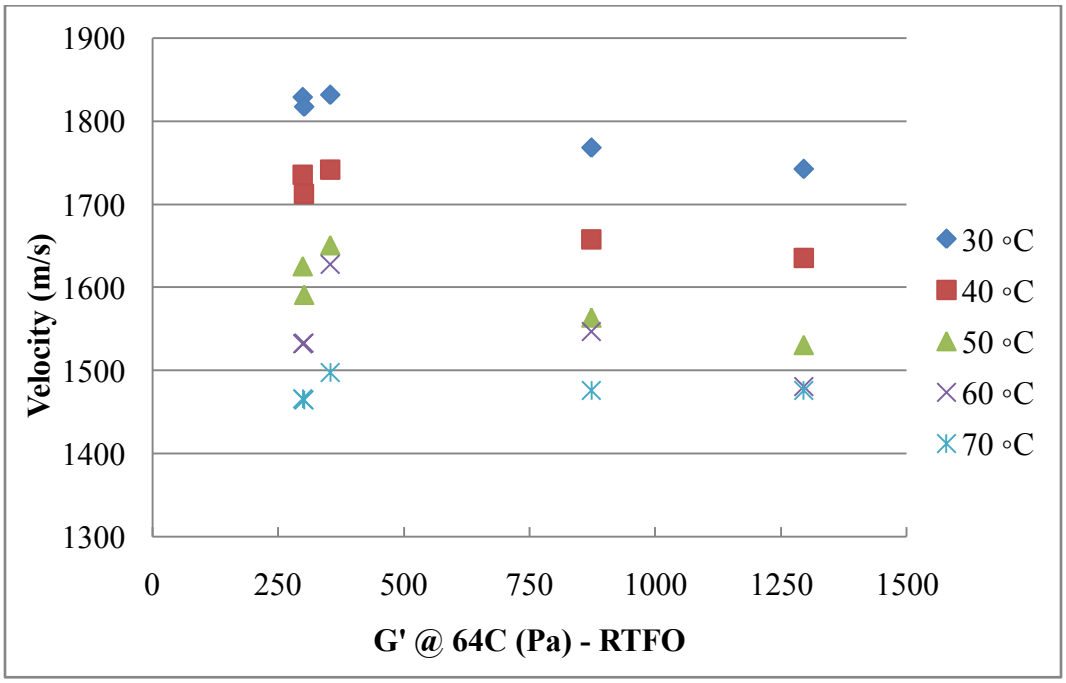

Figure 7-14Velocity vs. Elastic Shear Modulus at 64◦C for RTFO-aged

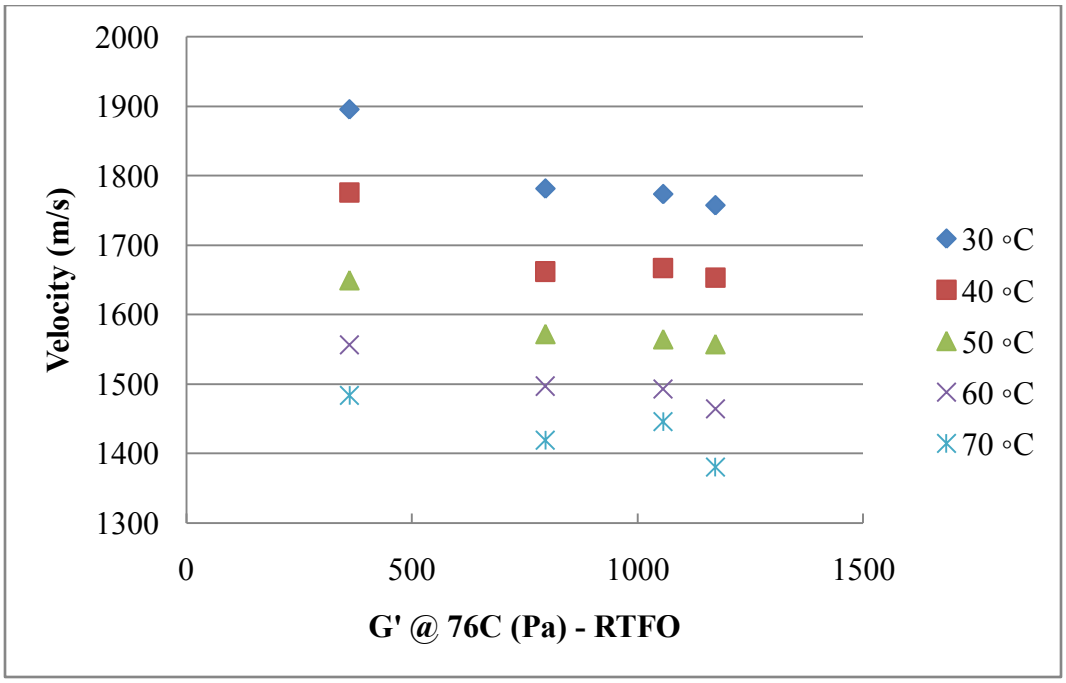

Figure 7-15Velocity vs. Elastic Shear Modulus at 76◦C for RTFO-aged

For complex shear modulus at medium temperature measured on PAV-aged samples a different behavior was observed. Figure 7-16 shows the variation of elastic portion of the complex shear modulus of PAV-ages samples measured at 31◦C with the Velocity of the same grade measured at different temperatures.

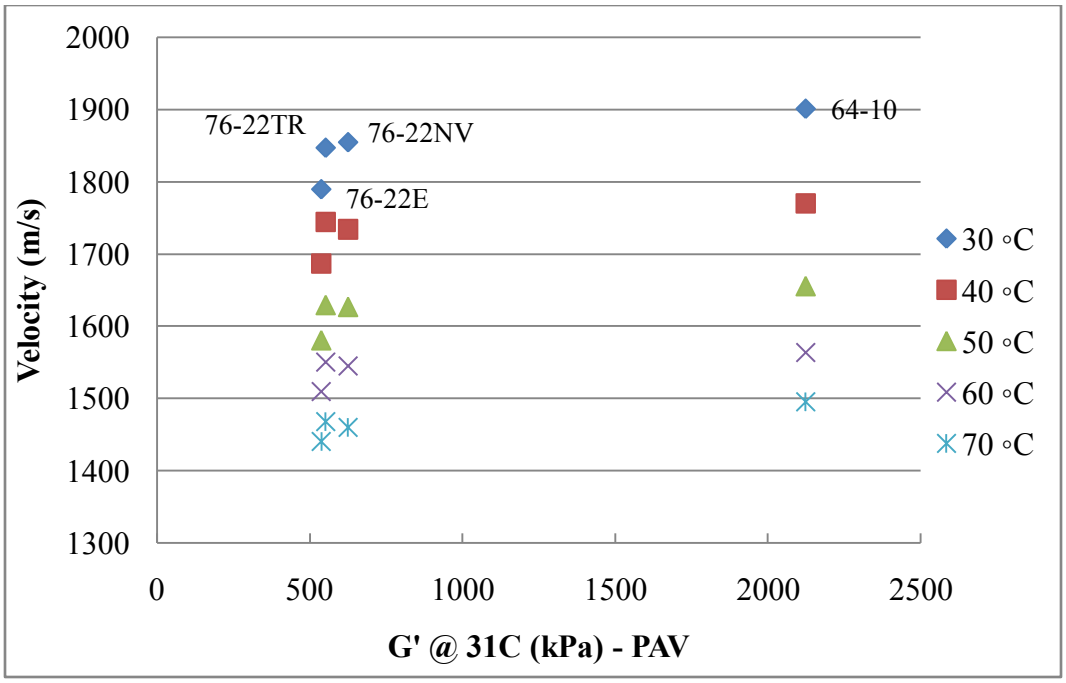

Figure 7-16Velocity vs. Elastic Shear Modulus at 31◦C for PAV-aged

As the plot shows, un-modified asphalt cement which has higher elastic shear modulus at medium temperature happens to have a higher velocity also.

7.2.2 Stiffness of Bending Beam

The variation of Stiffness, measured at low temperature, in asphalt binders with Velocity is studied in section. Figure 7-17 shows the variation of stiffness of PAV-ages samples measured at -12◦C with the Velocity of the same grade measured at different temperatures. Excluding the non-modified asphalt cement (PG64-22) from the plot, increase in stiffness occurs with increase in the Velocity.

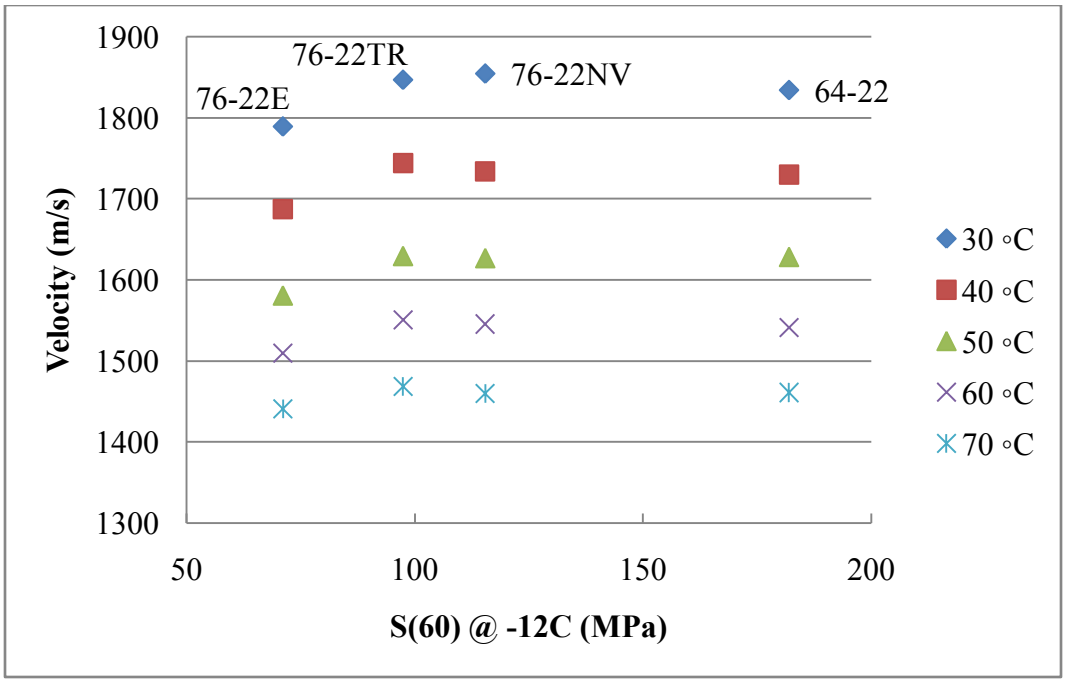

Figure 7-17Velocity vs. Stiffness at -12◦C for PAV-aged

7.3 Discriminant Function Analysis

Discriminant Function Analysis (DA) undertakes the same task as multiple linear regressions by predicting an outcome. The main purpose of a DA is to predict group membership based on a linear combination of the interval variables. The procedure begins with a set of observations where both group membership and the values of the interval variables are known. The end result of the procedure is a model that allows prediction of group membership when only the interval variables are known. A second purpose of discriminant function analysis is an understanding of the data set, as a careful examination of the prediction model that results from the procedure can give insight into the relationship between group membership and the variables used to predict group membership.

The purpose of applying DA for this research is to examine the ability of the ultrasound measured parameters to predict the grade of the asphalt binders. Software "R"

was used for DA in this research. Ultrasound parameters used were velocity, IR_1, IR_2, A_1 and A_2.

As it was shown earlier in this chapter ultrasound parameters vary significantly with temperature. Districting the data of different temperatures would improve the predicting process with DA. Data on aged samples was also significantly different from aged samples. Data from each temperature and each aging state (original, RTFO-aged, and PAV-aged) was categorized in different data sets for DA.

The final outcome of a discriminate function analysis is the probability of predicting the right grade with the developed model. Figure 7-18 shows this number for different aging state and all states combined for different temperatures.

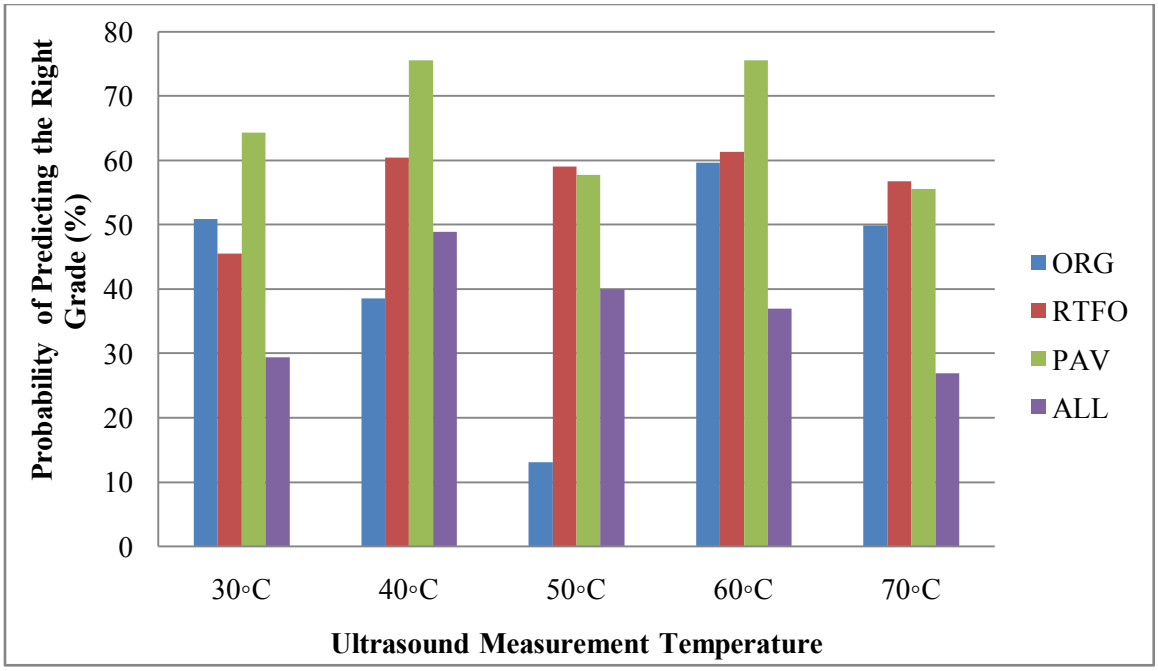

Figure 7-18 Probability of Predicting the Right Grade for Each Data Set

As the bar plot illustrates PAV-aged asphalt binder samples are the best for grade prediction. Temperatures of 40◦C and 60◦C are the best temperatures for that purpose.

7.3.1 Functions

Two data sets which showed higher probability (PAV-aged at 40◦C and 60◦C) were selected as examples for presenting the predictor functions. Two linear functions were produced to predict the grade in a two-dimensional coordinate. Each function is equal to sum of the products of each variable and the coefficient of that variable. For example, for data set of PAV-aged samples at 40◦C the functions are:

$$F_1 = -0.0443 \times \mathrm{Vel} + 0.957 \times \mathrm{IR}_1 - 0.334 \times \mathrm{IR}_2 - 358.689 \times \mathrm{A}_1 - 282.124 \times \mathrm{A}_2$$

$$F_2 = 0.0276 \times \mathrm{Vel} - 1.688 \times \mathrm{IR}_1 - 0.0358 \times \mathrm{IR}_2 + 320.67 \times \mathrm{A}_1 - 114.611 \times \mathrm{A}_2$$

Figure 7-19 illustrates the plotted points of each sample using Function1 and Function2. As plot shows the point corresponding to each grade are quit district in the two-dimension area.

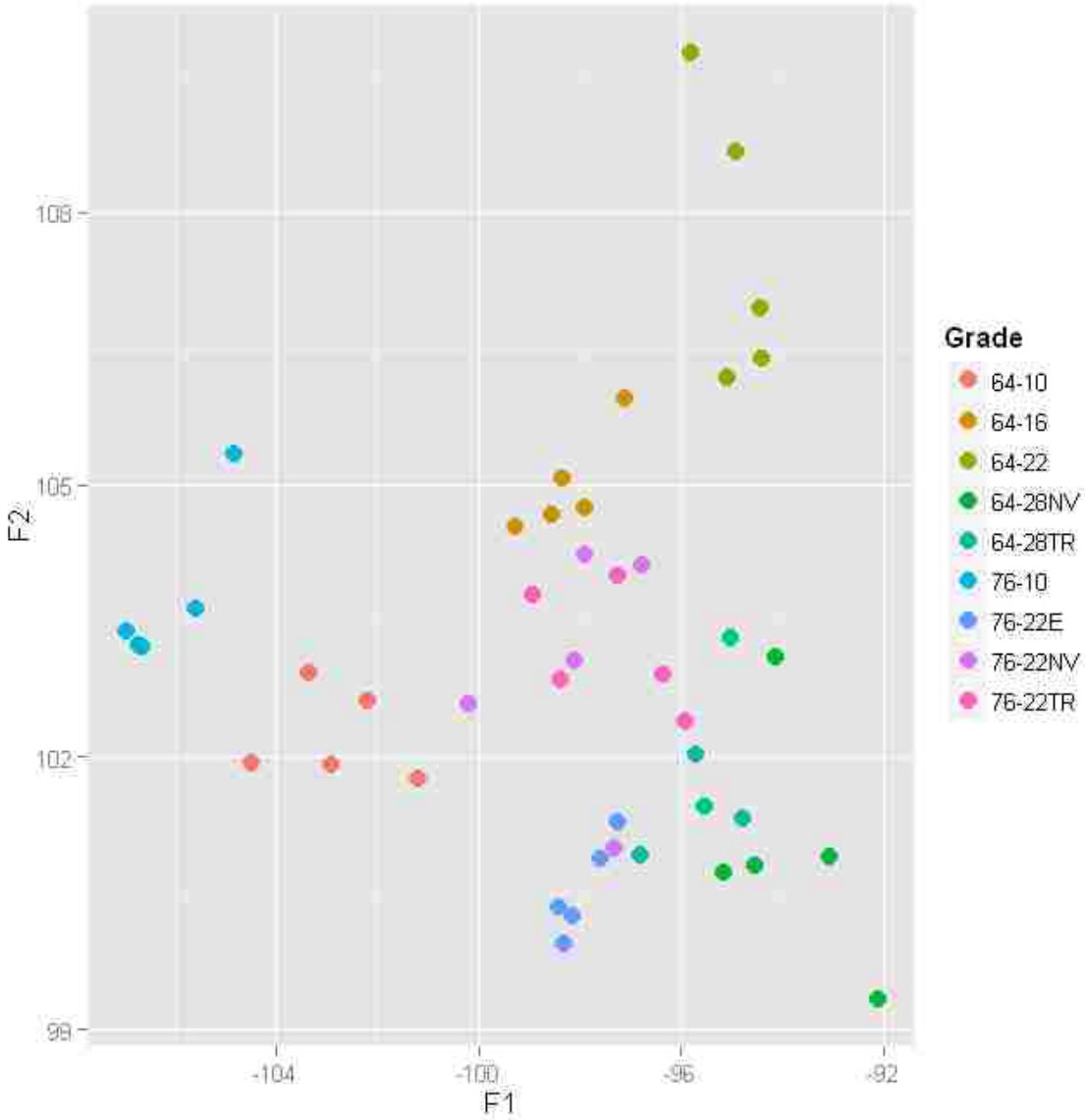

Figure 7-19 Plotted Data Point Using the Functions Produced for PAV-aged at 40◦C

The functions for data set of PAV-aged samples at 40◦C are;

$$F_1 = 0.0094\times \text{Vel} - 0.0707\times \text{IR}_1 + 0.199\times \text{IR}_2 - 70.456\times \text{A}_1 + 623.875\times \text{A}_2$$

$$F_2 = -0.0269\times \text{Vel} + 0.609\times \text{IR}_1 + 0.0432\times \text{IR}_2 - 661.138\times \text{A}_1 - 281.127\times \text{A}_2$$

Plotted data points for these functions are illustrated in Figure 7-20.

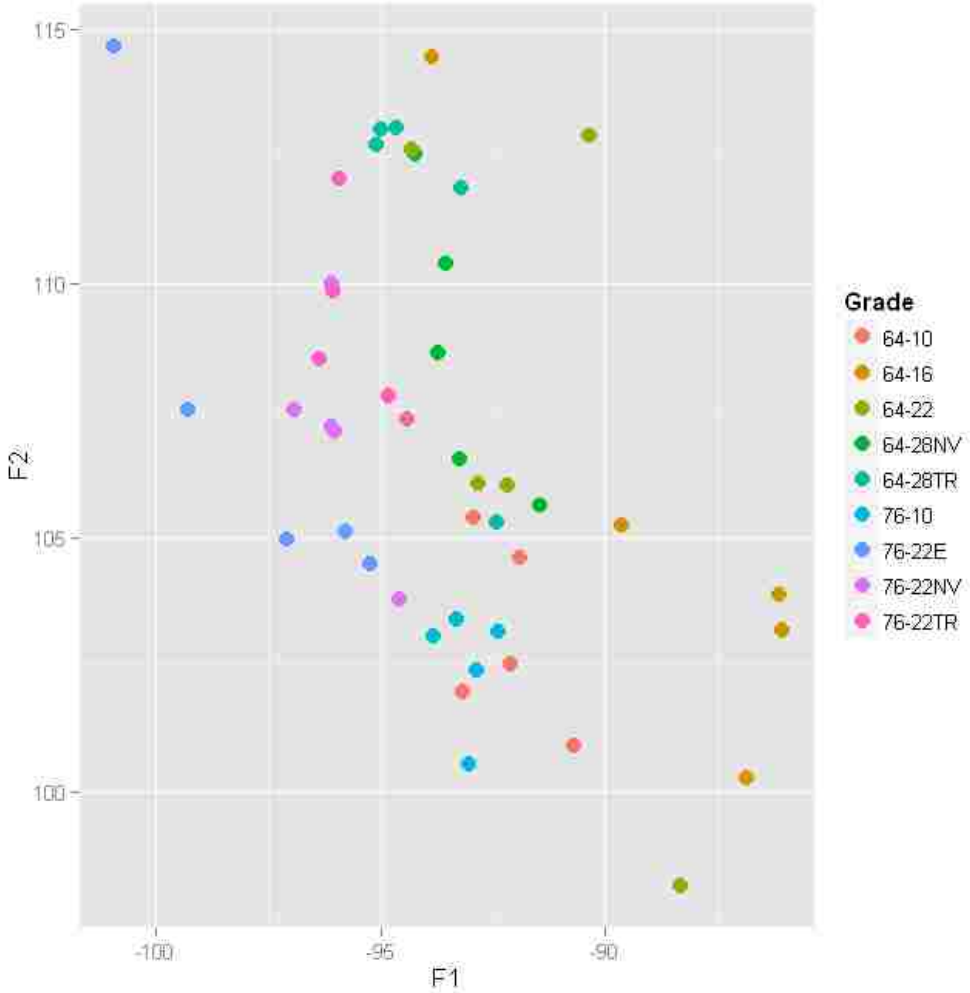

Figure 7-20 Plotted Data Point Using the Functions Produced for PAV-aged at 60◦C

8. CHAPTER 8 :CONCLUSIONS AND RECOMMENDATIONS

The use of ultrasound measurement as an alternative for determining the rheological properties of asphalt binders and also for prediction of the SUPERPAVE performance grade of asphalt binders was explored in this research project. The research was performed in two stages. In the first stage different ultrasound equipment and measurement configuration were examined to find the best system that can distinguish between two or more different asphalt binder grades. The second stage had two phases. In the first phase rheological properties of selected performance grade asphalt binders were determined with mechanical tests for grade verification. These properties were used later for possible correlation with ultrasound measured parameters. In the second stage selected measurement method from stage 1 was used to measure the ultrasound properties of the selected performance grade asphalt binders. Ultrasound measurements were performed at five different temperatures on original and aged samples. Following is the descriptive list of conclusions of this research.

8.1 Conclusions

Conclusions of this research project are presented in the following four categories;

- Feasibility
- Temperature Dependence of the Ultrasonic Measurements
- Correlations between Asphalt Binder Rheological Properties and Ultrasonic Measurements
- Prediction of the Performance Grade Using Discriminant Analysis

8.2 Feasibility

- The use of non-contact ultrasound in the work of previous researchers did not show promising results. Therefore, was not selected for this research project. The need for a test chamber for elevated temperature measurements was also one of the reasons that the idea of using non-contact ultrasound vanished.
- Contact ultrasound was examined with two couplants of gel and water. Due to the small size of the asphalt sample, the thickness of the couplant gel which was hard to have control on had unwanted effect on the measured ultrasound parameters. Use of water as the couplant for contact transducers showed some hopeful results.
- The use of high frequency transducer, specified for immersion ultrasound measurements, resulted in the most reliable responses and those transducers in an immersion configuration was selected for the main body of the research.
- Submerging of the asphalt sample, poured in a tin cup, gave the opportunity of elevated temperature testing. Ultrasound measurements were performed with an immersion transducer in a water bath with temperature control.
- On account of the pulse/echo ultrasound method the effect of holding material (tin cup) was eliminated from the measurements.

8.3 Temperature Dependence of Ultrasonic Measurements

- Ultrasonic pulse velocity of the asphalt binders decreases with increasing the temperature. A logarithmic curve fits the best with the data points.
- Aged samples showed higher velocity than original samples due to heavier and more solid constituents.

- Modified asphalt binders showed lower velocity compared to un-modified ones. This confirms the results of the researches which show the use of polymer modifiers in Portland cement concrete decreases the compression elastic modulus. Velocity of the compression waves, which were used in this research, has a direct relationship with compression elastic modulus.

8.3.1 Correlations between Asphalt Binder Rheological Properties and Ultrasonic Measurements

- Use of polymer or rubber modifiers in asphalt binder improves the elastic shear modulus whilst they reduce the compression elastic modulus. This behavior was observed at high temperature. Velocity of the compression ultrasound wave has a linear relationship with square root of compression elastic modulus.
- At medium temperature asphalt binder with modifiers showed higher velocity at higher elastic shear modulus.
- Stiffness of the modified asphalt binder, which is the flexural stiffness of the asphalt beam sample, was higher when ultrasound measurements showed higher velocity.

8.3.2 Prediction of the Performance Grade Using Discriminant Analysis

- When data of ultrasound parameters of PAV-aged asphalt binders at 40◦C or 60◦C was used the DA could predict the right grade with 75% chance. Other aging states and temperatures showed lower numbers.
- Two linear functions were produced to predict the grade of asphalt binders and plotting them in a two-dimension coordinate.

8.4 Recommendations

- This research used compression ultrasound wave as an alternative for mechanical test. The use of shear ultrasound wave could correlate better with shear properties of materials. Since the shear wave does not propagate in the liquids and air, contact ultrasound measurements which could be performed at elevated temperatures is a suitable configurations. Adhesive surface of the asphalt samples specially at elevated temperatures, need for a temperature control chamber and etc. are some of the difficulties involved with contact ultrasound.
- Ultrasound measurements in this research were performed at room temperature an higher. Performing the ultrasound measurements at temperatures lower than room temperature might results in better correlations with the results of the BBR and the low temperature ductility.
- This research used limited number of asphalt binder grades; other researches may expand the data base of the ultrasound measurements by selecting other grades.
- Discriminant Function Analysis was used in this research; one may consider other prediction methods such as Neural Network or Fuzzy Logic.
- In order to promote the experimental proposed method to a route standard test, agencies which deal with grade verification of the asphalt binders may adopt the ultrasound measurements and perform it besides mechanical testing. This will help to expand the data base of the ultrasound measurements as well as enhance the measurement procedure and find more sources of errors. After reaching a high and acceptable reliability the mechanical tests can be replaced by the ultrasound measurements.

A. APPENDIX A;

Test Data from Mechanical Tests on Asphalt Binders

Table A-1 DSR Data on PG 64-28NV

	DSR (Original)		DSR (RTFO)		DSR (PAV)	
Sample #	G* (kPa)	δ (◦)	G* (kPa)	δ (◦)	G* (kPa)	δ (◦)
1	1.42	69.9	3.04	65.1	2170	48.9
2	1.40	70.2	2.95	65.3	2010	48.6
3	1.41	70.2	3.23	64.8		
AVG	1.41	70.1	3.07	65.1	2090	48.8
G'	0.48		1.30		1378	
G"	1.33		2.79		1571	

Table A-2 BBR Data on PG 64-28NV

	Sample #					
	1		2		AVG	
t (sec)	S (MPa)	m-value	S (MPa)	m-value	S (MPa)	m-value
8	240	0.274	248	0.273	244.0	0.274
15	201	0.292	207	0.294	204	0.293
30	163	0.311	167	0.316	165	0.314
60	131	0.331	134	0.339	132.5	0.335
120	103	0.350	105	0.361	104	0.356
240	80.4	0.370	80.8	0.384	80.6	0.377

Table A-3 DSR Data PG64-28TR

	DSR (Original)		DSR (RTFO)		DSR (PAV)	
Sample #	G* (kPa)	δ (◦)	G* (kPa)	δ (◦)	G* (kPa)	δ (◦)
1	1.36	72.6	2.4	69.8	2260	52.1
2	1.35	72.9	2.53	69.7	2260	52.1
3	1.37	72.7	2.61	69.5		
AVG	1.36	72.7	2.51	69.7	2260	52.1
G'	0.40		0.87		1388	
G"	1.30		2.36		1783	

Table A-4 BBR Data PG64-28TR

	Sample #					
	1		2		AVG	
t (sec)	S (MPa)	m-value	S (MPa)	m-value	S (MPa)	m-value
8	316	0.264	307	0.271	312	0.268
15	265	0.287	256	0.292	261	0.290
30	216	0.312	208	0.315	212	0.314
60	173	0.337	166	0.338	170	0.338
120	135	0.362	130	0.361	133	0.362
240	104	0.387	101	0.384	103	0.386

Table A-5 DSR Data PG76-22NV

	DSR (Original)		DSR (RTFO)		DSR (PAV)	
Sample	G* (kPa)	δ (◦)	G* (kPa)	δ (◦)	G* (kPa)	δ (◦)
1	1.22	59.5	1.71	62.4	1170	55.1
2	1.17	58.7	1.78	63.1	1030	55.7
3	1.11	59.5	1.79	63.9		
AVG	1.17	59.2	1.76	63.1	1100	55.4
G'	0.60		0.80		625	
G"	1.00		1.57		905	

Table A-6 BBR Data PG76-22NV

	Sample #					
	1		2		AVG	
t (sec)	S (MPa)	m-value	S (MPa)	m-value	S (MPa)	m-value
8	219	0.277	213	0.271	216	0.274
15	182	0.297	177	0.292	180	0.295
30	147	0.319	143	0.315	145	0.317
60	117	0.341	114	0.338	116	0.340
120	91.8	0.363	88.9	0.361	90	0.362
240	70.7	0.386	68.4	0.384	70	0.385

Table A-7 DSR Data PG76-22TR

	DSR (Original)		DSR (RTFO)		DSR (PAV)	
Sample #	G* (kPa)	δ (◦)	G* (kPa)	δ (◦)	G* (kPa)	δ (◦)
1	1.29	66.2	2.19	60.0	928	52.9
2	1.24	68.6	2.14	60.1	904	53.1
3	1.27	68.6	2.08	61.0		
AVG	1.27	67.8	2.14	60.4	916	53.0
G'	0.48		1.06		551	
G"	1.17		1.86		732	

Table A-8 BBR Data PG76-22TR

	Sample #					
	1		2		AVG	
t (sec)	S (MPa)	m-value	S (MPa)	m-value	S (MPa)	m-value
8	191	0.311	196	0.306	194	0.309
15	157	0.330	160	0.327	159	0.329
30	123	0.352	127	0.349	125	0.351
60	96.1	0.373	98.9	0.372	98	0.373
120	73.6	0.395	75.8	0.395	75	0.395
240	55.6	0.416	57.2	0.418	56	0.417

Table A-9 DSR Data PG64-22

	DSR (Original)		DSR (RTFO)		DSR (PAV)	
Sample	G* (kPa)	δ (◦)	G* (kPa)	δ (◦)	G* (kPa)	δ (◦)
1	1.16	87.3	2.84	84.3	4900	48.2
2	1.12	87.3	2.86	84.1	4730	48.2
3	1.12	87.3	3.11	83.9		
AVG	1.133	87.30	2.94	84.10	4815	48.2
G'	0.05		0.30		3209	
G"	1.13		2.92		3589	

Table A-10 BBR Data PG64-22

	Sample #					
	1		2		AVG	
t (sec)	S (MPa)	m-value	S (MPa)	m-value	S (MPa)	m-value
8	329	0.259	325	0.254	327	0.257
15	277	0.279	274	0.276	276	0.278
30	228	0.301	225	0.3	227	0.301
60	183	0.322	181	0.324	182	0.323
120	145	0.344	143	0.348	144	0.346
240	113	0.366	112	0.372	113	0.369

Table A-11 DSR Data PG76-22E

	DSR (Original)		DSR (RTFO)		DSR (PAV)	
Sample	G* (kPa)	δ (◦)	G* (kPa)	δ (◦)	G* (kPa)	δ (◦)
1	1.25	64.7	2.22	58.5	822	48.7
2	1.23	64.8	2.23	58.2	803	48.6
3	1.25	64.9	2.23	58		
AVG	1.24	64.80	2.23	58.2	813	48.7
G'	0.53		1.17		537	
G"	1.13		1.89		610	

Table A-12 BBR Data PG76-22E

	Sample #					
	1		2		AVG	
t (sec)	S (MPa)	m-value	S (MPa)	m-value	S (MPa)	m-value
8	142	0.312	140	0.309	141	0.311
15	116	0.328	115	0.327	116	0.328
30	91.4	0.346	90.7	0.346	91	0.346
60	71.6	0.363	70.8	0.365	71	0.364
120	55.5	0.381	54.7	0.385	55	0.383
240	42.2	0.399	41.6	0.404	42	0.402

Table A-13 DSR Data PG64-10

	DSR (Original)		DSR (RTFO)		DSR (PAV)	
	PG64-10		PG64-10		PG64-10	
Sample	G* (kPa)	δ (◦)	G* (kPa)	δ (◦)	G* (kPa)	δ (◦)
1	1.67	88.2	4.21	86.3	3180	47
2	1.65	88.3	4.29	86.2	3120	46.9
3	1.64	88.2	4.62	86	3030	46.9
AVG	1.65	88.2	4.25	86.2	3110	46.9
G'	0.05		4.47	86.1	2124	
G"	1.65		4.65	85.9	2272	
			4.42	86.1		
			0.30			
			4.40			

Table A-14 BBR Data PG64-10

	Sample #					
	1		2		AVG	
t (sec)	S (MPa)	m-value	S (MPa)	m-value	S (MPa)	m-value
8	118	0.319	111	0.319	115	0.319
15	95.3	0.351	89.9	0.349	93	0.350
30	73.8	0.386	69.8	0.382	72	0.384
60	56	0.421	53.1	0.415	55	0.418
120	41.4	0.456	39.4	0.448	40	0.452
240	29.6	0.491	28.4	0.481	29	0.486

Table A-15 DSR Data PG76-10

	DSR (Original)		DSR (RTFO)		DSR (PAV)	
	PG76-10		PG76-10		PG76-10	
Sample	G* (kPa)	δ (◦)	G* (kPa)	δ (◦)	G* (kPa)	δ (◦)
1	1.00	84.6	2.43	81	2990	47.3
2	1.01	84.6	2.27	81.4	2890	47.3
3	1.01	84.6	2.02	81.9	2890	47.3
AVG	1.01	84.6	2.56	80.8	2923	47.3
G'	0.09		2.54	81	1982	
G"	1.00		2.36	81.2	2148	
			0.36			
			2.34			

Table A-16 BBR Data PG76-10

	Sample #					
	1		2		AVG	
t (sec)	S (MPa)	m-value	S (MPa)	m-value	S (MPa)	m-value
8	166	0.284	166	0.289	166	0.287
15	138	0.304	137	0.309	138	0.307
30	111	0.327	110	0.331	111	0.329
60	87.7	0.350	87	0.353	87	0.352
120	68.1	0.373	67.6	0.376	68	0.375
240	52.2	0.396	51.6	0.398	52	0.397

Table A-17DSR Data on PG64-16

	DSR (Original)		DSR (RTFO)		DSR (PAV)	
	PG64-16		PG64-16		PG64-16	
Sample	G* (kPa)	δ (◦)	G* (kPa)	δ (◦)	G* (kPa)	δ (◦)
1	1.37	86.9	3.59	84.3	3120	45.8
2	1.35	86.9	3.6	84.3	3120	46.3
3	1.39	86.9	3.56	84.4	3130	46.3
AVG	1.37	86.9	3.58	84.3	3123	46.1
G'	0.07		0.35		2164	
G"	1.37		3.57		2252	

Table A-18 BBR Data PG64-16

	Sample #					
	1		2		AVG	
t (sec)	S (MPa)	m-value	S (MPa)	m-value	S (MPa)	m-value
8	203	0.298	200	0.302	202	0.300
15	167	0.324	164	0.325	166	0.325
30	131	0.354	130	0.351	131	0.353
60	102	0.383	101	0.376	102	0.380
120	77.96	0.412	77.2	0.401	78	0.407
240	57.6	0.442	57.8	0.427	58	0.435

B. APPENDIX B;

Row Data of Ultrasound Measurements on Asphalt Binders

Table B-1 PG 64-28NV

	Temperature	30◦C					40◦C				
	Sample #	Vel	IR1	IR2	A1	A2	Vel	IR1	IR2	A1	A2
Original	1	1664.2	-21.43	-42.84	0.050	0.004	1578.5	-27.74	-42.34	0.024	0.004
	2	1725.3	-21.73	-44.36	0.048	0.004	1616.6	-26.25	-42.68	0.028	0.004
	3	1678.8	-20.86	-43.66	0.054	0.004	1576.6	-26.27	-41.49	0.028	0.005
	4	1688.4	-21.35	-42.34	0.052	0.004	1585.9	-26.34	-41.50	0.028	0.005
	5	1704.5	-21.19	-42.72	0.052	0.004	1625.2	-26.11	-46.35	0.029	0.003
	AVG	**1692.3**	**-21.31**	**-43.19**	**0.051**	**0.004**	**1596.59**	**-26.24**	**-42.00**	**0.028**	**0.004**
RTFO	1	1761.9	-24.16	-47.36	0.036	0.002	1633.4	-28.84	-44.98	0.020	0.004
	2	1729.6	-22.79	-46.75	0.042	0.003	1618.8	-29.76	-43.61	0.019	0.004
	3	1752.0	-21.59	-45.19	0.048	0.003	1650.8	-30.27	-45.02	0.018	0.004
	4	1734.8	-21.33	-44.49	0.048	0.003	1644.1	-27.39	-45.59	0.025	0.004
	5	1732.4	-21.85	-45.65	0.048	0.003	1630.4	-26.02	-45.26	0.029	0.004
	AVG	**1742.1**	**-21.89**	**-45.89**	**0.044**	**0.003**	**1635.49**	**-28.66**	**-44.89**	**0.022**	**0.004**
PAV	1	1743.2	-28.97	-49.37	0.021	0.002	1635.2	-30.21	-43.84	0.018	0.004
	2	1694.3	-27.44	-49.21	0.025	0.002	1597.2	-27.50	-43.89	0.024	0.004
	3	1737.2	-25.51	-50.15	0.032	0.002	1661.5	-26.42	-49.90	0.028	0.003
	4	1756.5	-25.43	-49.78	0.032	0.002	1655.8	-26.76	-44.70	0.027	0.003
	5	1758.7	-26.55	-49.41	0.028	0.002	1664.1	-26.00	-44.99	0.030	0.003
	AVG	**1738.0**	**-26.23**	**-49.58**	**0.028**	**0.002**	**1642.74**	**-26.67**	**-44.36**	**0.025**	**0.003**

	Temperature	50◦C					60◦C				
	Sample #	Vel	IR1	IR2	A1	A2	Vel	IR1	IR2	A1	A2
Original	1	1485.4	-37.65	-35.78	0.008	0.010	1409.9	-31.50	-30.91	0.016	0.018
	2	1509.8	-39.04	-35.17	0.007	0.010	1445.6	-30.46	-28.59	0.018	0.022
	3	1484.8	-33.77	-36.31	0.012	0.010	1407.4	-31.74	-28.17	0.015	0.024
	4	1493.0	-33.77	-35.57	0.012	0.010	1413.3	-32.41	-28.18	0.014	0.024
	5	1492.3	-32.30	-37.50	0.014	0.008	1413.4	-31.36	-29.88	0.016	0.018
	AVG	**1493.1**	**-33.28**	**-36.06**	**0.011**	**0.010**	**1417.9**	**-31.49**	**-29.15**	**0.016**	**0.021**
RTFO	1	1466.7	-40.18	-38.99	0.006	0.007	1456.8	-34.70	-33.86	0.010	0.012
	2	1604.1	-41.01	-38.55	0.005	0.007	1495.6	-38.54	-30.51	0.006	0.018
	3	1533.2	-29.97	-38.77	0.020	0.007	1467.8	-27.74	-31.06	0.024	0.016
	4	1527.4	-31.10	-39.48	0.017	0.007	1485.1	-27.04	-32.09	0.026	0.014
	5	1521.7	-30.88	-41.15	0.017	0.006	1499.5	-37.12	-31.59	0.008	0.016
	AVG	**1530.6**	**-30.65**	**-39.39**	**0.013**	**0.007**	**1481.0**	**-33.03**	**-31.31**	**0.016**	**0.016**
PAV	1	1529.8	-42.43	-44.44	0.004	0.004	1465.9	-38.93	-38.09	0.006	0.008
	2	1503.2	-39.08	-44.79	0.004	0.004	1415.3	-37.78	-37.28	0.008	0.009
	3	1544.8	-36.00	-44.87	0.010	0.003	1447.1	-40.36	-38.41	0.005	0.006
	4	1567.7	-36.68	-46.63	0.009	0.003	1480.8	-36.96	-38.53	0.009	0.008
	5	1566.1	-35.84	-45.31	0.010	0.004	1499.9	-40.40	-42.74	0.006	0.005
	AVG	**1542.3**	**-36.90**	**-45.21**	**0.007**	**0.003**	**1461.8**	**-38.89**	**-38.08**	**0.007**	**0.007**

	Temperature	70◦C				
	Sample #	Vel	IR1	IR2	A1	A2
Original	1	1338.7	-26.06	-20.76	0.026	0.054
	2	1379.7	-26.67	-20.34	0.026	0.058
	3	1355.8	-28.28	-24.10	0.022	0.060
	4	1351.0	-26.71	-20.36	0.026	0.058
	5	1365.8	-27.35	-24.62	0.024	0.058
	AVG	**1358.2**	**-27.02**	**-22.03**	**0.025**	**0.058**
RTFO	1	1593.9	-26.53	-21.07	0.026	0.049
	2	1366.8	-42.17	-22.09	0.005	0.047
	3	1513.7	-31.80	-22.82	0.013	0.042
	4	1478.9	-32.02	-23.78	0.016	0.037
	5	1435.3	-30.97	-26.43	0.016	0.030
	AVG	**1476.0**	**-31.59**	**-22.90**	**0.011**	**0.042**
PAV	1	1388.0	-25.89	-25.02	0.028	0.032
	2	1356.9	-27.49	-25.03	0.024	0.034
	3	1412.9	-34.93	-33.94	0.010	0.013
	4	1417.2	-32.69	-31.12	0.013	0.017
	5	1401.0	-34.62	-28.87	0.013	0.020
	AVG	**1395.2**	**-31.12**	**-27.51**	**0.020**	**0.026**

Table B -2PG 64-28TR

	Temperature	30◦C					40◦C				
	Sample #	Vel	IR1	IR2	A1	A2	Vel	IR1	IR2	A1	A2
Original	1	1741.4	-20.35	-42.43	0.058	0.004	1666.9	-24.52	-46.54	0.035	0.003
	2	1717.7	-20.04	-44.57	0.058	0.004	1629.7	-24.60	-45.99	0.035	0.003
	3	1746.4	-20.11	-46.70	0.060	0.004	1612.1	-24.82	-44.05	0.034	0.004
	4	1707.0	-19.99	-42.28	0.060	0.004	1631.3	-24.63	-45.99	0.034	0.035
	5	1750.7	-23.77	-43.13	0.039	0.004	1636.3	-27.83	-42.99	0.024	0.004
	AVG	**1732.7**	**-20.12**	**-43.82**	**0.055**	**0.004**	**1627.3**	**-24.64**	**-45.11**	**0.032**	**0.010**
RTFO	1	1755.9	-20.68	-43.86	0.049	0.003	1645.7	-27.01	-45.09	0.027	0.004
	2	1775.6	-22.29	-42.55	0.046	0.004	1681.4	-28.45	-45.03	0.022	0.003
	3	1774.9	-22.34	-48.25	0.046	0.003	1646.6	-25.74	-45.29	0.030	0.004
	4	1764.7	-20.07	-44.04	0.060	0.004	1658.2	-27.84	-44.90	0.024	0.004
	5										
	AVG	**1767.8**	**-21.35**	**-43.48**	**0.050**	**0.004**	**1658.0**	**-27.26**	**-45.08**	**0.026**	**0.003**
PAV	1	1779.8	-23.79	-46.97	0.040	0.003	1659.4	-27.62	-44.07	0.024	0.004
	2	1787.5	-26.58	-48.88	0.028	0.002	1738.9	-27.04	-52.06	0.025	0.002
	3	1781.5	-23.56	-47.80	0.038	0.003	1710.8	-24.73	-49.82	0.034	0.002
	4	1749.8	-26.49	-48.01	0.027	0.002	1701.6	-24.15	-47.64	0.037	0.004
	5	1817.1	-23.56	-51.82	0.040	0.002	1733.9	-24.65	-52.15	0.034	0.002
	AVG	**1783.1**	**-23.64**	**-47.92**	**0.037**	**0.002**	**1708.9**	**-24.51**	**-50.41**	**0.154**	**0.013**
	Temperature	50◦C					60◦C				
	Sample #	Vel	IR1	IR2	A1	A2	Vel	IR1	IR2	A1	A2
Original	1	1536.9	-33.01	-37.55	0.013	0.007	1479.4	-35.85	-34.55	0.010	0.013
	2	1521.4	-29.76	-39.36	0.019	0.006	1419.7	-32.32	-32.20	0.015	0.015
	3	1510.1	-31.96	-38.76	0.015	0.007	1424.7	-33.78	-31.76	0.012	0.015
	4				0.015	0.006	1417.9	-34.12	-32.03	0.012	0.015
	5	1537.8	-30.39	-38.72	0.018	0.007	1446.6	-34.78	-33.18	0.011	0.013
	AVG	**1526.5**	**-31.28**	**-38.60**	**0.016**	**0.007**	**1437.7**	**-34.17**	**-32.74**	**0.012**	**0.014**
RTFO	1	1555.8	-28.26	-41.16	0.023	0.005	1559.5	-38.57	-34.62	0.007	0.012
	2	1584.3	-31.16	-39.58	0.016	0.006	1536.4	-33.01	-31.67	0.013	0.016
	3	1540.8	-26.60	-41.30	0.028	0.006	1536.8	-35.96	-35.56	0.025	0.014
	4	1574.2	-30.11	-43.66	0.019	0.004	1554.7	-35.54	-37.45	0.009	0.011
	5										
	AVG	**1563.8**	**-29.03**	**-41.42**	**0.022**	**0.005**	**1546.8**	**-35.75**	**-35.09**	**0.014**	**0.013**
PAV	1	1561.2	-40.83	-46.73	0.006	0.025	1494.2	-40.86	-40.80	0.005	0.006
	2	1572.5	-38.51	-46.95	0.007	0.003	1503.1	-40.78	-41.51	0.005	0.005
	3	1575.8	-33.36	-46.33	0.013	0.004	1480.4	-41.26	-41.21	0.005	0.005
	4	1592.0	-34.85	-49.36	0.010	0.002	1517.1	-39.52	-45.06	0.006	0.003
	5	1596.0	-33.47	-49.32	0.012	0.002	1521.0	-35.12	-41.43	0.010	0.006
	AVG	**1579.5**	**-35.05**	**-47.74**	**0.009**	**0.007**	**1503.2**	**-40.60**	**-41.24**	**0.006**	**0.005**
	Temperature	70◦C									
	Sample #	Vel	IR1	IR2	A1	A2					
Original	1	1449.6	-33.13	-24.96	0.012	0.036					
	2	1375.5	-32.71	-26.60	0.009	0.040					
	3	1361.2	-36.27	-23.70	0.014	0.036					
	4	1364.9	-30.27	-24.21	0.018	0.036					
	5	1376.7	-28.05	-24.89	0.024	0.034					
	AVG	**1369.6**	**-32.03**	**-24.44**	**0.017**	**0.036**					
RTFO	1	1475.6	-28.23	-26.10	0.022	0.029					
	2	1500.3	-28.59	-25.00	0.022	0.032					
	3	1434.9	-24.37	-26.75	0.036	0.028					
	4	1492.5	-30.01	-27.39	0.017	0.026					
	5										
	AVG	**1475.8**	**-28.41**	**-26.31**	**0.024**	**0.029**					
PAV	1	1406.4	-35.34	-32.41	0.010	0.015					
	2	1431.3	-34.91	-32.40	0.010	0.014					
	3	1411.3	-36.27	-32.23	0.009	0.015					
	4	1403.2	-38.77	-33.22	0.007	0.013					
	5	1466.8	-43.12	-34.22	0.004	0.011					
	AVG	**1423.8**	**-36.32**	**-32.90**	**0.008**	**0.014**					

Table B -3PG 76-22NV

	Temperature	30◦C					40◦C				
	Sample #	Vel	IR1	IR2	A1	A2	Vel	IR1	IR2	A1	A2
Original	1	1685.3	-22.60	-43.05	0.045	0.005	1572.0	-33.36	-44.32	0.013	0.004
	2	1723.0	-20.89	-45.24	0.054	0.004	1607.6	-24.71	-43.54	0.036	0.004
	3	1734.2	-21.72	-42.69	0.050	0.005	1623.4	-25.97	-42.24	0.030	0.004
	4	1779.7	-23.47	-41.31	0.040	0.005	1669.7	-25.64	-40.93	0.032	0.005
	5	1765.0	-22.25	-43.60	0.048	0.004	1654.2	-26.07	-43.19	0.030	0.004
	AVG	**1737.4**	**-22.19**	**-43.18**	**0.047**	**0.005**	**1638.7**	**-25.90**	**-42.84**	**0.028**	**0.004**
RTFO	1	1820.6	-23.34	-49.27	0.041	0.004	1659.8	-27.21	-43.20	0.026	0.004
	2	1781.3	-22.27	-45.61	0.045	0.004	1632.0	-28.26	-43.35	0.023	0.004
	3	1716.6	-21.00	-42.69	0.054	0.004	1654.9	-25.39	-42.73	0.032	0.004
	4	1806.0	-22.68	-46.51	0.044	0.003	1710.9	-26.28	-49.91	0.029	0.003
	5	1782.9	-19.55	-43.76	0.064	0.003	1652.8	-24.12	-42.68	0.038	0.004
	AVG	**1781.5**	**-21.98**	**-44.64**	**0.050**	**0.004**	**1662.1**	**-26.29**	**-42.99**	**0.030**	**0.004**
PAV	1	1813.4	-21.27	-42.09	0.043	0.003	1703.8	-25.21	-44.51	0.032	0.004
	2	1835.6	-21.49	-41.56	0.045	0.003	1761.2	-25.73	-48.21	0.030	0.003
	3	1868.8	-21.39	-42.56	0.050	0.004	1757.8	-24.89	-44.22	0.034	0.004
	4	1874.9	-22.20	-48.77	0.046	0.003	1762.5	-26.94	-49.23	0.027	0.003
	5	1879.2	-24.18	-52.37	0.037	0.002	1684.3	-29.47	-43.89	0.021	0.004
	AVG	**1854.4**	**-21.59**	**-43.75**	**0.046**	**0.003**	**1733.9**	**-25.69**	**-44.21**	**0.029**	**0.004**

	Temperature	50◦C					60◦C				
	Sample #	Vel	IR1	IR2	A1	A2	Vel	IR1	IR2	A1	A2
Original	1	1490.6	-34.76	-43.48	0.010	0.004	1429.7	-36.97	-31.79	0.008	0.016
	2	1516.8	-34.17	-43.50	0.011	0.004	1456.7	-32.34	-32.89	0.014	0.014
	3	1526.9	-36.72	-42.51	0.009	0.005	1461.0	-35.00	-30.31	0.010	0.019
	4	1583.3	-36.88	-42.45	0.009	0.005	1508.4	-35.77	-29.56	0.009	0.020
	5	1544.2	-38.00	-45.78	0.008	0.003	1503.1	-37.58	-32.70	0.008	0.013
	AVG	**1532.3**	**-36.11**	**-43.55**	**0.009**	**0.004**	**1471.8**	**-36.33**	**-31.45**	**0.010**	**0.016**
RTFO	1	1560.7	-30.02	-38.18	0.018	0.007	1496.5	-37.94	-33.71	0.007	0.012
	2	1553.4	-31.48	-38.48	0.016	0.007	1489.3	-37.06	-33.49	0.008	0.012
	3	1557.6	-29.57	-38.60	0.020	0.007	1488.7	-36.64	-33.91	0.009	0.012
	4	1623.3	-27.75	-44.92	0.024	0.004	1516.6	-30.80	-38.11	0.018	0.007
	5	1563.9	-28.02	-38.45	0.024	0.007	1493.9	-32.88	-35.81	0.013	0.008
	AVG	**1571.8**	**-28.84**	**-38.43**	**0.020**	**0.007**	**1497.0**	**-36.13**	**-34.23**	**0.009**	**0.011**
PAV	1	1600.8	-31.59	-40.98	0.020	0.005	1516.7	-34.43	-36.03	0.011	0.009
	2	1633.6	-29.62	-46.69	0.021	0.006	1553.6	-35.86	-37.70	0.010	0.007
	3	1652.8	-27.56	-41.02	0.025	0.006	1568.1	-36.08	-37.51	0.009	0.008
	4	1647.3	-27.56	-42.57	0.024	0.004	1570.4	-35.50	-39.05	0.010	0.007
	5	1598.8	-31.17	-41.31	0.017	0.005	1516.6	-38.81	-38.02	0.007	0.008
	AVG	**1626.7**	**-28.98**	**-41.47**	**0.022**	**0.005**	**1545.1**	**-35.47**	**-37.66**	**0.009**	**0.008**

	Temperature	70◦C				
	Sample #	Vel	IR1	IR2	A1	A2
Original	1	1369.0	-28.84	-27.76	0.020	0.024
	2	1372.1	-29.20	-22.57	0.019	0.040
	3	1416.9	-29.07	-26.71	0.020	0.028
	4	1442.9	-32.72	-23.09	0.012	0.042
	5	1412.8	-35.47	-25.11	0.009	0.035
	AVG	**1402.7**	**-29.04**	**-25.05**	**0.016**	**0.034**
RTFO	1	1422.0	-31.42	-24.84	0.015	0.033
	2	1421.4	-31.66	-25.70	0.015	0.030
	3	1412.7	-30.83	-26.15	0.016	0.029
	4	1423.2	-30.45	-29.39	0.018	0.018
	5	1412.8	-30.93	-27.71	0.016	0.024
	AVG	**1418.4**	**-31.06**	**-26.52**	**0.016**	**0.028**
PAV	1	1428.7	-44.83	-29.17	0.004	0.020
	2	1462.0	-37.80	-29.31	0.007	0.020
	3	1492.9	-39.82	-30.01	0.006	0.020
	4	1461.1	-39.30	-31.17	0.007	0.017
	5	1453.9	-34.44	-30.87	0.011	0.018
	AVG	**1459.7**	**-38.97**	**-30.11**	**0.007**	**0.019**

Table B-4 PG 76-22TR

		30◦C					40◦C				
		Vel	IR1	IR2	A1	A2	Vel	IR1	IR2	A1	A2
Original	1	1647.0	-23.91	-46.42	0.040	0.003	1562.7	-29.30	-50.11	0.020	0.002
	2	1761.4	-35.82	-46.64	0.009	0.003	1596.8	-44.07	-46.22	0.004	0.003
	3	1710.8	-24.39	-44.71	0.037	0.003	1599.8	-26.35	-44.63	0.030	0.004
	4	1601.8	-43.53	-45.76	0.005	0.003	1566.7	-32.38	-45.74	0.015	0.003
	5	1735.3	-26.40	-45.09	0.029	0.003	1619.6	-36.40	-44.57	0.009	0.004
	AVG	**1691.3**	**-24.90**	**-45.72**	**0.024**	**0.003**	**1589.1**	**-31.11**	**-45.29**	**0.015**	**0.003**
RTFO	1	1739.8	-28.47	-50.06	0.023	0.002	1631.2	-31.32	-50.47	0.016	0.002
	2	1834.6	-22.20	-52.11	0.046	0.003	1707.0	-26.26	-52.25	0.029	0.002
	3	1794.9	-22.01	-45.81	0.048	0.003	1659.7	-27.16	-49.93	0.010	0.002
	4	1786.4	-22.25	-47.57	0.047	0.002				0.026	0.002
	5	1712.2	-22.85	-43.77	0.042	0.003	1670.5	-26.19	-54.06	0.029	0.002
	AVG	**1773.6**	**-22.33**	**-47.81**	**0.039**	**0.002**	**1667.1**	**-26.54**	**-51.68**	**0.022**	**0.002**
PAV	1	1828.0	-21.15	-43.98	0.046	0.002	1769.9	-25.84	-53.30	0.031	0.003
	2	1803.9	-22.19	-44.02	0.047	0.002	1701.2	-26.50	-47.95	0.029	0.003
	3	1810.6	-23.86	-47.57	0.038	0.003	1720.0	-26.28	-49.58	0.030	0.003
	4	1902.2	-22.56	-47.03	0.046	0.002	1774.3	-25.94	-48.11	0.030	0.003
	5	1889.1	-20.99	-48.12	0.054	0.003	1755.4	-24.53	-49.64	0.036	0.003
	AVG	**1846.8**	**-21.72**	**-46.19**	**0.043**	**0.002**	**1744.2**	**-25.81**	**-48.82**	**0.031**	**0.003**

		50◦C					60◦C				
		Vel	IR1	IR2	A1	A2	Vel	IR1	IR2	A1	A2
Original	1	1475.4	-36.32	-48.37	0.009	0.003	1409.9	-36.07	-34.12	0.009	0.012
	2	1494.0	-38.61	-47.89	0.007	0.002	1448.7	-35.97	-36.56	0.010	0.010
	3	1515.9	-36.30	-48.37	0.009	0.002	1468.5	-37.61	-34.33	0.008	0.012
	4	1468.7	-41.92	-47.96	0.005	0.002	1404.4	-37.07	-34.09	0.008	0.011
	5	1527.7	-35.35	-46.18	0.010	0.003	1488.9	-36.20	-36.20	0.009	0.010
	AVG	**1496.4**	**-36.64**	**-47.75**	**0.008**	**0.002**	**1444.1**	**-36.58**	**-35.06**	**0.009**	**0.011**
RTFO	1	1530.4	-35.11	-44.84	0.011	0.003	1489.7	-40.41	-41.87	0.005	0.004
	2	1596.3	-29.16	-48.50	0.021	0.003	1496.7	-43.36	-38.36	0.004	0.006
	3	1579.6	-35.45	-45.65	0.010	0.003	1509.4	-44.54	-40.78	0.004	0.006
	4	1585.3	-31.16	-47.79	0.017	0.003	1503.7	-37.94	-41.87	0.008	0.005
	5	1529.6	-30.52	-43.51	0.018	0.004	1465.6	-41.98	-37.67	0.005	0.008
	AVG	**1564.3**	**-32.28**	**-46.06**	**0.015**	**0.003**	**1493.0**	**-41.92**	**-40.11**	**0.005**	**0.006**
PAV	1	1607.1	-28.75	-43.18	0.020	0.003	1519.2	-38.50	-38.29	0.007	0.007
	2	1605.8	-29.57	-44.44	0.020	0.004	1519.6	-36.65	-39.43	0.009	0.007
	3	1634.6	-30.62	-45.43	0.018	0.003	1554.5	-39.13	-42.18	0.007	0.005
	4	1665.2	-29.63	-44.29	0.020	0.004	1578.3	-36.24	-40.21	0.010	0.007
	5	1633.6	-28.69	-43.75	0.022	0.004	1578.7	-35.56	-42.29	0.010	0.005
	AVG	**1629.3**	**-29.45**	**-44.22**	**0.020**	**0.004**	**1550.1**	**-37.22**	**-40.48**	**0.009**	**0.006**

		70◦C				
		Vel	IR1	IR2	A1	A2
Original	1	1366.8	-30.27	-28.07	0.018	0.024
	2	1380.9	-28.98	-24.48	0.021	0.035
	3	1358.2	-31.09	-25.36	0.018	0.020
	4	1411.5	-31.82	-26.08	0.016	0.032
	5				0.015	0.028
	AVG	**1379.3**	**-30.54**	**-25.31**	**0.018**	**0.029**
RTFO	1	1425.0	-39.08	-31.92	0.007	0.015
	2	1438.6	-36.55	-35.70	0.009	0.011
	3	1463.9	-38.29	-31.43	0.006	0.015
	4	1453.7	-32.13	-33.71	0.014	0.013
	5	1443.3	-39.95	-36.32	0.006	0.010
	AVG	**1445.3**	**-38.47**	**-33.78**	**0.010**	**0.013**
PAV	1	1456.0	-35.76	-31.48	0.010	0.016
	2	1441.2	-37.03	-32.57	0.008	0.013
	3	1459.2	-36.02	-32.76	0.009	0.013
	4	1500.5	-37.81	-34.55	0.008	0.012
	5	1483.3	-38.48	-33.49	0.007	0.013
	AVG	**1468.0**	**-37.02**	**-32.97**	**0.008**	**0.013**

Table B-5 PG64-22

	Temperature	30◦C					40◦C				
	Sample #	Vel	IR1	IR2	A1	A2	Vel	IR1	IR2	A1	A2
Original	1	1759.5	-24.51	-45.24	0.035	0.004	1655.2	-28.31	-52.07	0.022	0.002
	2	1788.4	-26.44	-47.22	0.028	0.003	1679.5	-30.69	-54.33	0.017	0.002
	3	1762.2	-25.75	-45.73	0.030	0.003	1685.4	-30.58	-54.66	0.018	0.002
	4	1784.0	-25.43	-44.54	0.032	0.004	1689.6	-31.70	-53.89	0.015	0.002
	5	1767.0	-22.92	-46.99	0.012	0.003	1716.2	-36.29	-57.23	0.009	0.001
	AVG	**1772.2**	**-25.53**	**-45.94**	**0.027**	**0.003**	**1685.2**	**-30.99**	**-54.43**	**0.016**	**0.001**
RTFO	1	1797.4	-22.46	-43.76	0.044	0.004	1706.7	-30.09	-54.43	0.019	0.002
	2	1819.9	-23.56	-45.20	0.040	0.035	1724.5	-32.85	-57.48	0.013	0.001
	3	1818.9	-20.27	-44.45	0.059	0.003	1739.6	-27.44	-57.05	0.025	0.001
	4	1829.0	-22.83	-47.97	0.042	0.003	1711.9	-30.53	-57.42	0.018	0.001
	5	1819.9	-22.16	-44.47	0.046	0.003	1680.8	-32.57	-54.61	0.014	0.001
	AVG	**1817.0**	**-22.75**	**-45.17**	**0.046**	**0.010**	**1712.7**	**-31.06**	**-56.20**	**0.018**	**0.001**
PAV	1	1821.5	-23.36	-42.31	0.039	0.004	1758.6	-32.49	-55.29	0.014	0.001
	2	1809.4	-23.78	-40.56	0.039	0.006	1701.4	-31.18	-50.80	0.016	0.002
	3	1852.5	-22.47	-44.55	0.046	0.003	1707.8	-32.76	-52.30	0.014	0.001
	4	1825.6	-22.91	-42.70	0.043	0.004	1759.5	-29.62	-57.69	0.020	0.001
	5	1861.7	-22.32	-44.31	0.046	0.003	1722.8	-30.11	-51.66	0.019	0.002
	AVG	**1834.1**	**-22.97**	**-42.89**	**0.043**	**0.004**	**1730.0**	**-31.23**	**-52.51**	**0.016**	**0.001**

	Temperature	50◦C					60◦C				
	Sample #	Vel	IR1	IR2	A1	A2	Vel	IR1	IR2	A1	A2
Original	1	1575.1	-37.50	-44.43	0.007	0.003	1538.2	-43.26	-37.72	0.004	0.008
	2	1574.9	-26.70	-43.27	0.027	0.004	1534.0	-33.66	-38.06	0.012	0.007
	3	1593.0	-29.54	-45.02	0.020	0.004	1590.6	-40.09	-39.39	0.005	0.006
	4	1579.7	-29.45	-46.76	0.020	0.003	1596.7	-43.79	-39.77	0.004	0.006
	5	1543.7	-28.25	-50.51	0.023	0.002	1520.6	-39.35	-40.83	0.006	0.005
	AVG	**1573.3**	**-29.08**	**-44.87**	**0.019**	**0.003**	**1556.0**	**-40.03**	**-39.15**	**0.006**	**0.007**
RTFO	1	1590.3	-31.72	-48.36	0.015	0.003	1551.2	-50.57	-42.71	0.002	0.005
	2	1602.0	-33.02	-51.25	0.013	0.002	1537.1	-35.43	-45.02	0.010	0.004
	3	1600.7	-31.26	-51.09	0.016	0.002	1582.4	-50.23	-46.34	0.002	0.003
	4	1571.9	-37.90	-49.17	0.008	0.002	1475.0	-45.36	-45.29	0.004	0.004
	5	1590.8	-28.74	-48.93	0.021	0.002	1519.4	-34.45	-44.49	0.010	0.004
	AVG	**1591.1**	**-32.00**	**-49.76**	**0.015**	**0.002**	**1533.0**	**-43.21**	**-44.77**	**0.005**	**0.004**
PAV	1	1658.1	-36.53	-47.00	0.010	0.003	1377.1	-42.55	-43.59	0.006	0.004
	2	1616.4	-32.16	-45.92	0.014	0.003	1523.0	-35.41	-42.00	0.010	0.005
	3	1616.3	-30.53	-49.59	0.016	0.002	1511.7	-28.54	-44.38	0.022	0.004
	4	1613.6	-30.12	-51.86	0.019	0.002	1548.0	-39.47	-45.35	0.006	0.003
	5	1636.3	-30.09	-50.51	0.019	0.002	1580.5	-33.98	-44.80	0.012	0.004
	AVG	**1628.1**	**-30.73**	**-48.97**	**0.016**	**0.002**	**1540.8**	**-35.99**	**-44.02**	**0.011**	**0.004**

	Temperature	70◦C				
	Sample #	Vel	IR1	IR2	A1	A2
Original	1	1436.4	-37.84	-28.72	0.007	0.022
	2	1418.2	-37.16	-30.17	0.008	0.018
	3	1436.3	-38.45	-30.75	0.007	0.017
	4	1463.1	-33.27	-35.69	0.011	0.011
	5	1304.7	-44.25	-35.92	0.006	0.010
	AVG	**1438.5**	**-37.81**	**-29.88**	**0.008**	**0.016**
RTFO	1	1483.2	-40.78	-34.93	0.005	0.011
	2	1480.6	-41.41	-36.00	0.004	0.010
	3	1427.0	-35.07	-33.89	0.010	0.012
	4	1340.0	-42.82	-40.92	0.005	0.006
	5	1466.3	-36.22	-40.23	0.008	0.006
	AVG	**1464.2**	**-39.26**	**-37.19**	**0.006**	**0.009**
PAV	1	1511.8	-42.25	-39.37	0.005	0.006
	2	1522.3	-40.88	-38.84	0.005	0.007
	3	1398.5	-38.18	-42.84	0.007	0.005
	4	1410.0	-41.27	-43.21	0.004	0.004
	5	1622.0	-47.50	-43.71	0.002	0.005
	AVG	**1460.7**	**-41.47**	**-43.25**	**0.004**	**0.005**

Table B-6 PG 76-22E

	Temperature	30◦C					40◦C				
	Sample #	Vel	IR1	IR2	A1	A2	Vel	IR1	IR2	A1	A2
Original	1	1749.9	-24.04	-49.87	0.039	0.002	1604.0	-29.29	-48.64	0.020	0.002
	2	1702.6	-23.61	-46.45	0.039	0.002	1588.4	-27.78	-44.27	0.024	0.004
	3	1738.1	-26.83	-48.42	0.030	0.002	1635.5	-28.09	-46.52	0.023	0.003
	4	1740.5	-24.42	-44.79	0.037	0.003	1629.0	-26.93	-42.67	0.028	0.004
	5	1724.6	-26.95	-46.91	0.027	0.003	1613.6	-24.92	-42.83	0.034	0.004
	AVG	**1731.1**	**-24.02**	**-47.29**	**0.034**	**0.002**	**1614.1**	**-27.60**	**-44.07**	**0.027**	**0.004**
RTFO	1	1760.8	-22.95	-46.39	0.043	0.003	1650.6	-24.51	-42.63	0.036	0.004
	2	1736.6	-22.84	-44.87	0.043	0.003	1650.2	-28.93	-44.26	0.021	0.004
	3	1767.0	-22.49	-48.70	0.045	0.003	1650.2	-23.32	-44.43	0.041	0.004
	4	1732.1	-22.42	-44.69	0.046	0.003	1646.1	-28.16	-43.80	0.024	0.004
	5	1790.7	-24.42	-53.85	0.037	0.002	1669.9	-24.86	-47.22	0.034	0.004
	AVG	**1757.4**	**-22.68**	**-46.16**	**0.044**	**0.003**	**1653.4**	**-25.96**	**-43.78**	**0.031**	**0.004**
PAV	1	1779.7	-22.41	-46.32	0.046	0.003	1677.1	-24.56	-41.81	0.036	0.005
	2	1773.9	-22.28	-46.35	0.046	0.003	1703.9	-23.91	-47.68	0.039	0.003
	3	1804.3	-24.27	-48.03	0.038	0.003	1685.1	-24.69	-44.00	0.036	0.004
	4	1826.9	-25.93	-50.98	0.031	0.002	1667.5	-23.98	-41.49	0.039	0.005
	5	1762.2	-23.42	-45.23	0.039	0.003	1701.7	-23.09	-43.72	0.041	0.003
	AVG	**1789.4**	**-23.10**	**-46.48**	**0.042**	**0.003**	**1687.1**	**-24.05**	**-42.75**	**0.038**	**0.004**

	Temperature	50◦C					60◦C				
	Sample #	Vel	IR1	IR2	A1	A2	Vel	IR1	IR2	A1	A2
Original	1	1501.5	-35.37	-39.61	0.010	0.005	1430.0	-34.52	-30.52	0.011	0.017
	2	1514.2	-32.75	-38.12	0.014	0.007	1422.3	-33.14	-29.48	0.013	0.020
	3	1541.3	-29.88	-37.53	0.020	0.008	1445.2	-30.95	-29.42	0.017	0.020
	4	1531.0	-34.25	-35.58	0.012	0.010	1442.7	-36.60	-28.12	0.008	0.024
	5	1513.5	-32.17	-38.26	0.015	0.007	1434.1	-34.13	-30.42	0.012	0.019
	AVG	**1520.3**	**-33.05**	**-37.82**	**0.014**	**0.007**	**1434.9**	**-33.93**	**-29.59**	**0.012**	**0.020**
RTFO	1	1555.3	-31.51	-38.22	0.016	0.008	1470.7	-33.89	-30.90	0.012	0.017
	2	1557.6	-35.89	-39.97	0.010	0.006	1452.0	-39.59	-30.68	0.006	0.017
	3	1546.4	-28.95	-39.59	0.021	0.006	1456.4	-30.14	-32.75	0.019	0.014
	4	1552.3	-35.02	-40.51	0.011	0.006	1464.5	-37.77	-34.05	0.008	0.012
	5	1574.3	-32.28	-43.31	0.014	0.005	1478.2	-35.44	-35.60	0.011	0.011
	AVG	**1557.2**	**-32.73**	**-39.57**	**0.015**	**0.007**	**1464.4**	**-35.70**	**-32.57**	**0.013**	**0.014**
PAV	1	1585.0	-30.57	-40.53	0.018	0.006	1508.3	-35.80	-35.31	0.010	0.011
	2	1558.8	-31.09	-38.43	0.017	0.007	1502.7	-35.29	-35.38	0.011	0.011
	3	1579.3	-31.54	-39.09	0.016	0.007	1492.4	-38.36	-31.56	0.007	0.016
	4	1570.4	-31.78	-38.37	0.018	0.008	1512.7	-35.90	-33.38	0.009	0.013
	5	1610.4	-29.35	-44.05	0.020	0.004	1530.2	-42.14	-34.94	0.004	0.011
	AVG	**1580.8**	**-30.87**	**-39.10**	**0.017**	**0.007**	**1509.2**	**-36.34**	**-34.75**	**0.008**	**0.011**

	Temperature	70◦C				
	Sample #	Vel	IR1	IR2	A1	A2
Original	1	1366.4	-28.94	-23.93	0.036	0.020
	2	1370.1	-27.24	-23.58	0.025	0.040
	3	1382.5	-27.42	-22.48	0.024	0.042
	4	1377.1	-27.59	-21.27	0.024	0.054
	5	1358.1	-28.72	-25.01	0.021	0.036
	AVG	**1370.8**	**-27.98**	**-23.75**	**0.027**	**0.035**
RTFO	1	1381.7	-30.59	-23.93	0.017	0.038
	2	1380.3	-33.08	-25.17	0.013	0.032
	3	1369.1	-29.28	-27.05	0.020	0.028
	4	1376.2	-36.97	-25.85	0.008	0.032
	5	1392.5	-32.99	-29.87	0.014	0.022
	AVG	**1379.9**	**-32.22**	**-26.02**	**0.014**	**0.031**
PAV	1	1435.9	-31.94	-27.54	0.014	0.026
	2	1435.0	-32.75	-28.71	0.013	0.022
	3	1423.2	-32.16	-27.06	0.014	0.024
	4	1451.4	-31.94	-30.86	0.015	0.018
	5	1457.2	-31.25	-31.79	0.016	0.016
	AVG	**1440.5**	**-32.01**	**-29.04**	**0.014**	**0.022**

Table B-7 PG64-10

	Temperature	30◦C					40◦C				
	Sample #	Vel	IR1	IR2	A1	A2	Vel	IR1	IR2	A1	A2
Original	1	1787.5	-20.75	-40.12	0.055	0.006	1702.4	-24.58	-46.59	0.035	0.004
	2	1825.8	-21.30	-38.37	0.051	0.006	1718.2	-22.44	-42.49	0.044	0.005
	3	1799.2	-22.95	-39.81	0.042	0.006	1719.4	-26.21	-47.85	0.028	0.003
	4	1814.7	-20.68	-38.47	0.055	0.007	1708.3	-23.70	-43.38	0.038	0.004
	5	1814.0	-21.59	-40.48	0.050	0.006	1692.9	-23.80	-43.18	0.039	0.004
	AVG	**1808.2**	**-21.08**	**-39.45**	**0.051**	**0.006**	**1708.3**	**-24.03**	**-43.91**	**0.037**	**0.004**
RTFO	1	1833.5	-20.09	-38.01	0.060	0.007	1729.2	-22.54	-41.67	0.044	0.005
	2	1803.9	-19.93	-38.29	0.061	0.007	1731.4	-25.53	-44.36	0.031	0.004
	3	1836.0	-20.39	-38.54	0.058	0.006	1753.5	-23.24	-47.02	0.041	0.003
	4	1841.2	-21.45	-39.79	0.050	0.006	1720.8	-23.49	-43.74	0.040	0.004
	5	1828.4	-21.61	-38.71	0.049	0.006	1743.3	-25.45	-44.06	0.031	0.004
	AVG	**1828.6**	**-20.70**	**-38.67**	**0.056**	**0.006**	**1735.6**	**-24.05**	**-43.46**	**0.037**	**0.004**
PAV	1	1884.8	-21.04	-41.68	0.054	0.005	1756.8	-23.30	-43.06	0.040	0.004
	2	1869.8	-19.39	-38.30	0.065	0.007	1754.0	-21.30	-40.95	0.052	0.005
	3	1896.0	-20.38	-39.84	0.058	0.006	1776.4	-23.49	-43.23	0.040	0.004
	4	1929.6	-19.23	-44.05	0.064	0.004	1794.4	-21.58	-45.89	0.049	0.004
	5	1923.2	-19.04	-44.08	0.066	0.004	1765.7	-23.83	-40.14	0.038	0.006
	AVG	**1900.7**	**-19.51**	**-42.41**	**0.061**	**0.005**	**1769.4**	**-22.70**	**-41.84**	**0.043**	**0.005**
	Temperature	50◦C					60◦C				
	Sample #	Vel	IR1	IR2	A1	A2	Vel	IR1	IR2	A1	A2
Original	1	1606.7	-41.07	-46.32	0.005	0.003	1486.0	-36.41	-41.65	0.008	0.005
	2	1613.7	-36.82	-44.28	0.008	0.004	1545.3	-40.95	-42.26	0.005	0.005
	3	1580.3	-26.45	-43.74	0.028	0.004	1502.3	-35.23	-42.45	0.010	0.004
	4	1605.7	-28.57	-44.23	0.021	0.004	1525.5	-31.77	-42.18	0.015	0.005
	5	1580.1	-26.37	-43.87	0.028	0.004	1513.6	-34.37	-42.49	0.010	0.005
	AVG	**1597.3**	**-31.86**	**-44.49**	**0.018**	**0.004**	**1514.5**	**-35.74**	**-42.20**	**0.010**	**0.005**
RTFO	1	1613.4	-25.96	-42.89	0.029	0.004	1512.9	-41.42	-40.28	0.005	0.006
	2	1613.1	-29.64	-43.77	0.019	0.004	1528.7	-36.54	-41.77	0.008	0.005
	3	1647.9	-27.73	-48.76	0.024	0.003	1545.7	-44.00	-43.97	0.003	0.004
	4	1622.1	-26.09	-44.01	0.028	0.004	1530.4	-39.34	-41.02	0.006	0.005
	5	1632.1	-29.93	-43.08	0.019	0.004	1544.5	-35.61	-40.57	0.009	0.006
	AVG	**1625.7**	**-27.87**	**-43.44**	**0.024**	**0.004**	**1532.5**	**-39.10**	**-40.91**	**0.007**	**0.006**
PAV	1	1631.7	-27.68	-43.68	0.024	0.004	1538.2	-30.77	-42.17	0.017	0.004
	2	1643.4	-25.20	-41.33	0.032	0.005	1567.9	-33.15	-44.76	0.013	0.004
	3	1648.1	-26.21	-41.12	0.029	0.005	1559.3	-31.42	-40.05	0.016	0.006
	4	1680.5	-25.62	-46.72	0.031	0.004	1589.4	-33.47	-44.46	0.012	0.004
	5	1672.8	-25.84	-46.09	0.030	0.003	1564.4	-31.48	-42.55	0.016	0.004
	AVG	**1655.3**	**-26.11**	**-43.05**	**0.029**	**0.004**	**1563.8**	**-32.06**	**-43.48**	**0.015**	**0.004**
	Temperature	70◦C									
	Sample #	Vel	IR1	IR2	A1	A2					
Original	1	1429.8	-32.16	-38.91	0.012	0.007					
	2	1490.5	-38.57	-35.68	0.007	0.010					
	3	1415.5	-33.29	-35.62	0.013	0.010					
	4	1461.7	-33.99	-38.22	0.012	0.008					
	5	1525.7	-37.41	-42.77	0.007	0.005					
	AVG	**1464.7**	**-35.09**	**-37.11**	**0.010**	**0.008**					
RTFO	1	1479.5	-44.06	-36.04	0.003	0.010					
	2	1454.2	-42.03	-38.55	0.004	0.008					
	3	1450.3	-38.65	-38.91	0.004	0.005					
	4	1465.5	-37.99	-40.95	0.006	0.007					
	5	1480.7	-37.32	-43.00	0.008	0.005					
	AVG	**1466.1**	**-40.01**	**-39.47**	**0.005**	**0.007**					
PAV	1	1478.5	-36.82	-41.04	0.009	0.005					
	2	1473.8	-36.69	-40.45	0.009	0.006					
	3	1499.0	-38.37	-39.81	0.007	0.006					
	4	1530.4	-40.47	-40.88	0.005	0.005					
	5	1493.6	-37.22	-42.26	0.008	0.005					
	AVG	**1495.1**	**-37.28**	**-40.89**	**0.007**	**0.005**					

Table B-8 PG76-10

	Temperature	30◦C					40◦C				
	Sample #	Vel	IR1	IR2	A1	A2	Vel	IR1	IR2	A1	A2
Original	1	1820.9	-18.85	-37.23	0.066	0.008	1747.4	-21.95	-47.34	0.046	0.003
	2	1850.8	-18.22	-39.08	0.073	0.006	1765.0	-22.08	-50.09	0.046	0.003
	3	1869.1	-18.88	-37.87	0.067	0.008	1742.5	-22.03	-44.21	0.047	0.004
	4	1843.3	-19.92	-37.44	0.060	0.008	1738.8	-21.66	-46.35	0.048	0.003
	5	1843.7	-19.01	-37.00	0.066	0.007	1723.4	-21.44	-47.62	0.050	0.003
	AVG	**1845.6**	**-18.98**	**-37.72**	**0.066**	**0.007**	**1743.4**	**-21.83**	**-47.12**	**0.047**	**0.003**
RTFO	1	1862.5	-18.58	-37.34	0.071	0.007	1749.8	-21.33	-44.44	0.052	0.004
	2	1902.2	-18.76	-39.01	0.070	0.007	1798.1	-20.95	-49.13	0.054	0.002
	3	1875.5	-18.21	-36.99	0.075	0.008	1755.9	-21.96	-41.89	0.048	0.005
	4	1896.6	-19.09	-39.73	0.066	0.006	1748.3	-21.98	-43.22	0.048	0.004
	5	1941.2	-18.27	-39.35	0.073	0.008	1824.1	-21.27	-49.21	0.052	0.002
	AVG	**1895.6**	**-18.58**	**-38.48**	**0.071**	**0.007**	**1775.3**	**-21.50**	**-45.58**	**0.051**	**0.003**
PAV	1	1943.6	-17.73	-37.16	0.080	0.008	1801.5	-21.09	-41.38	0.053	0.005
	2	1930.6	-18.22	-34.49	0.073	0.010	1804.7	-21.15	-41.02	0.053	0.005
	3	1980.4	-17.77	-40.32	0.080	0.006	1805.7	-20.83	-42.12	0.054	0.005
	4	1992.9	-17.78	-42.40	0.079	0.004	1855.1	-21.65	-49.49	0.050	0.002
	5	1892.1	-17.53	-34.02	0.080	0.010	1806.9	-21.50	-43.14	0.051	0.004
	AVG	**1947.9**	**-17.80**	**-37.68**	**0.078**	**0.008**	**1814.8**	**-21.24**	**-41.92**	**0.053**	**0.005**
	Temperature	50◦C					60◦C				
	Sample #	Vel	IR1	IR2	A1	A2	Vel	IR1	IR2	A1	A2
Original	1	1631.0	-26.36	-46.69	0.027	0.003	1538.4	-34.52	-40.56	0.011	0.006
	2	1632.1	-25.59	-46.99	0.030	0.003	1583.6	-32.45	-43.61	0.014	0.004
	3	1634.7	-26.07	-46.27	0.030	0.003	1558.2	-31.79	-43.33	0.015	0.004
	4	1636.6	-26.04	-47.31	0.029	0.003	1520.0	-32.74	-42.82	0.014	0.004
	5	1639.6	-26.83	-46.23	0.027	0.003	1547.4	-32.88	-44.80	0.013	0.004
	AVG	**1634.8**	**-26.18**	**-46.70**	**0.029**	**0.003**	**1549.5**	**-32.88**	**-43.03**	**0.013**	**0.004**
RTFO	1	1651.9	-26.05	-47.65	0.030	0.003	1543.7	-33.59	-43.95	0.012	0.004
	2	1648.9	-25.21	-45.39	0.032	0.003	1555.8	-31.81	-44.28	0.015	0.004
	3	1641.7	-25.83	-44.85	0.030	0.004	1546.8	-33.05	-43.83	0.013	0.004
	4	1639.7	-26.56	-45.42	0.028	0.003	1547.2	-31.96	-46.05	0.015	0.003
	5	1664.4	-25.82	-45.02	0.030	0.004	1588.0	-39.55	-46.31	0.006	0.003
	AVG	**1649.3**	**-25.89**	**-45.66**	**0.030**	**0.003**	**1556.3**	**-32.60**	**-44.88**	**0.012**	**0.004**
PAV	1	1692.0	-24.34	-43.55	0.036	0.004	1605.1	-28.49	-42.94	0.022	0.004
	2	1696.0	-24.97	-43.60	0.033	0.004	1617.8	-30.51	-43.73	0.018	0.004
	3	1709.5	-24.60	-45.44	0.035	0.004	1639.6	-30.03	-46.96	0.019	0.003
	4	1696.9	-25.05	-44.81	0.033	0.004	1608.2	-30.25	-44.53	0.018	0.004
	5	1720.4	-24.90	-47.48	0.034	0.003	1609.1	-30.79	-45.78	0.017	0.003
	AVG	**1702.9**	**-24.77**	**-44.98**	**0.034**	**0.004**	**1616.0**	**-30.01**	**-44.79**	**0.019**	**0.004**
	Temperature	70◦C									
	Sample #	Vel	IR1	IR2	A1	A2					
Original	1	1501.9	-43.85	-33.80	0.004	0.012					
	2	1532.2	-35.40	-34.32	0.010	0.011					
	3	1489.6	-34.03	-33.30	0.011	0.013					
	4	1483.5	-33.39	-36.37	0.012	0.009					
	5	1525.4	-36.33	-35.33	0.009	0.010					
	AVG	**1506.5**	**-34.79**	**-34.62**	**0.009**	**0.011**					
RTFO	1	1475.7	-34.96	-37.67	0.011	0.008					
	2	1488.2	-38.18	-37.33	0.007	0.009					
	3	1482.2	-37.47	-37.09	0.008	0.008					
	4	1491.3	-37.19	-38.65	0.008	0.007					
	5	1480.4	-38.08	-37.16	0.007	0.009					
	AVG	**1483.5**	**-37.18**	**-37.58**	**0.008**	**0.008**					
PAV	1	1529.1	-39.63	-38.91	0.006	0.007					
	2	1537.2	-39.87	-41.18	0.006	0.006					
	3	1554.7	-35.28	-39.33	0.010	0.007					
	4	1524.4	-36.35	-41.43	0.009	0.006					
	5	1525.3	-38.90	-42.04	0.007	0.005					
	AVG	**1534.1**	**-38.69**	**-40.58**	**0.008**	**0.006**					

Table B-9 PG64-16

	Temperature	30◦C					40◦C				
	Sample #	Vel	IR1	IR2	A1	A2	Vel	IR1	IR2	A1	A2
Original	1	1824.9	-24.06	-49.06	0.038	0.004	1671.9	-23.31	-45.72	0.040	0.003
	2	1728.9	-22.71	-42.12	0.044	0.004	1726.7	-24.76	-50.06	0.035	0.002
	3	1840.5	-20.86	-45.23	0.054	0.003	1714.7	-27.42	-48.33	0.025	0.003
	4	1828.0	-25.60	-47.44	0.032	0.004	1636.2	-23.26	-46.62	0.041	0.002
	5	1809.4	-21.45	-42.09	0.031	0.004	1703.6	-26.68	-46.79	0.028	0.003
	AVG	**1806.3**	**-22.94**	**-44.22**	**0.040**	**0.004**	**1690.6**	**-24.50**	**-47.50**	**0.034**	**0.002**
RTFO	1	1823.4	-19.78	-39.22	0.062	0.007	1735.7	-27.43	-52.89	0.024	0.001
	2	1821.0	-23.43	-38.08	0.040	0.007	1716.6	-25.46	-50.91	0.032	0.002
	3	1841.3	-18.56	-39.33	0.072	0.007	1767.2	-30.14	-54.42	0.019	0.002
	4	1839.0	-21.93	-41.82	0.048	0.005	1748.5	-26.67	-53.80	0.028	0.001
	5	1832.1	-23.71	-40.18	0.039	0.006	1740.3	-31.02	-51.12	0.017	0.002
	AVG	**1831.4**	**-21.48**	**-39.73**	**0.052**	**0.006**	**1741.7**	**-28.15**	**-52.62**	**0.024**	**0.001**
PAV	1	1873.8	-19.67	-38.24	0.063	0.008	1778.0	-26.08	-49.88	0.031	0.002
	2	1864.3	-19.82	-38.26	0.063	0.008	1781.6	-26.82	-49.91	0.028	0.002
	3	1850.0	-23.54	-38.27	0.040	0.007	1730.0	-29.83	-47.68	0.020	0.003
	4	1869.4	-18.65	-36.57	0.071	0.009	1767.8	-26.67	-46.86	0.029	0.003
	5	1844.1	-19.69	-36.72	0.063	0.008	1781.1	-26.22	-51.64	0.030	0.002
	AVG	**1860.3**	**-19.46**	**-37.61**	**0.060**	**0.008**	**1767.7**	**-26.45**	**-49.19**	**0.028**	**0.002**

	Temperature	50◦C					60◦C				
	Sample #	Vel	IR1	IR2	A1	A2	Vel	IR1	IR2	A1	A2
Original	1	1559.7	-28.75	-46.17	0.021	0.003	1507.8	-36.87	-44.63	0.008	0.004
	2	1622.4	-27.41	-50.95	0.025	0.002	1512.9	-43.35	-45.91	0.003	0.003
	3	1606.4	-28.12	-49.60	0.024	0.002	1528.6	-37.18	-47.58	0.008	0.003
	4	1592.8	-26.76	-50.65	0.027	0.002	1507.8	-37.45	-49.14	0.008	0.002
	5	1580.5	-30.56	-46.62	0.018	0.004	1499.0	-40.99	-44.99	0.005	0.004
	AVG	**1592.4**	**-27.76**	**-48.80**	**0.023**	**0.003**	**1511.2**	**-38.12**	**-46.45**	**0.006**	**0.003**
RTFO	1	1624.1	-33.85	-52.60	0.012	0.002	1628.8	-47.55	-46.03	0.002	0.003
	2	1680.7	-37.35	-47.34	0.008	0.002	1630.9	-35.82	-46.02	0.008	0.004
	3	1658.3	-34.21	-50.14	0.012	0.002	1754.8	-44.32	-48.65	0.032	0.002
	4	1649.4	-30.24	-54.66	0.018	0.001	1615.9	-26.29	-52.55	0.028	0.001
	5	1642.9	-32.53	-48.23	0.014	0.002	1633.7	-35.42	-41.90	0.010	0.004
	AVG	**1651.1**	**-33.63**	**-49.58**	**0.012**	**0.002**	**1627.3**	**-37.88**	**-46.90**	**0.014**	**0.003**
PAV	1	1647.8	-29.95	-47.72	0.020	0.002	1463.0	-32.33	-43.96	0.013	0.004
	2	1691.0	-41.33	-47.97	0.005	0.002	1439.4	-35.33	-45.31	0.008	0.003
	3	1643.0	-34.75	-47.14	0.012	0.003	1482.2	-41.94	-44.18	0.005	0.004
	4	1587.3	-29.54	-48.03	0.020	0.002	1412.4	-35.78	-45.17	0.010	0.003
	5	1649.8	-32.77	-47.69	0.014	0.003	1461.0	-36.35	-41.87	0.008	0.005
	AVG	**1643.8**	**-31.76**	**-47.71**	**0.014**	**0.002**	**1451.6**	**-34.95**	**-44.10**	**0.009**	**0.004**

	Temperature	70◦C				
	Sample #	Vel	IR1	IR2	A1	A2
Original	1	1443.8	-33.48	-33.67	0.012	0.011
	2	1440.1	-33.14	-33.08	0.012	0.012
	3	1459.7	-32.84	-37.60	0.013	0.008
	4	1451.9	-34.47	-34.96	0.011	0.012
	5	1432.2	-33.31	-32.06	0.012	0.016
	AVG	**1445.5**	**-33.45**	**-33.44**	**0.012**	**0.013**
RTFO	1	1429.7	-40.65	-48.13	0.005	0.002
	2	1569.9	-42.20	-34.04	0.004	0.012
	3	1495.1	-27.35	-40.44	0.024	0.005
	4	1484.8	-29.31	-43.87	0.020	0.004
	5	1509.5	-36.77	-36.78	0.009	0.009
	AVG	**1497.8**	**-35.26**	**-40.36**	**0.018**	**0.006**
PAV	1	1533.4	-42.31	-36.47	0.005	0.009
	2	1395.2	-44.56	-36.25	0.003	0.010
	3	1623.6	-47.56	-36.65	0.003	0.010
	4	1525.8	-45.15	-36.35	0.003	0.010
	5	1552.3	-42.04	-36.99	0.005	0.009
	AVG	**1537.2**	**-43.52**	**-36.54**	**0.003**	**0.009**

Table B-10 PG58-28

	Temperature	30◦C					40◦C				
	Sample #	Vel	IR1	IR2	A1	A2	Vel	IR1	IR2	A1	A2
Original	1	1739.9	-26.86	-47.96	0.027	0.003	1618.7	-26.11	-48.06	0.029	0.003
	2	1746.2	-24.92	-48.21	0.035	0.003	1621.2	-29.84	-48.09	0.019	0.002
	3	1735.9	-22.52	-49.18	0.045	0.002	1680.0	-32.05	-52.78	0.015	0.002
	AVG	**1740.7**	**-24.77**	**-48.45**	**0.036**	**0.003**	**1639.9**	**-29.33**	**-48.08**	**0.024**	**0.002**
	Temperature	50◦C					60◦C				
	Sample #	Vel	IR1	IR2	A1	A2	Vel	IR1	IR2	A1	A2
Original	1	1506.4	-36.14	-46.55	0.009	0.003	1451.3	-38.61	-39.41	0.006	0.006
	2	1457.9	-40.26	-45.55	0.006	0.003	1430.1	-42.98	-40.98	0.004	0.006
	3	1501.2	-35.61	-45.11	0.010	0.004	1427.5	-41.13	-41.01	0.005	0.005
	AVG	**1488.5**	**-35.88**	**-45.73**	**0.008**	**0.003**	**1436.3**	**-40.91**	**-40.47**	**0.005**	**0.006**
	Temperature	70◦C									
	Sample #	Vel	IR1	IR2	A1	A2					
Original	1	1394.1	-35.75	-31.75	0.010	0.016					
	2	1361.6	-37.41	-26.22	0.007	0.030					
	3	1378.0	-30.44	-29.50	0.017	0.023					
	AVG	**1377.9**	**-34.53**	**-29.16**	**0.011**	**0.023**					

Table B-11 PG 70-28

	Temperature	30◦C					40◦C				
	Sample #	Vel	IR1	IR2	A1	A2	Vel	IR1	IR2	A1	A2
Original	1	1734.3	-24.67	-46.25	0.036	0.004	1644.0	-26.87	-45.82	0.027	0.004
	2	1771.0	-23.92	-49.16	0.039	0.003	1643.7	-27.55	-46.32	0.025	0.003
	3	1777.3	-23.70	-47.83	0.040	0.003	1653.9	-27.59	-45.73	0.025	0.003
	AVG	**1760.8**	**-24.09**	**-47.75**	**0.038**	**0.003**	**1647.2**	**-27.33**	**-45.95**	**0.026**	**0.003**
	Temperature	50◦C					60◦C				
	Sample #	Vel	IR1	IR2	A1	A2	Vel	IR1	IR2	A1	A2
Original	1	1544.1	-33.29	-41.41	0.013	0.005	1466.2	-37.97	-37.72	0.008	0.008
	2	1546.8	-33.86	-42.15	0.012	0.004	1483.9	-38.80	-39.83	0.007	0.007
	3	1548.6	-34.73	-41.13	0.011	0.006	1517.1	-38.30	-44.62	0.007	0.004
	AVG	**1546.5**	**-33.96**	**-41.56**	**0.012**	**0.005**	**1489.1**	**-38.35**	**-38.77**	**0.007**	**0.007**
	Temperature	70◦C									
	Sample #	Vel	IR1	IR2	A1	A2					
Original	1	1380.4	-31.72	-28.48	0.015	0.024					
	2	1396.9	-32.96	-29.14	0.013	0.022					
	3	1397.4	-33.54	-26.96	0.012	0.026					
	AVG	**1391.6**	**-32.74**	**-28.19**	**0.013**	**0.024**					

Table B-12 PG76-28

	Temperature	30◦C					40◦C				
	Sample #	Vel	IR1	IR2	A1	A2	Vel	IR1	IR2	A1	A2
Original	1	1763.3	-23.22	-49.41	0.0420	0.0020	1658.3	-26.64	-49.18	0.0280	0.0020
	2	1726.8	-27.79	-47.85	0.0250	0.0025	1630.9	-26.60	-44.76	0.0280	0.0037
	3	1734.8	-26.41	-48.19	0.0290	0.0025	1617.0	-27.88	-44.68	0.0240	0.0040
	AVG	**1741.6**	**-25.81**	**-48.48**	**0.0320**	**0.0023**	**1635.4**	**-27.04**	**-44.72**	**0.0260**	**0.0039**
	Temperature	50◦C					60◦C				
	Sample #	Vel	IR1	IR2	A1	A2	Vel	IR1	IR2	A1	A2
Original	1	1533.7	-38.16	-44.24	0.0078	0.0038	1425.5	-42.33	-37.79	0.0044	0.0072
	2	1515.3	-36.09	-40.45	0.0095	0.0050	1450.9	-39.31	-36.89	0.0064	0.0086
	3	1516.1	-32.93	-41.08	0.0130	0.0040	1432.3	-41.47	-37.79	0.0049	0.0079
	AVG	**1521.7**	**-35.73**	**-41.92**	**0.0101**	**0.0043**	**1436.2**	**-41.04**	**-37.49**	**0.0052**	**0.0079**
	Temperature	70◦C									
	Sample #	Vel	IR1	IR2	A1	A2					
Original	1	1412.1	-38.82	-25.83	0.0070	0.0300					
	2	1383.4	-31.05	-25.96	0.0160	0.0310					
	3	1386.6	-38.11	-26.53	0.0075	0.0280					
	AVG	**1394.1**	**-35.99**	**-26.11**	**0.0102**	**0.0297**					

Table B-13 PG58-34

	Temperature	30◦C					40◦C				
	Sample #	Vel	IR1	IR2	A1	A2	Vel	IR1	IR2	A1	A2
Original	1	1654.7	-27.80	-46.03	0.0240	0.0030	1577.7	-41.09	-49.75	0.0057	0.0020
	2	1674.2	-25.92	-47.76	0.0310	0.0020	1543.1	-37.19	-47.91	0.0080	0.0022
	3	1693.4	-24.74	-50.04	0.0340	0.0020	1582.2	-34.12	-50.33	0.0115	0.0020
	AVG	**1674.1**	**-26.15**	**-47.94**	**0.0297**	**0.0023**	**1567.7**	**-37.47**	**-49.33**	**0.0084**	**0.0021**
	Temperature	50◦C					60◦C				
	Sample #	Vel	IR1	IR2	A1	A2	Vel	IR1	IR2	A1	A2
Original	1	1429.3	-38.47	-39.46	0.0066	0.0064	1373.4	-29.96	-28.86	0.0170	0.0220
	2	1424.7	-37.07	-39.02	0.0080	0.0066	1379.7	-28.49	-28.59	0.0200	0.0230
	3	1498.8	-40.28	-38.22	0.0060	0.0078	1412.5	-36.52	-28.01	0.0090	0.0240
	AVG	**1450.9**	**-38.61**	**-38.90**	**0.0069**	**0.0069**	**1388.5**	**-31.66**	**-28.49**	**0.0153**	**0.0230**
	Temperature	70◦C									
	Sample #	Vel	IR1	IR2	A1	A2					
Original	1	1350.3	-30.89	-22.54	0.0160	0.0440					
	2	1274.1	-32.60	-23.94	0.0120	0.0038					
	3	1265.6	-40.53	-22.60	0.0500	0.0043					
	AVG	**1296.6**	**-34.68**	**-23.02**	**0.0260**	**0.0174**					

C. APPENDIX C;

Graphs of Variation of Ultrasound Measurments with Temparature

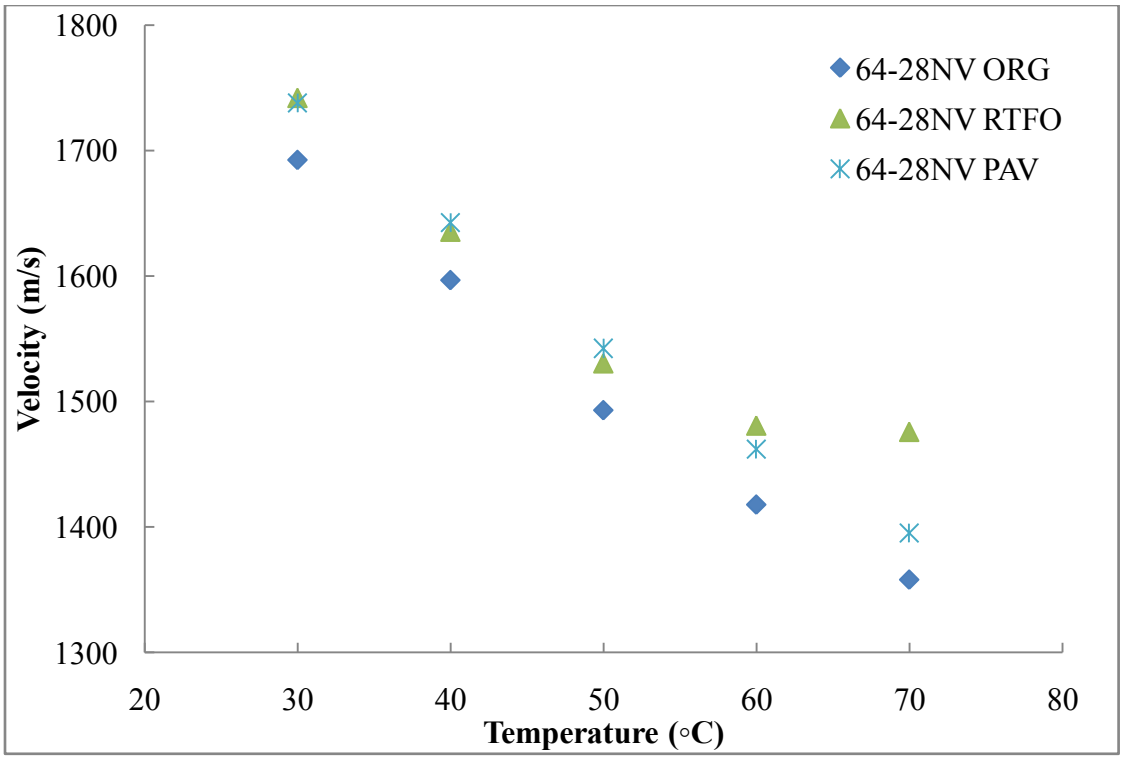

Figure C-1 Variation of Velocity with Temperature for PG 64-28NV

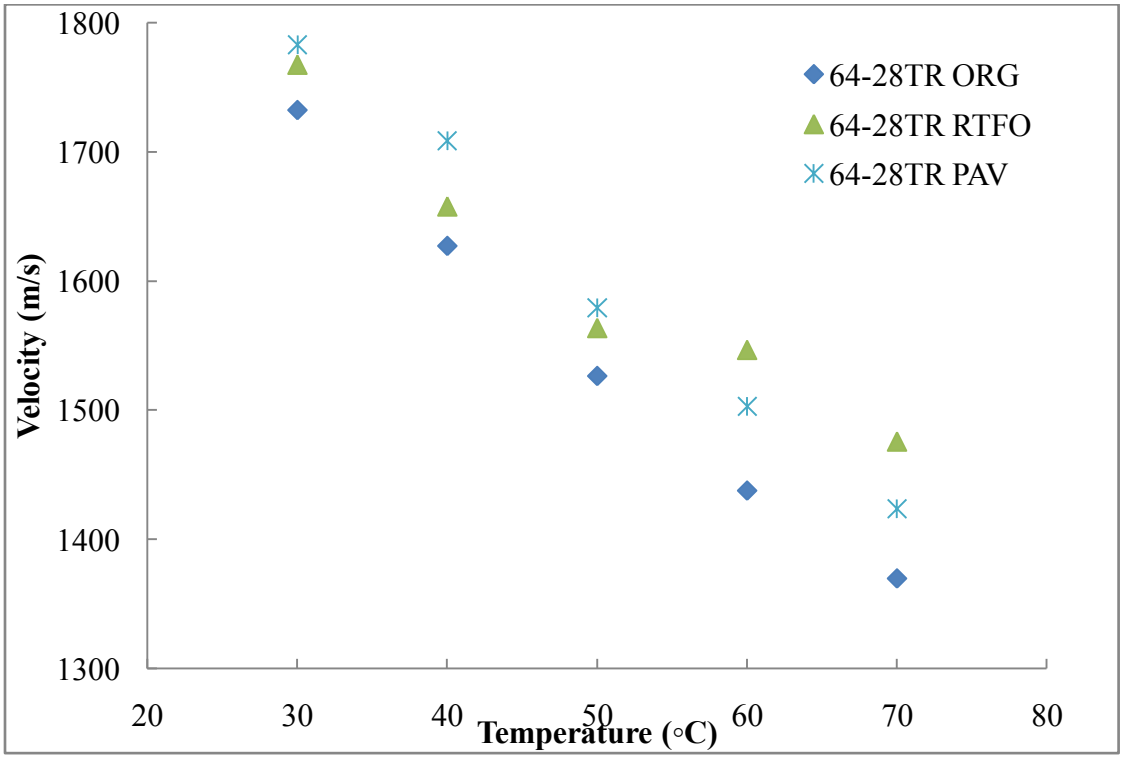

Figure C-2Variation of Velocity with Temperature for PG 64-28TR

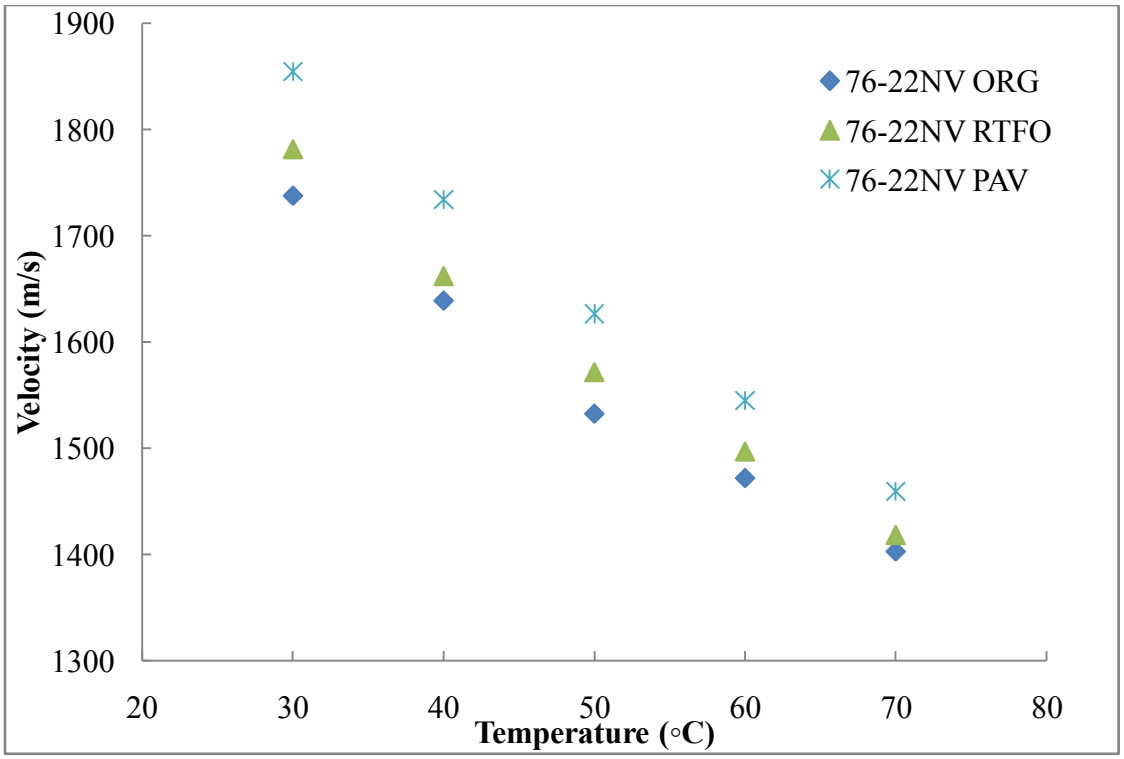

Figure C-3Variation of Velocity with Temperature for PG 76-22NV

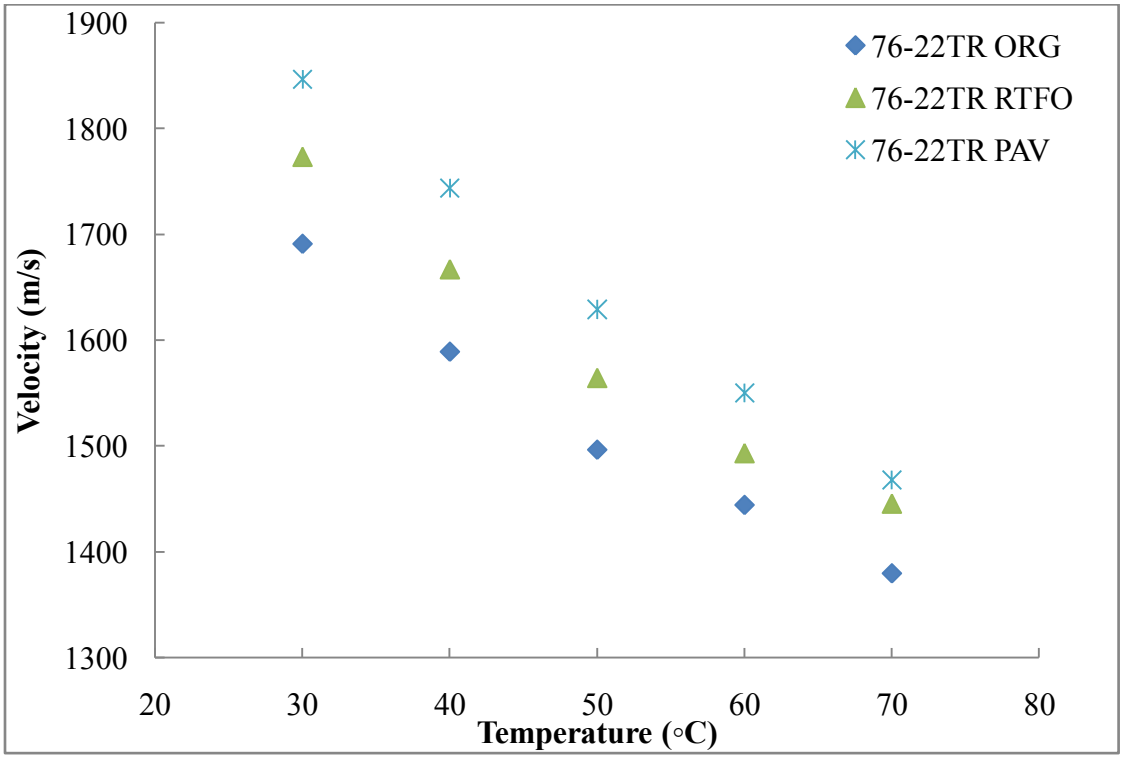

Figure C-4Variation of Velocity with Temperature for PG 76-22TR

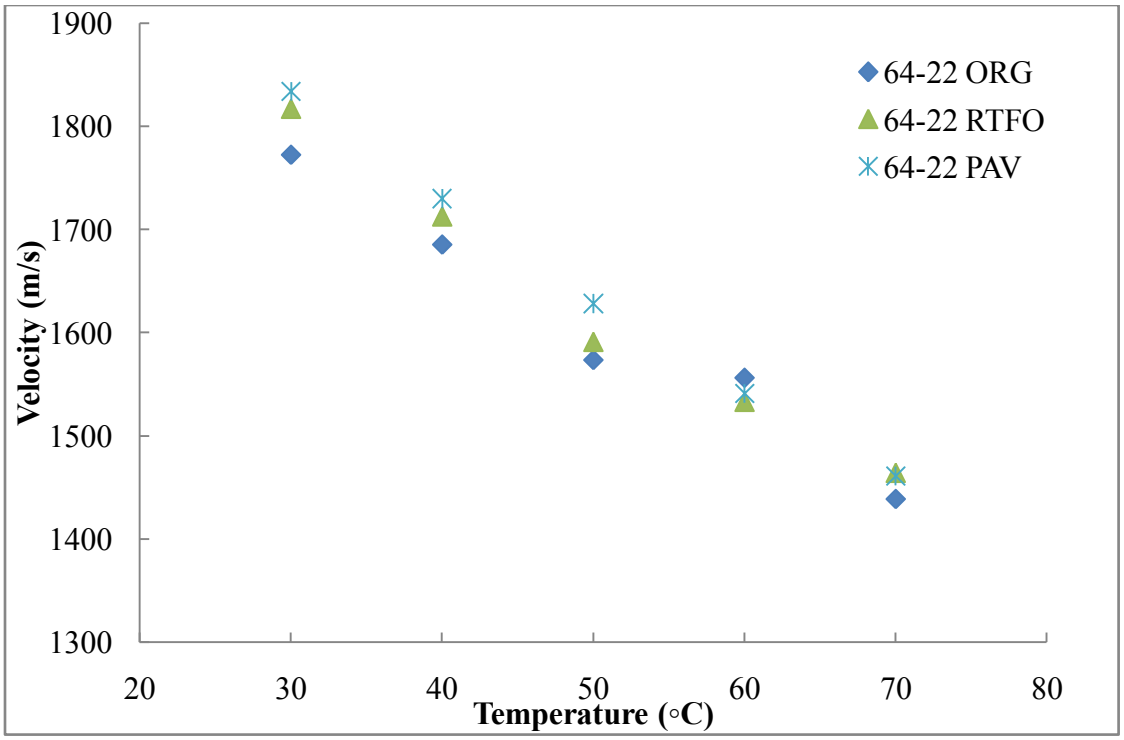

Figure C-5Variation of Velocity with Temperature for PG 64-22

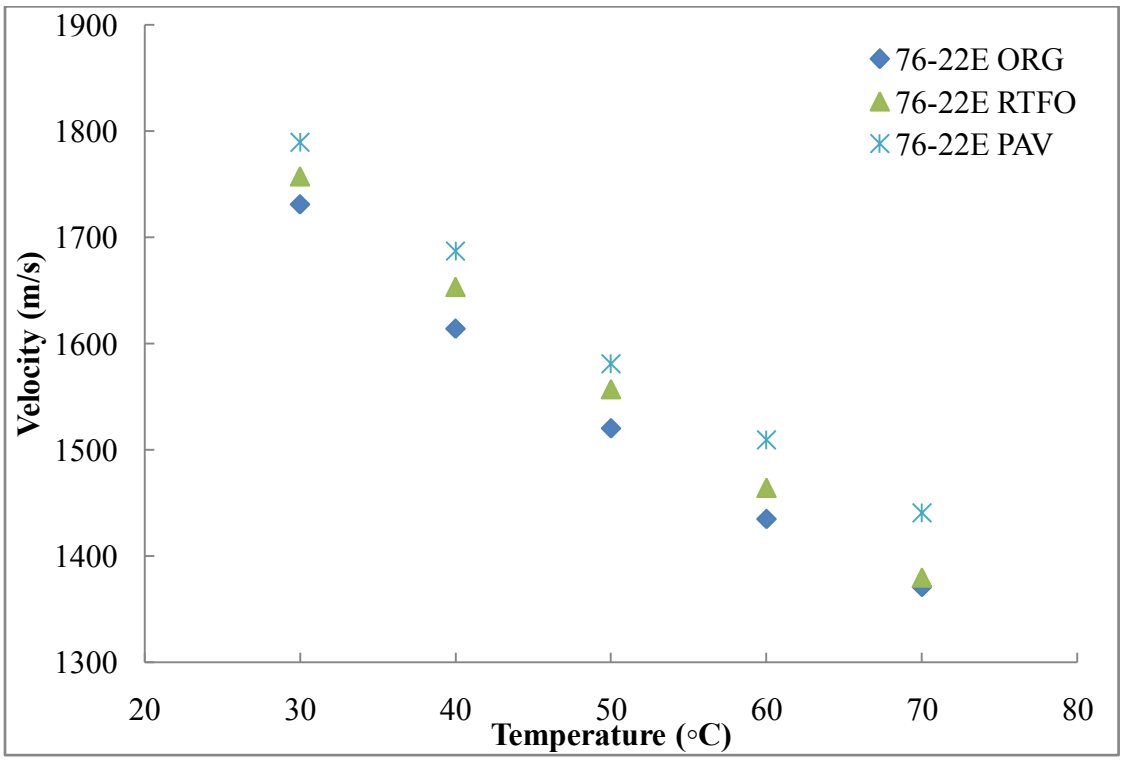

Figure C-6Variation of Velocity with Temperature for PG 76-22E

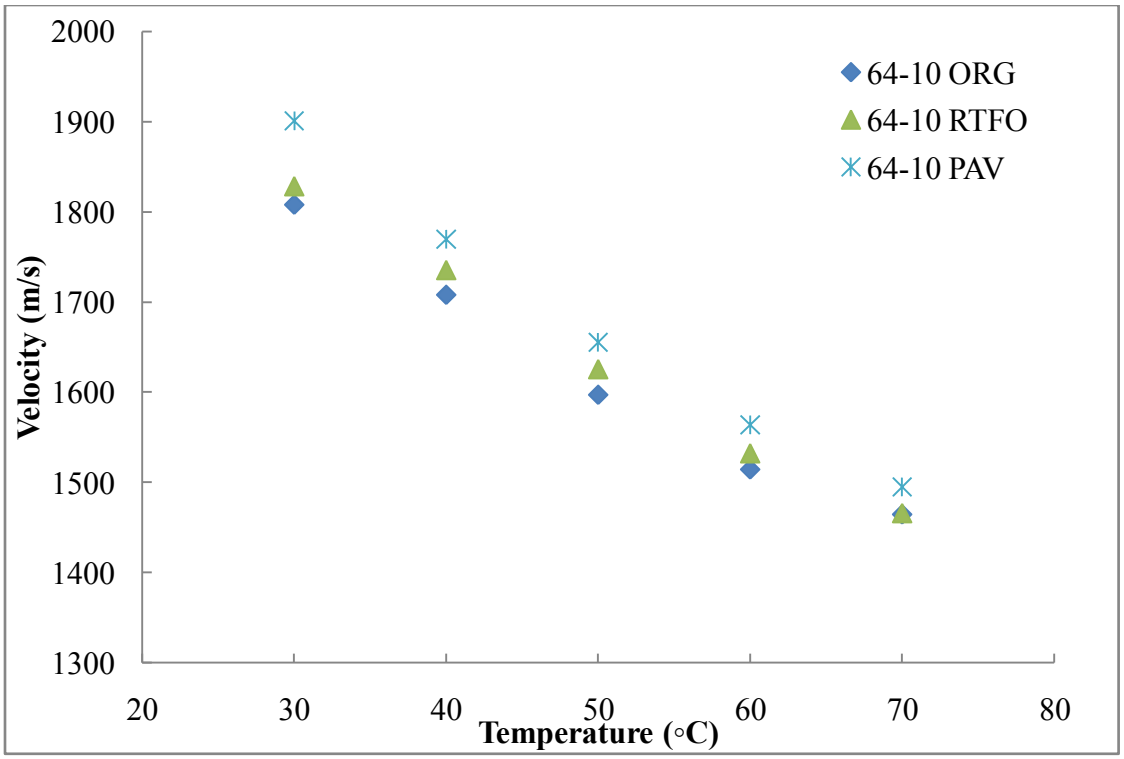

Figure C-7Variation of Velocity with Temperature for PG 64-10

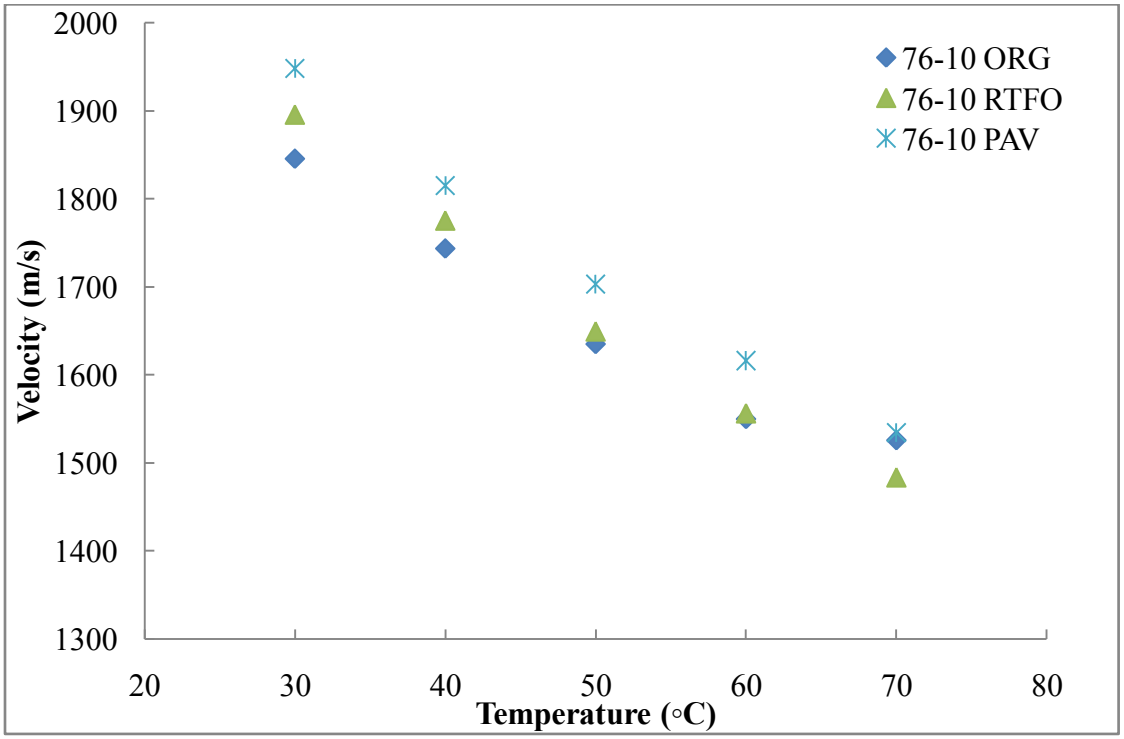

Figure C-8Variation of Velocity with Temperature for PG 76-10

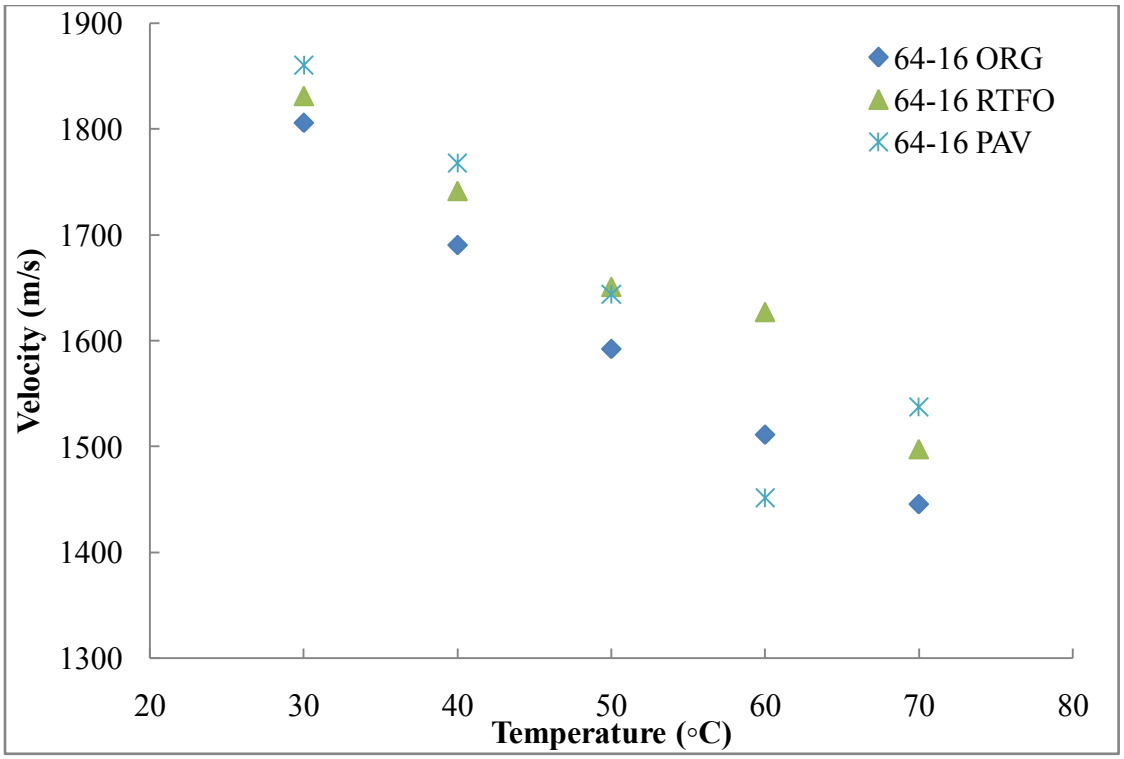

Figure C-9Variation of Velocity with Temperature for PG 64-16

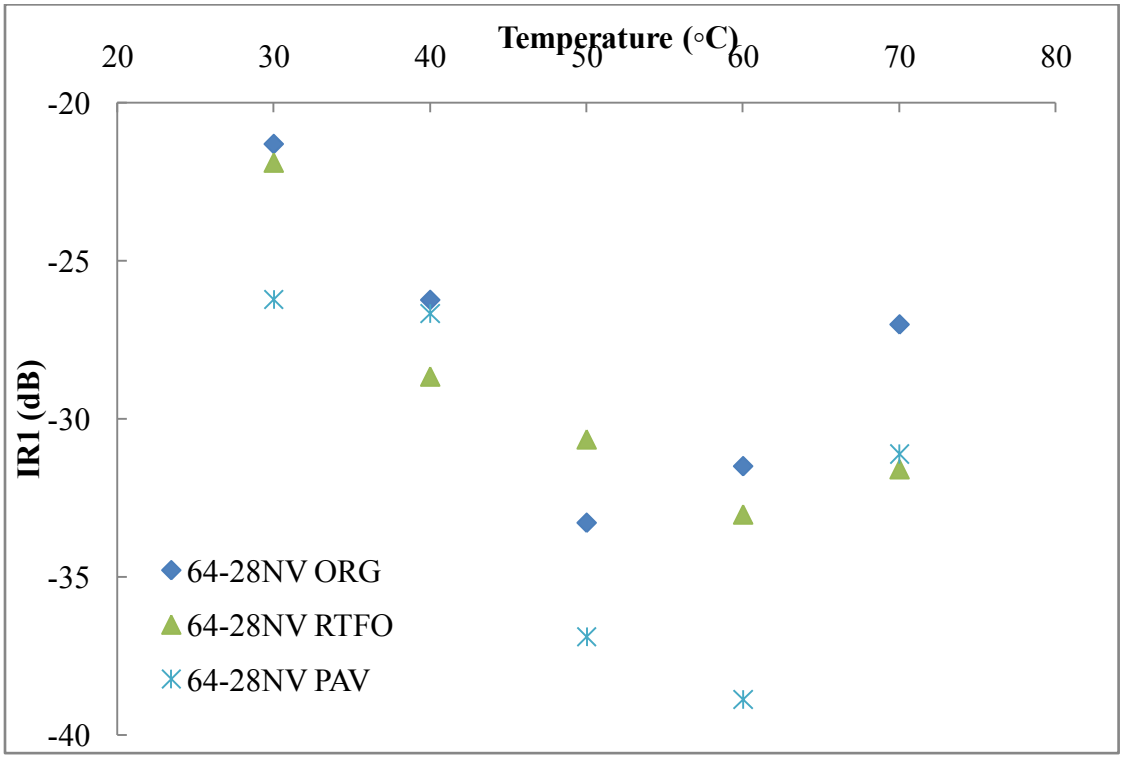

Figure C-10Variation of IR1 with Temperature for PG 64-28NV

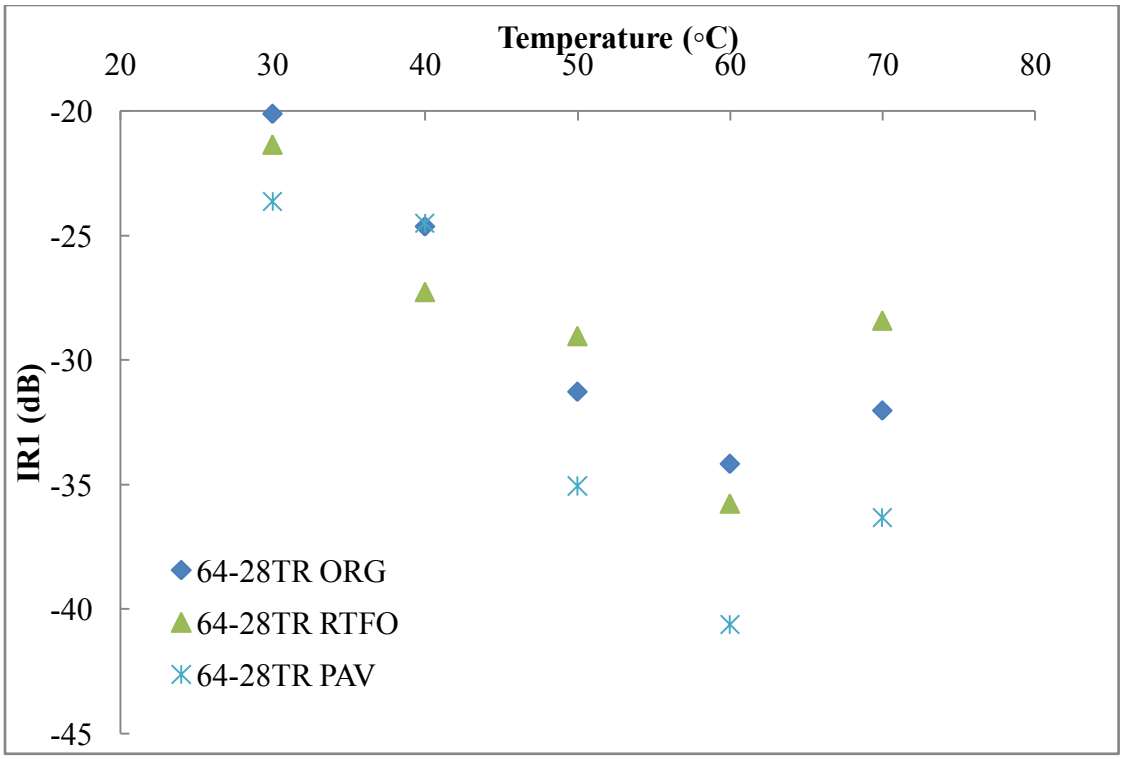

Figure C-11Variation of IR1 with Temperature for PG 64-28TR

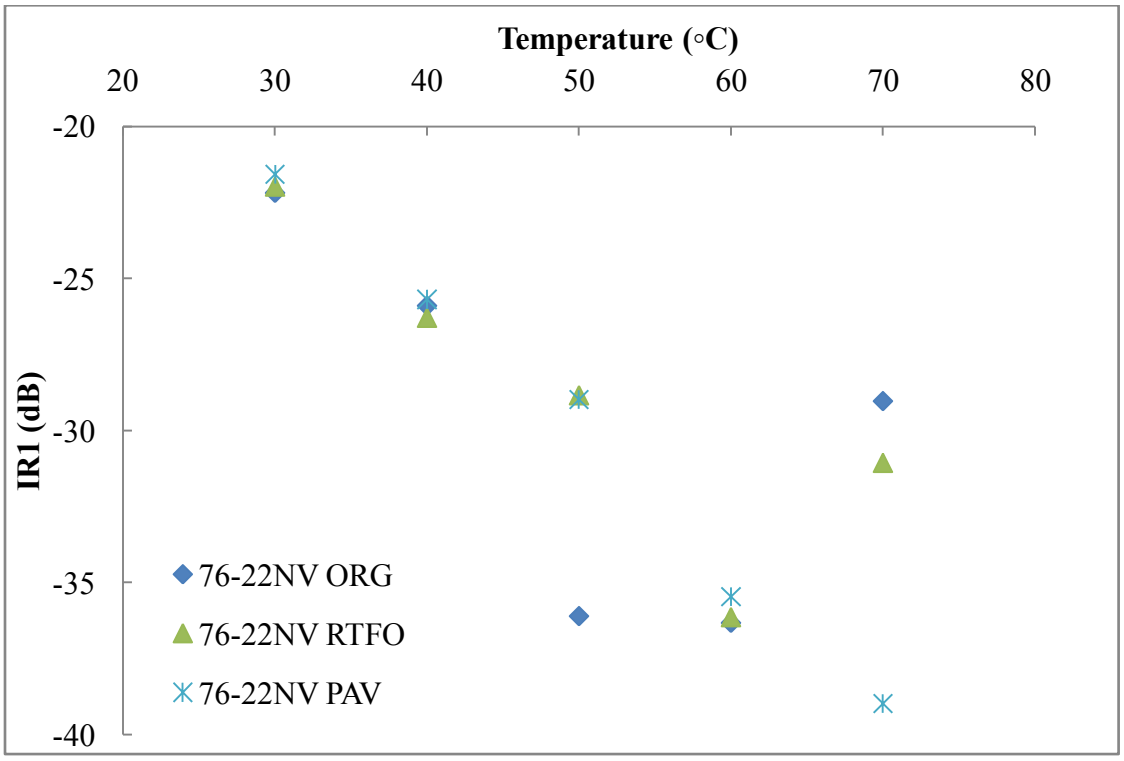

Figure C-12Variation of IR1 with Temperature for PG 76-22NV

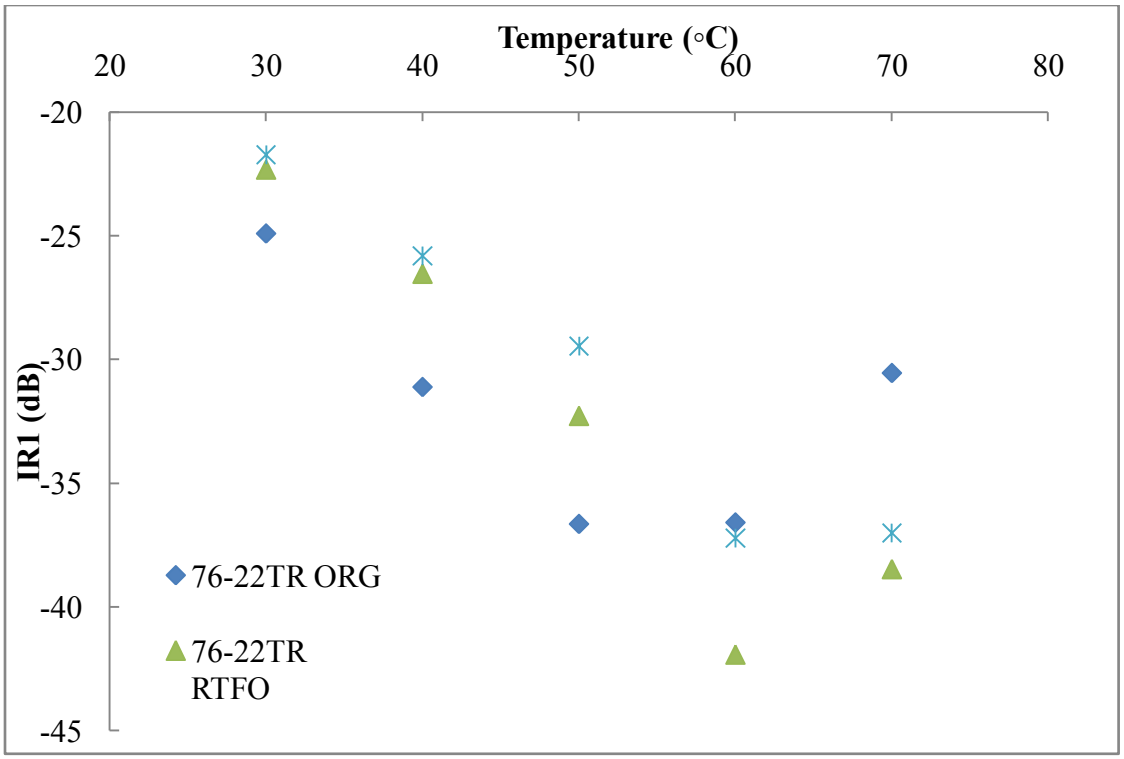

Figure C-13Variation of IR1 with Temperature for PG 76-22TR

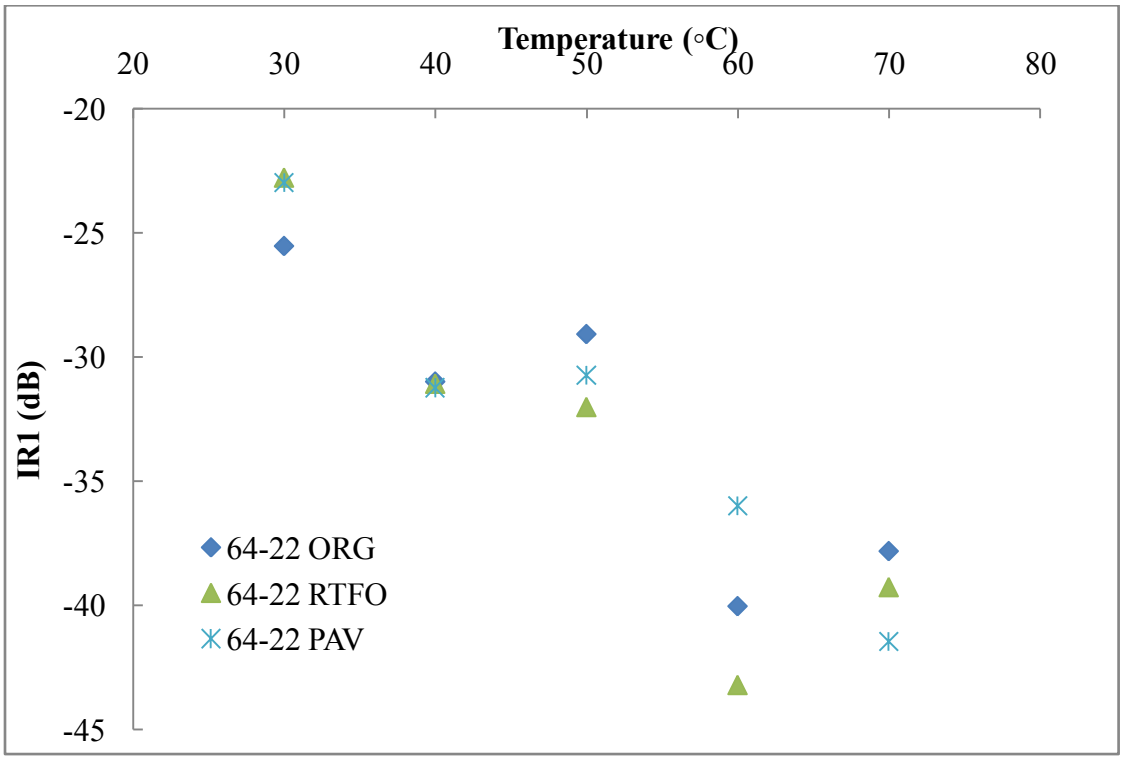

Figure C-14Variation of IR1 with Temperature for PG 64-22

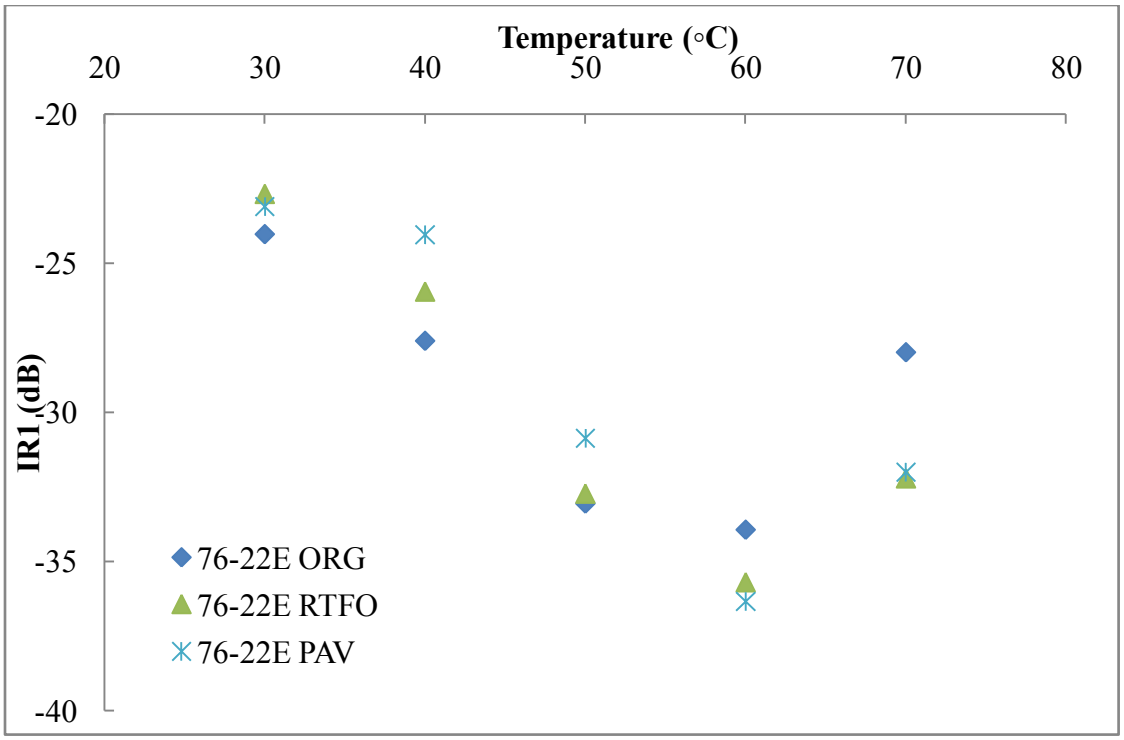

Figure C-15Variation of IR1 with Temperature for PG 76-22E

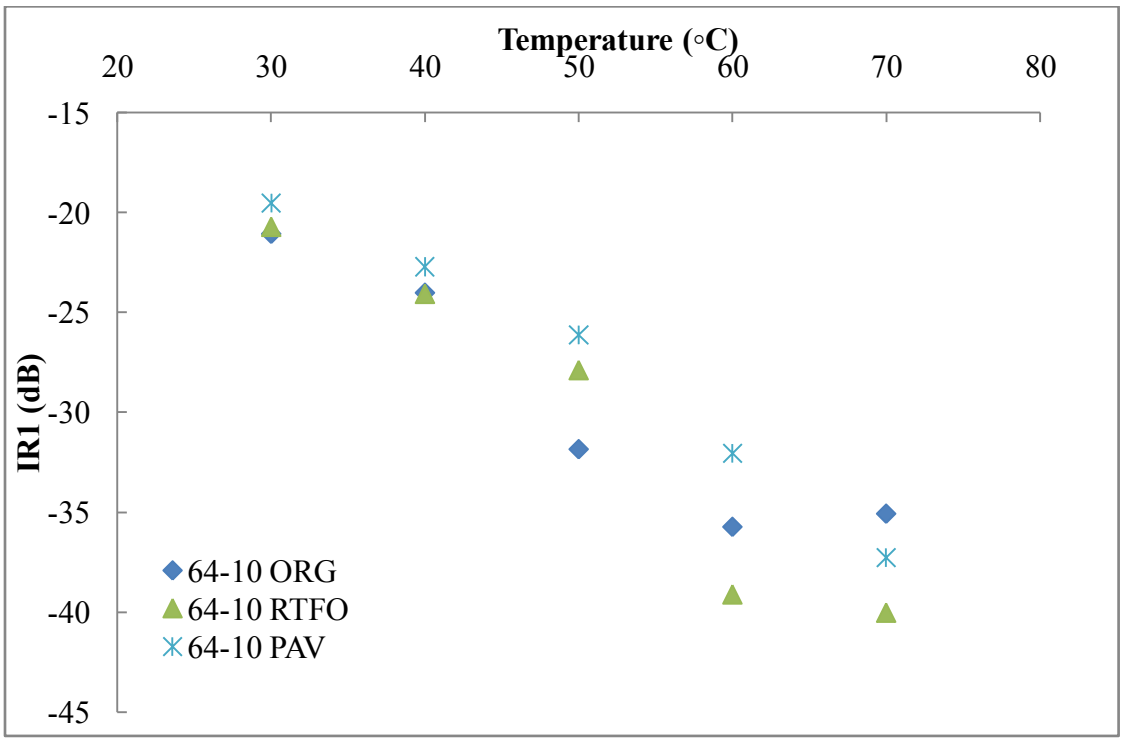

Figure C-16Variation of IR1 with Temperature for PG 64-10

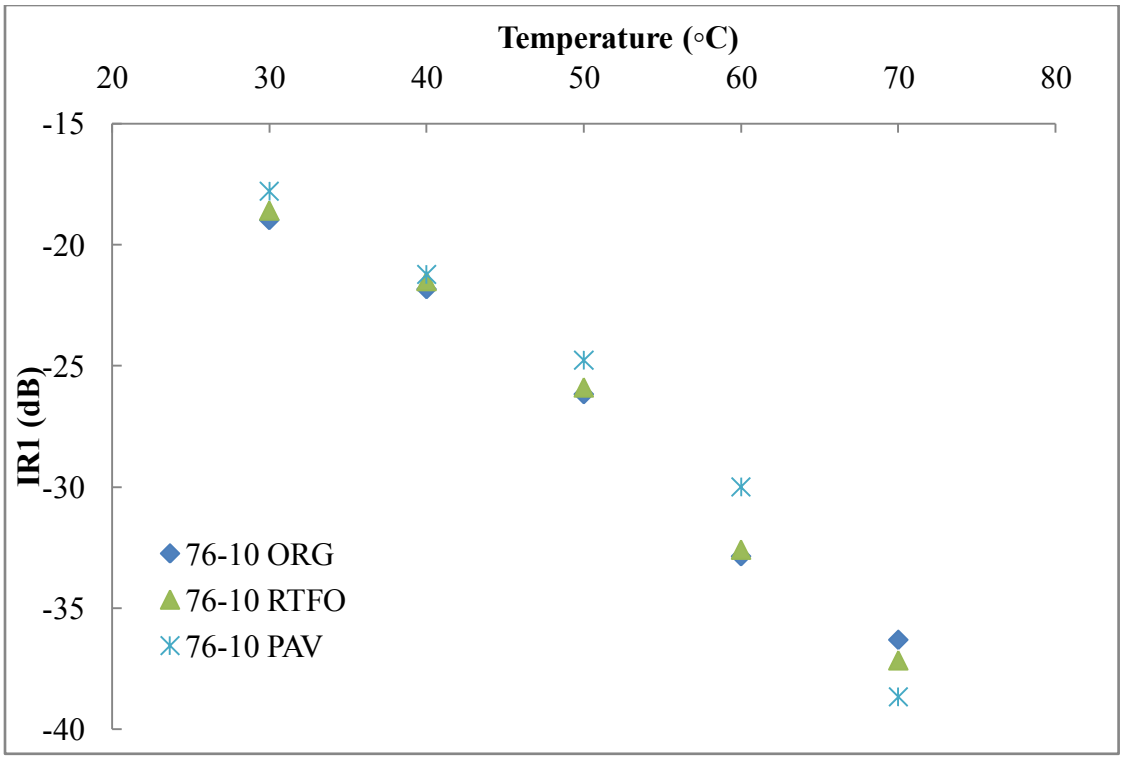

Figure C-17Variation of IR1 with Temperature for PG 76-10

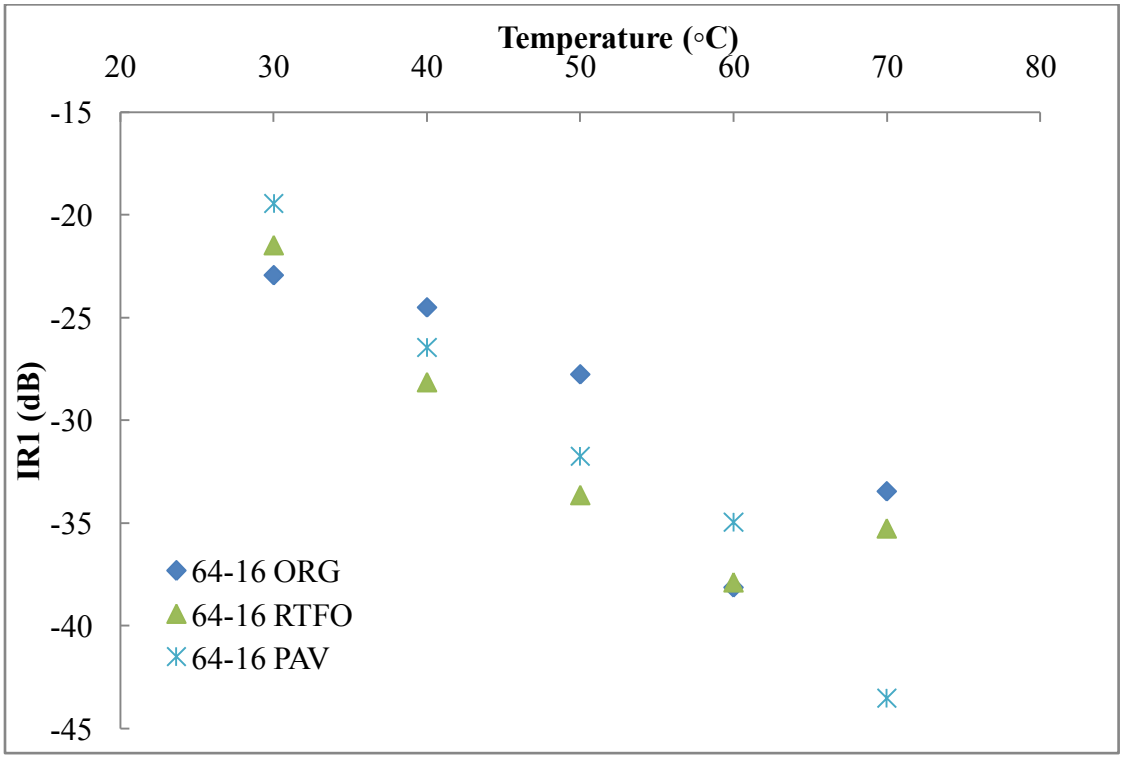

Figure C-18Variation of IR1 with Temperature for PG 76-10

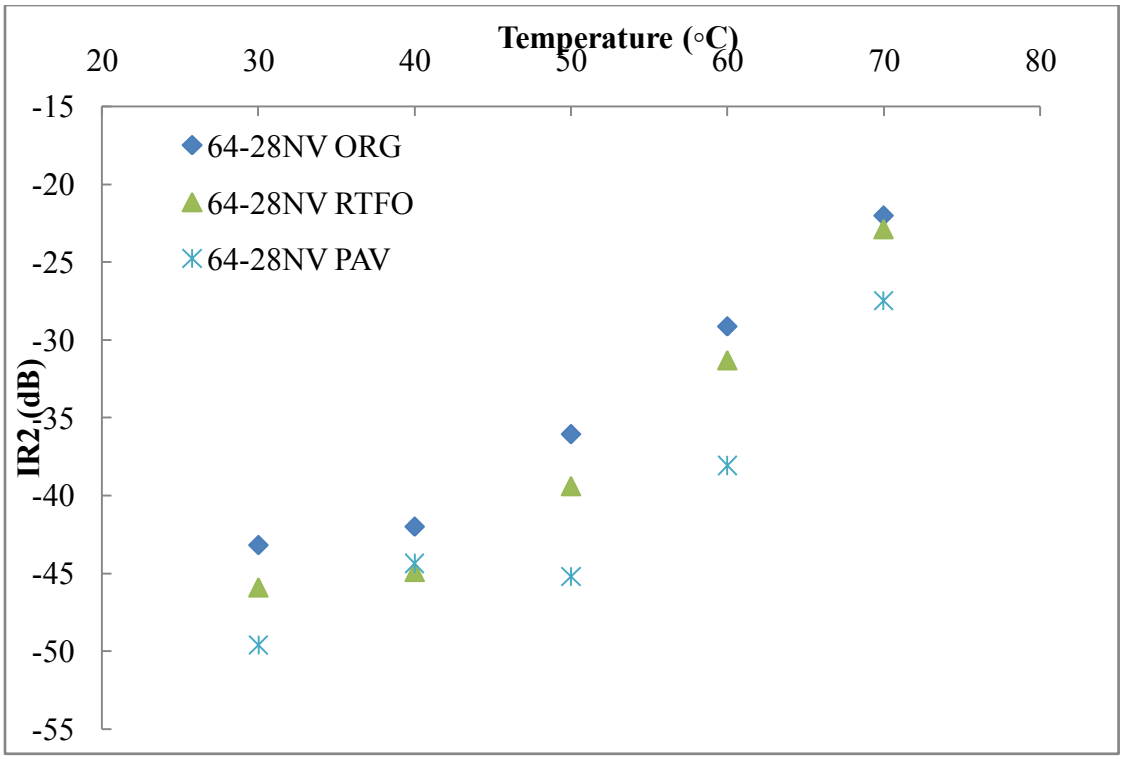

Figure C-19Variation of IR2 with Temperature for PG64-28NV

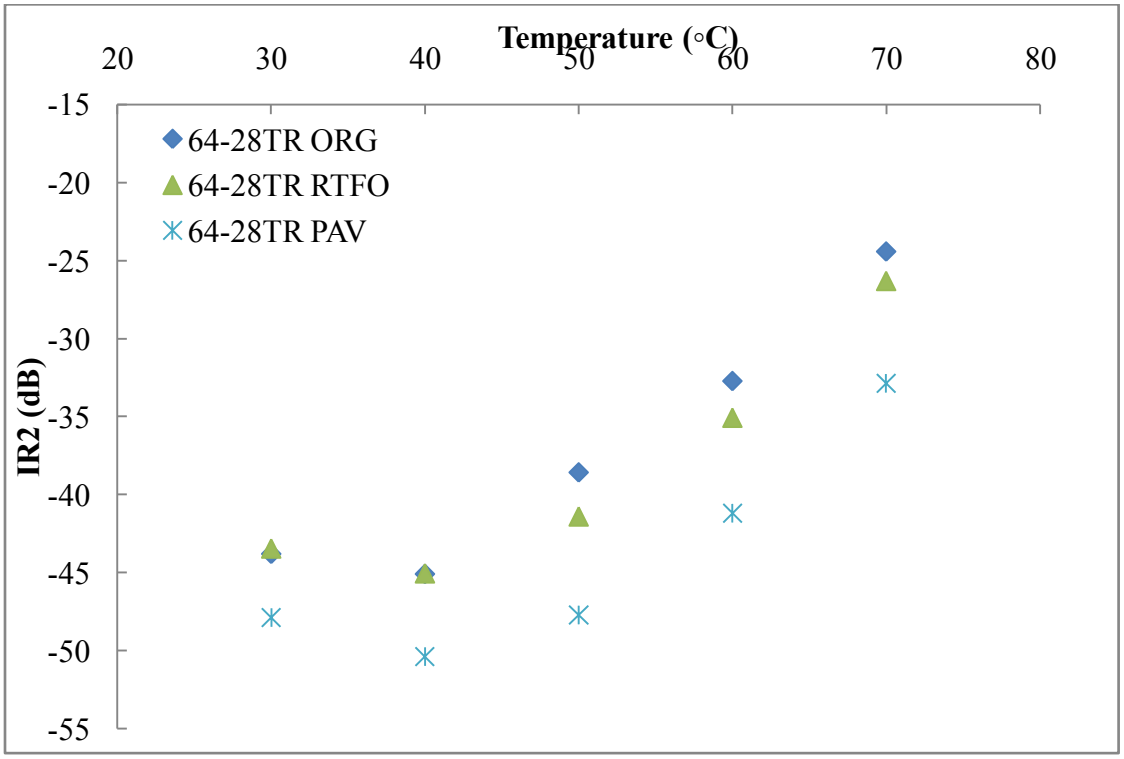

Figure C-20Variation of IR2 with Temperature for PG64-28TR

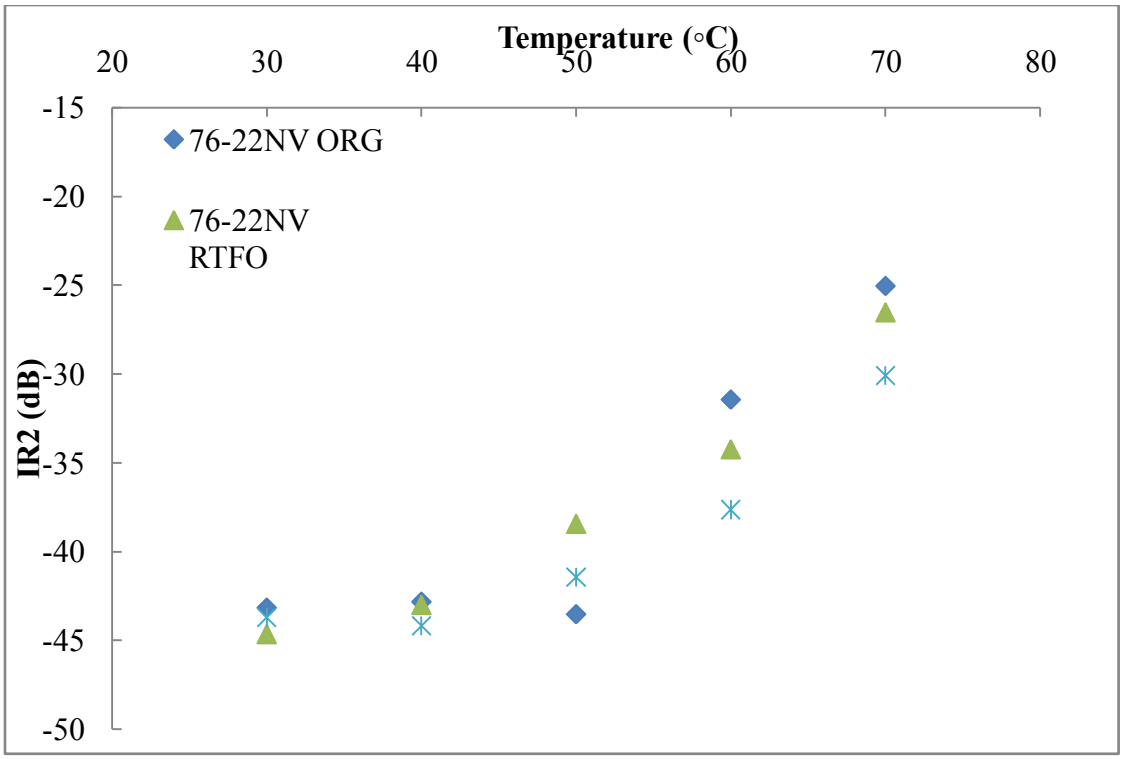

Figure C-21Variation of IR2 with Temperature for PG 76-22NV

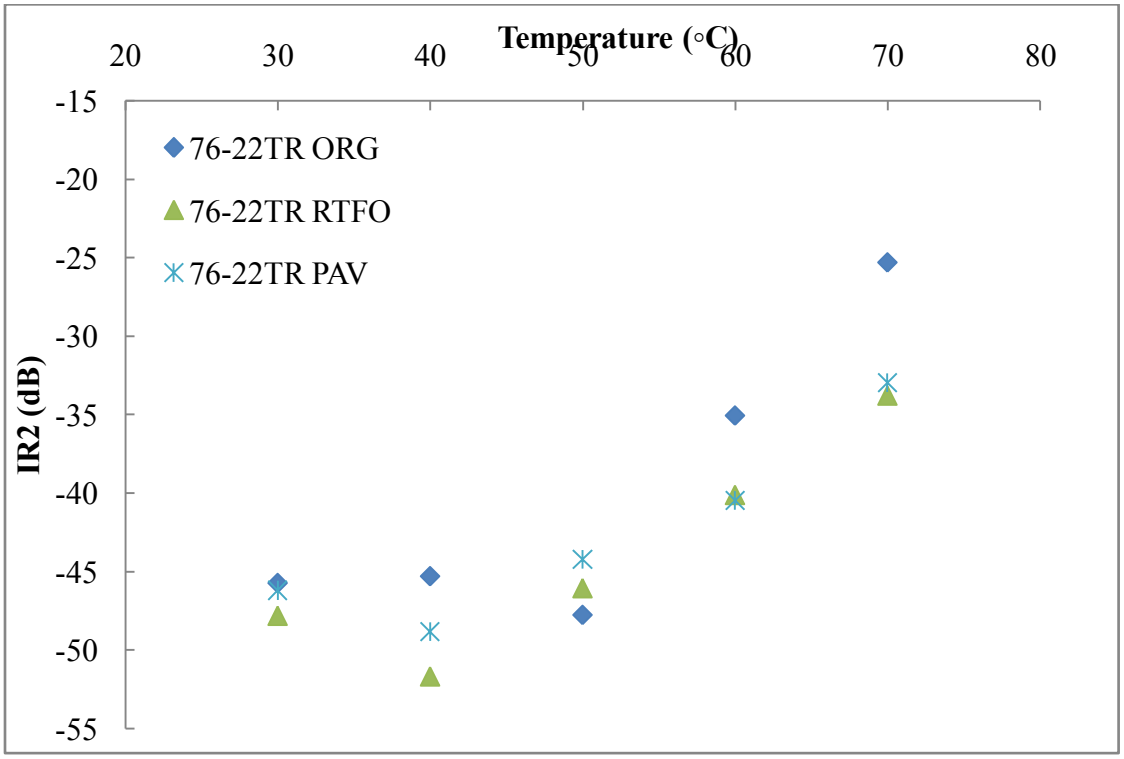

Figure C-22Variation of IR2 with Temperature for PG 76-22TR

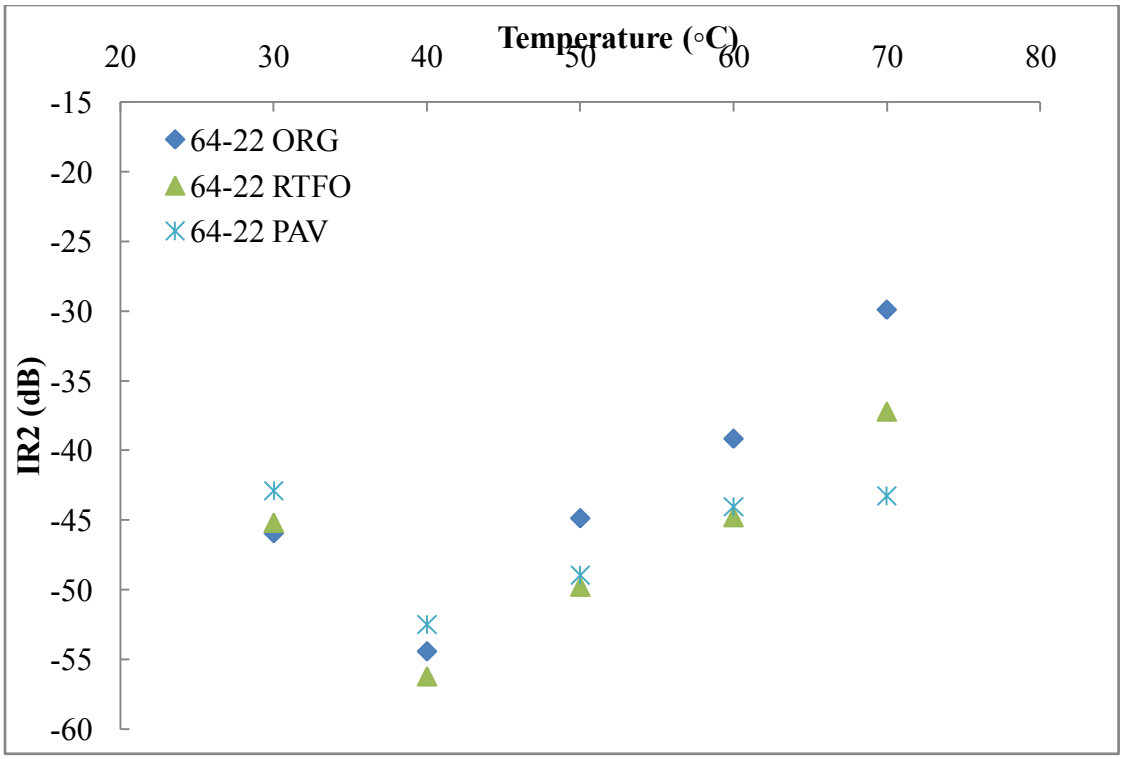

Figure C-23Variation of IR2 with Temperature for PG 64-22

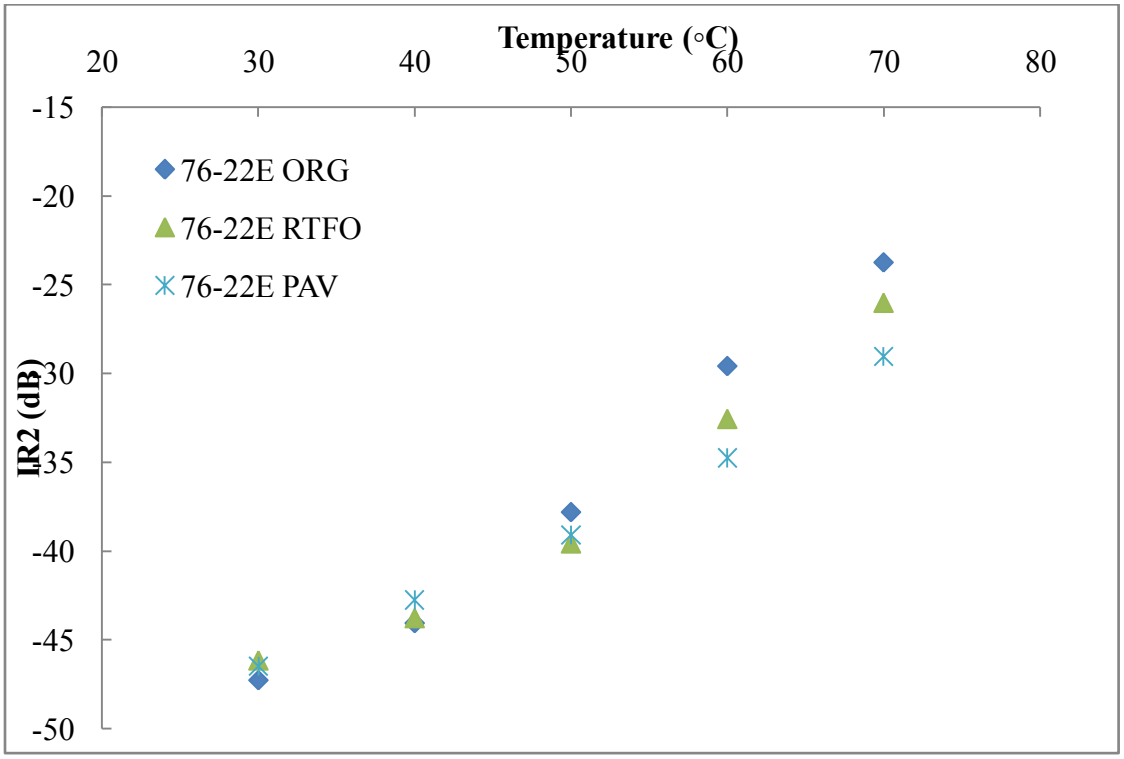

Figure C-24Variation of IR2 with Temperature for PG 76-22E

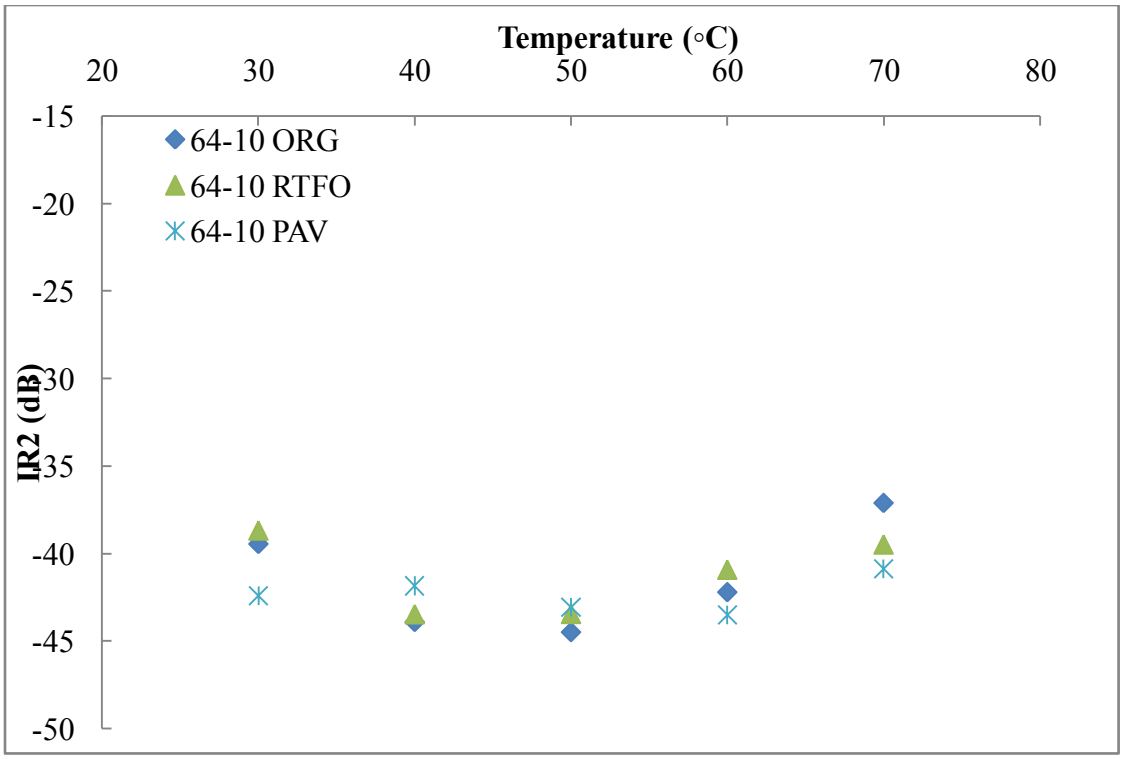

Figure C-25Variation of IR2 with Temperature for PG 64-10

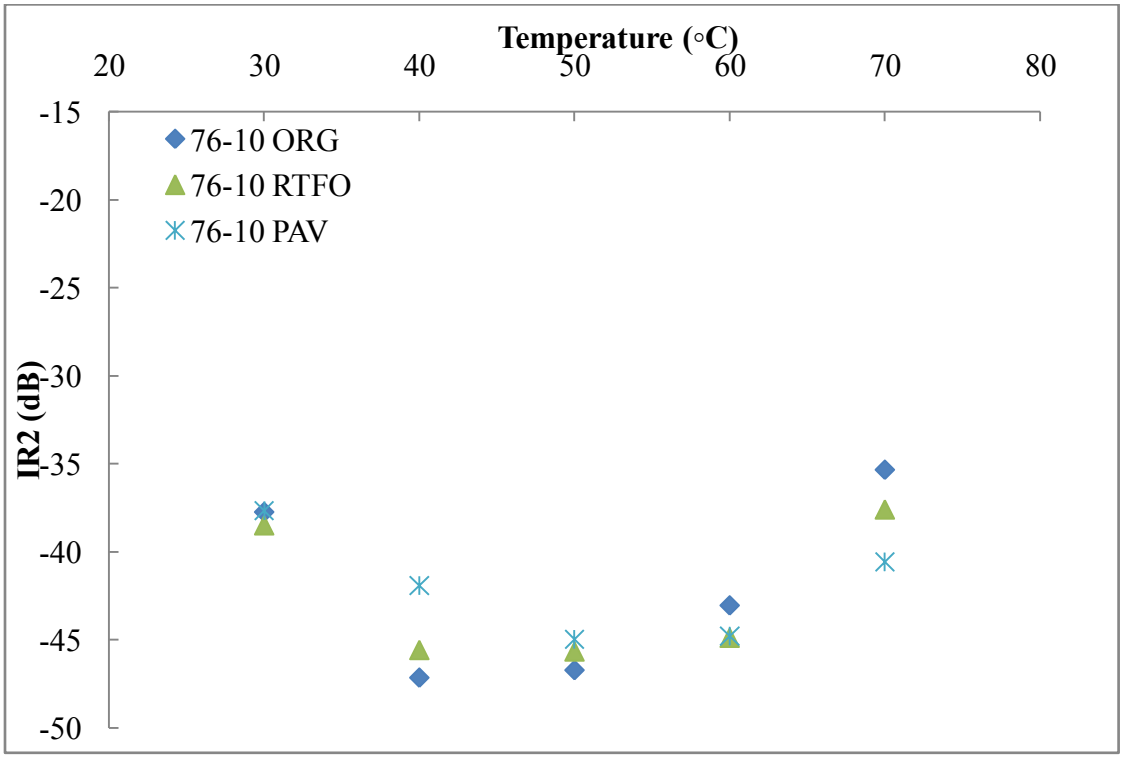

Figure C-26Variation of IR2 with Temperature for PG 76-10

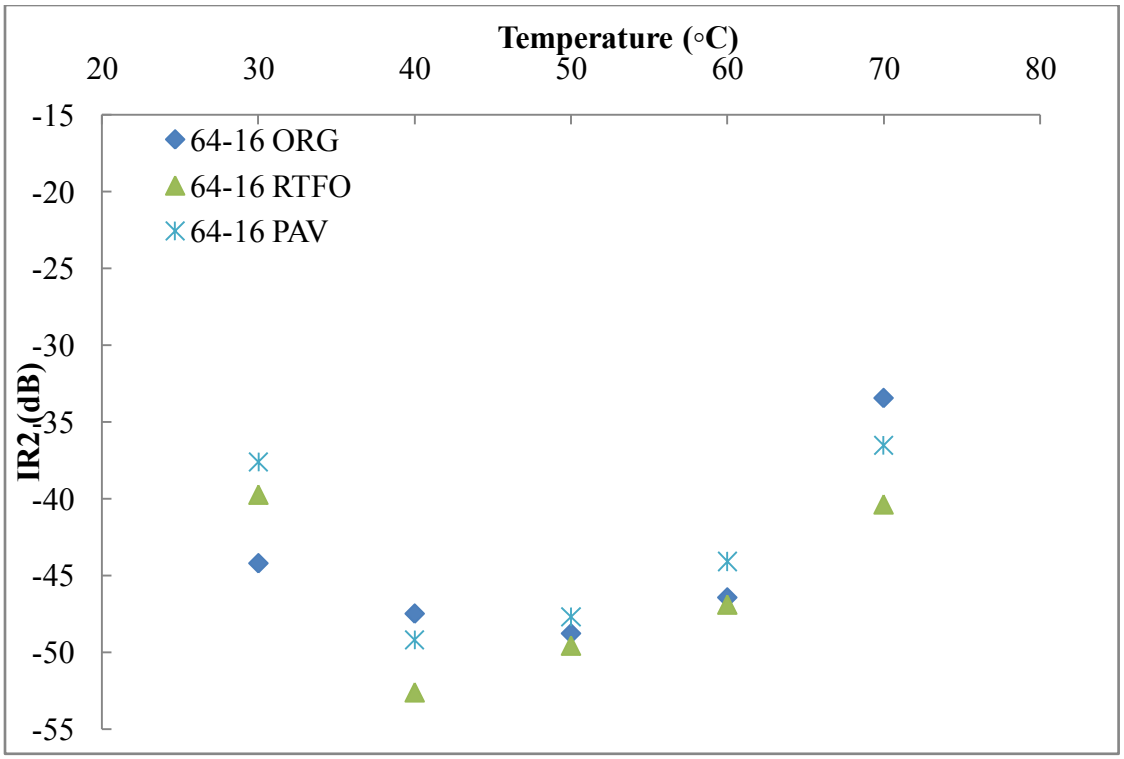

Figure C-27Variation of IR2 with Temperature for PG 64-16

D. APPENDIX D;
Effect of the Use of Polymer and Rubber on Elastic Modulus of Portland Cement Concrete(Siringi, 2012)

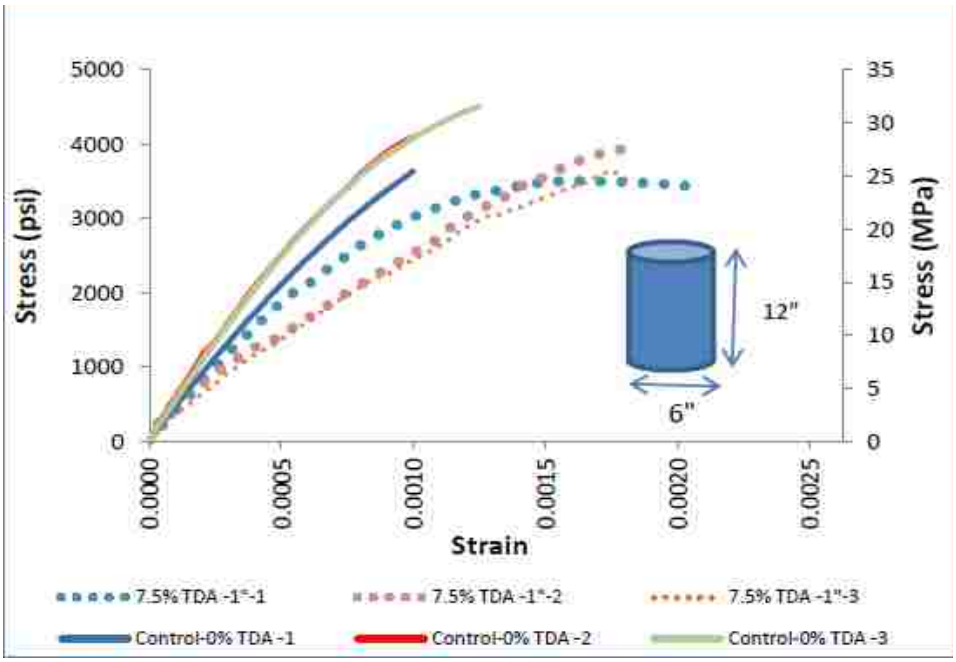

Figure D-28Stress vs. Strain Comparison between Control Concrete and TDA Concrete at 28 days (Siringi, 2012)

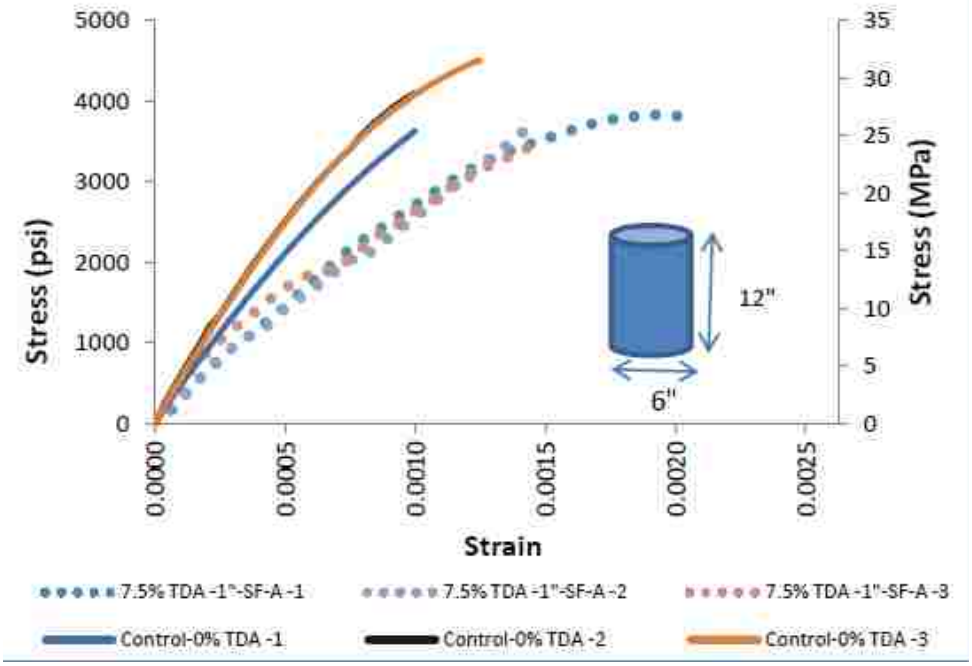

Figure D-29Stress vs. Strain Comparison between Control Concrete and TDA Concrete with Silica Fume at 28 days (Siringi, 2012)

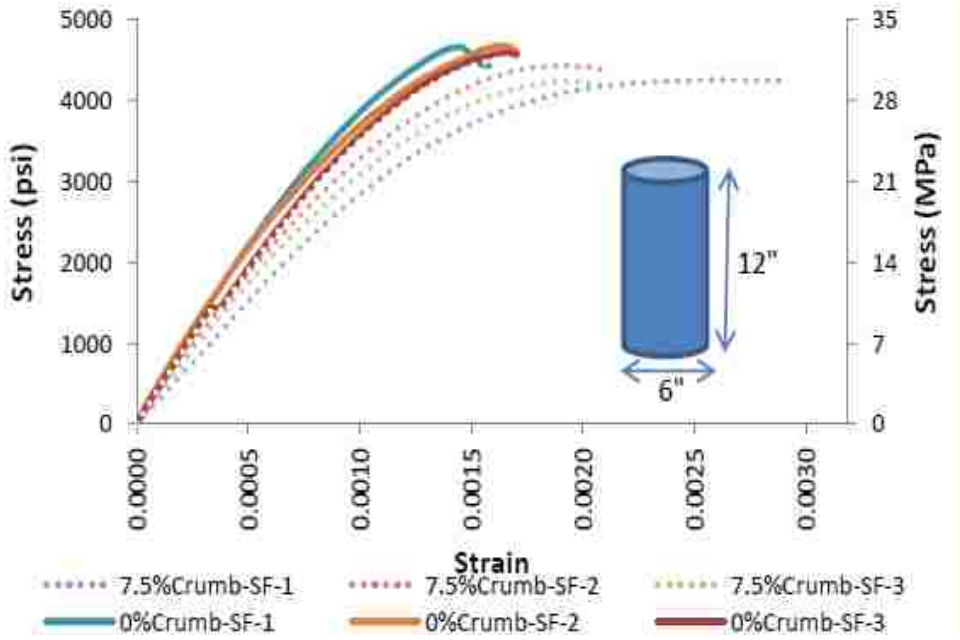

Figure D-30Stress vs. Strain Comparison for concrete with 7.5% Crumb with Silica Fume and Control with Silica Fume (Siringi, 2012)

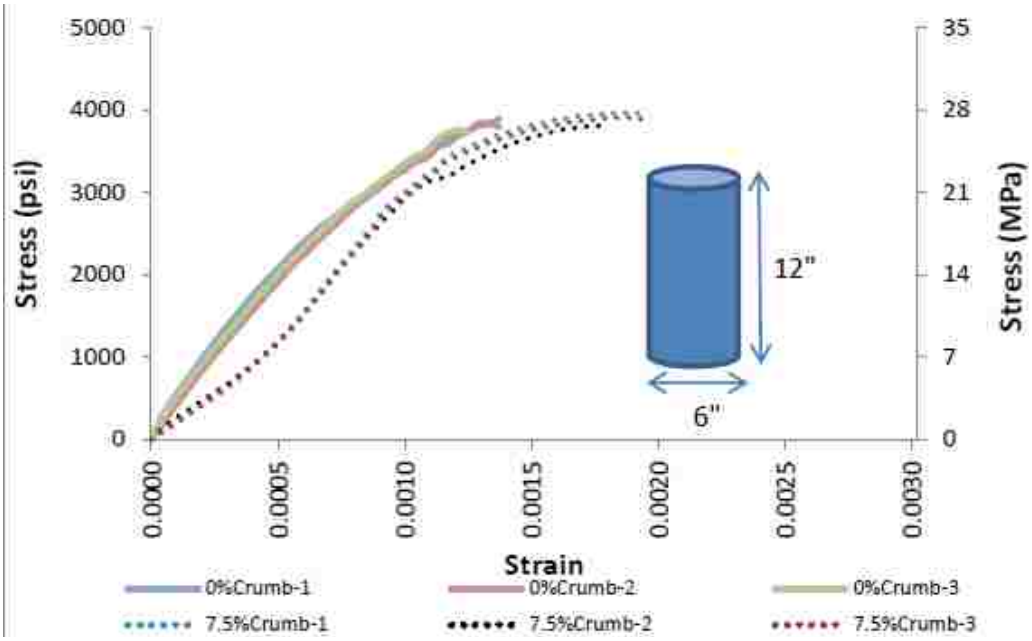

Figure D-31Stress vs. Strain Comparison for Control Concrete (0%Crumb) and Concrete with 7.5% of Fine Aggregate Replaced by Crumb Rubber (7.5%Crumb) (Siringi, 2012)

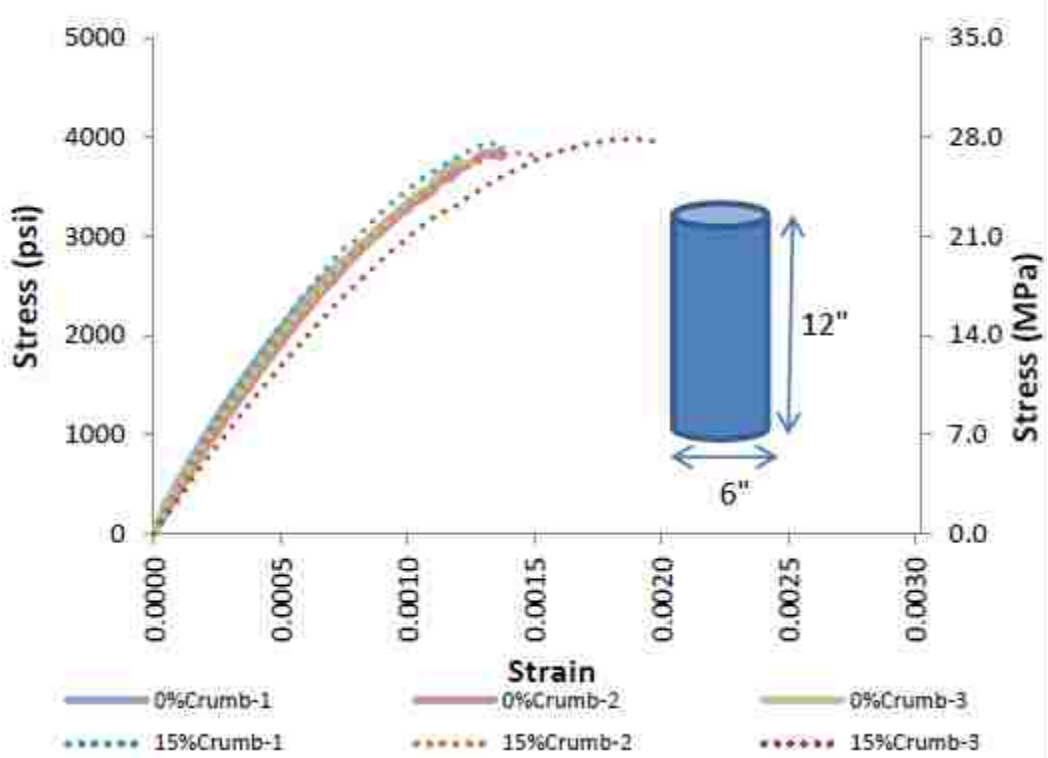

Figure D-32Stress vs. Strain Comparison for Control Concrete (0%Crumb) and Concrete with 15% of Fine Aggregate Replaced by Crumb Rubber (15%Crumb) (Siringi, 2012)

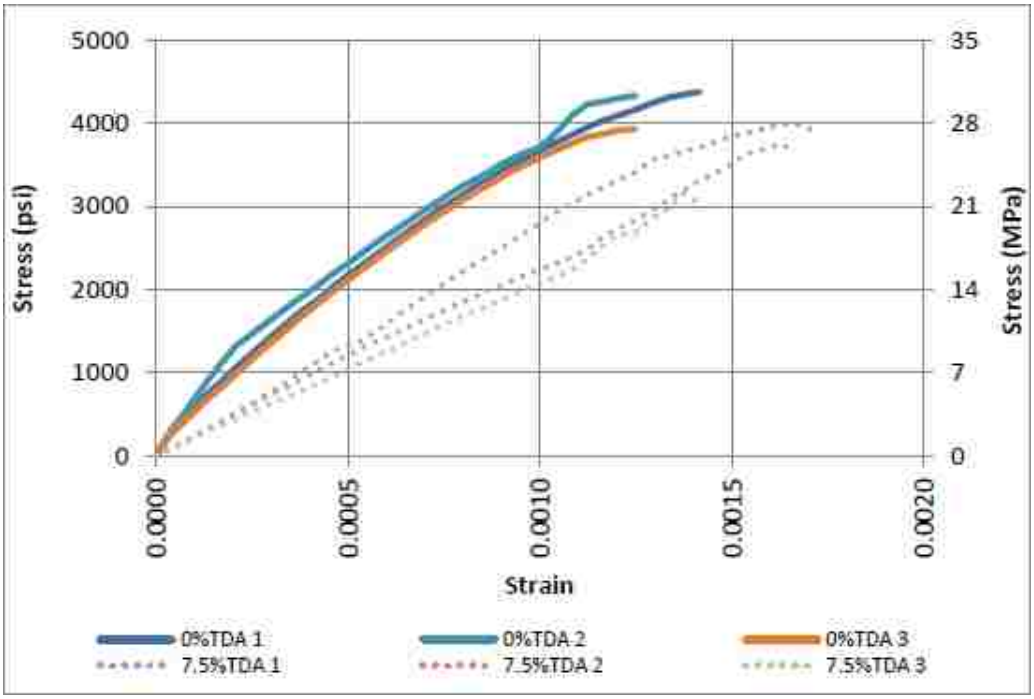

Figure D-33Stress vs. Strain curves for Control Concrete with and without Exposure to Elevated Temperature (Siringi, 2012)

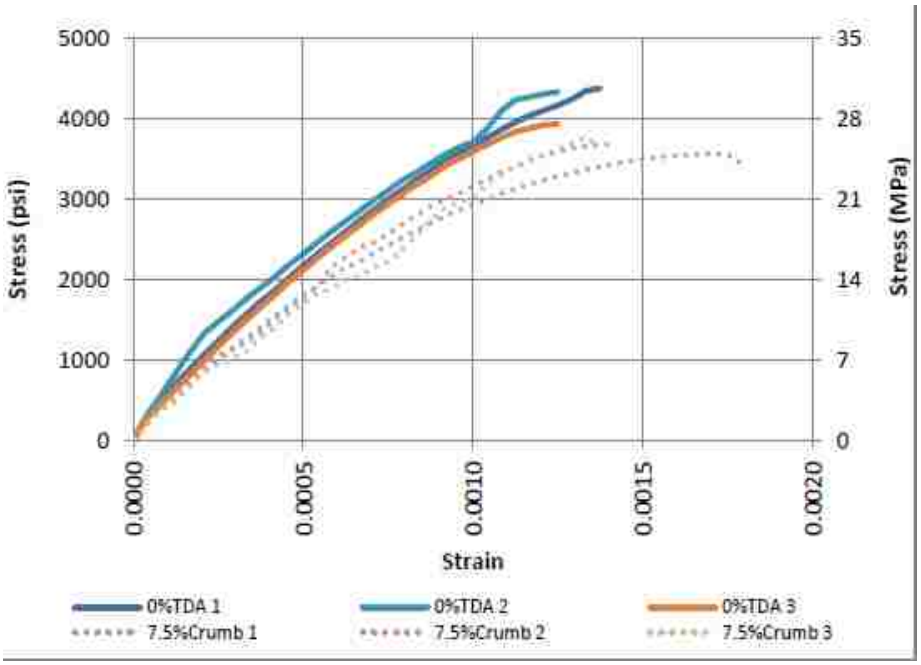

Figure D-34Stress vs. Strain Comparison between the Control Concrete (0%TDA) and Concrete Containing TDA (7.5%TDA) (Siringi, 2012)

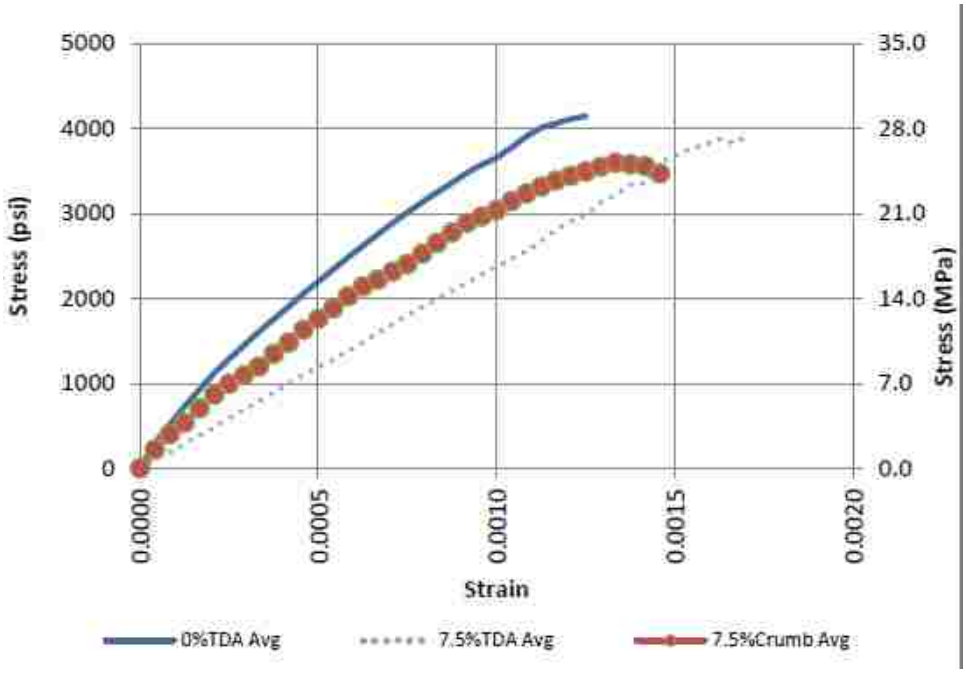

Figure D-35Average Stress vs. Strain Comparison for the Three Types of Concrete (Siringi, 2012)

E. APPENDIX E :
Economic Impact

Grade verification of the asphalt binders is a very time consuming process which requires expensive equipment and skillful labor. Ultrasound devices are inexpensive and operating them simple and could be fast. The application of the ultrasound as an alternative for mechanical tests on asphalt binder has the potential of economical saving for governmental and state agencies as well as private companies. Table E-1 compares the estimated cost of the proposed ultrasound method with the current grade verification routine.

Table E-1Economical Impact of the Propsed Method

	Grade Verification Routine	**Cost**	**Proposed Ultrasound Method**	**Cost**
Equipment	Dynamic Shear	$40,000	Pulser/Receiver and GUI	$10,000
	Bending Beam	$23,000	Transducer	$700
	Direct Tensile	$17,000	Water Bath	$1,000
Total		**$80,000**		**$11,700**
Sample Preparation Time (for 100 samples)	Dynamic Shear	$20	Tin cup	$40
	Bending Beam	$200		
	Direct Tensile	$250		
Total		**$470**		**$40**
Testing Time (for 100 tests)	Dynamic Shear	$625	Ultrasound shot	$60
	Bending Beam	$420		
	Direct Tensile	$625		
Total		**$1670**		**$60**

Proposed method could save 85%, 90%, and 95% in equipment, time value of samples preparation and time value of testing, respectively.

Additionally, unlike all mechanical tests on asphalt binder, the ultrasound measurement is a non-destructive method which its value could hardly be quantified. With a non-destructive ultrasound one sample can be tested repeatedly without imposing any change in the sample's condition.

Bibliography

Alexander, D. R. (1992). *In situ Material Characterization for Pavement Evaluation by the Spectral-Analysis-of-Surface-Waves (SASW) Method.* Geothecnical Laboratory DEPARTMENT OF ARMY.

Aspahlt-Institute. (2003). *SUPERPAVE Mix Design.* Lexington, KY: Aspahlt Institute.

ASTM. (2007). Standard Specification for Performance Graded Asphalt Binder. In *ASTM BooK of Standards.*

Atkins, H. N. (2003). *Highway Materials, Soils, and Concrete* (4th ed.). Columbus, OH: Prentice Hall.

Bhardwaj, M. (2004). *High Efficiency Non-contact Transducers and a Very High Coupling Piezoelectric Composite.* Boalsburg, PA: Ultran Group.

Brown, A. E. (1995). *Rationale and Summary of Methods for Determining Ultrasonic Properties of Materials at Lawrence Livermore National Laboratory.* Oak Ridge, TN.

Dunning, M. (1996). *Evaluation of Ultrasound Method for Detremining Aggregate Gradationin Asphaltic Concrete Mixes.* University of Nevada, Las Vegas.

Dunning, M. (2006). *Feasibility for the Use of Non-contact Ultrasoundfor Applicationwith Asphalt Concrete Materials.* University of Nevada, Las Vegas.

Gan T.H., H. D. (2001). The use of broadband acoustic transducers and pulse compression techniques for air coupled ultrasonic imaging. *Elsevier Science*.

Hyperphysics. (2011). *hyperphysics.edu*. Retrieved from Hyperphysics; Departement of Phusics and Astronomy, Georgia State University: http://hyperphysics.phy-astr.gsu.edu/hbase/hph.html

IllinoisDOT. (2005). *PAVEMENT TECHNOLOGY ADVISORY, POLYMER-MODIFIED HOT MIX ASPHALT.*

Interactive, P. (2012). Retrieved from Pavement Interactive: http://www.pavementinteractive.org/

Krishnan, A. (2005). *Material Characterization of Asphalt Binder Using Ultrasound Testing.* University of Nevada. Las Vegas.

Lakes, R. (2004). *Viscoelastic measurement techniques (Review of scientific instruments).* Madison WI: Dept of engineering Physics University of Wisconsin-Madison.

Lempriere, B. (2002). *Ultrasound and Elastic Waves Frequantly Asked Questions.* Academic Press.

McMaster, R. C. (1959). *Non Destructive Testing Handbook.* New York: The Roland Press.

McMaster, R. C. (1959). *Non Destructive Testing Handbook.* New York: The Roland Press.

NDT. (2012). *homepage, NDT Resource Center*. Retrieved from The Collaboration for NDT Education Center for NDE Iowa State University Ames, Iowa: www.ndt-ed.org

NDT-ed.org. (n.d.). Retrieved from The Collaboration for NDT Education Center for NDE Iowa State University Ames, Iowa: www.ndt-ed.org

Papagiannakis A.T., M. E. (2007). *Pavement Design and Materials.* Hoboken, NJ: John Wiley & Sons.

Reis, J. M. (2005). Mechanical Characterization of Fiber Reinforced Polymer Concrete. *Materials Research*, Vol. 8, No. 3, 357-360.

Siringi, G. M. (2012). *PROPERTIES OF CONCRETE WITH TIRE DERIVED AGGREGATE AND*. THE UNIVERSITY OF TEXAS AT ARLINGTON.

Sztukiewicz, R. (1991). *Application of Ultrasound methods in asphalt concrete testing institute of Civil Engineering*. Technical university Poznań, Poland Ultrasonics.

Zhao, B. b. (2004). Esimation of Ultrasound Attenuation and dispersion Using Short Time Fourier Transform. *Journal of Ultrasound*.

VITA

Mehdi Khalili

khalilim@unlv.nevada.edu

Mobile: 702-286-9167 **Office:** 702-895-1638

Education:

- **Jan 2010-Dec 2013:** PhD Student, University of Nevada Las Vegas, Haward H. Hughs Collage of Engineering, Civil and Environmental Engineering Department
GPA: 4.0/4.0
- **Sep 2004- Dec2006**: Graduate Student, Transportation Engineering, Civil Engineering, Engineering Department, Chamran University, Ahwaz, Iran.
Total GPA: 3.25/4 (First Honor)
- **Sep 2000- Sep2004**: Undergtaduate Student, Civil Engineering Department, Zanjan University, Zanjan, Iran.

Academic and ResearchExperiences:

Jan. 2010- Dec 2013, University of Nevada Las Vegas

- *Instructor of "Highway Construction Materials" (CEE410/610), "Soil Mechanics"(CEE 334), and "Soil Mechanics Laboratory" (CEE334L)*
  - Performing test for two sections of lab each semester
  - Developing an online course for CEE410/610 and CEE 334L (online assignments and lab performance videos)

Jun. 2007- Sep. 2009, University of Science and Technology, Tehran, Iran

Project title:"Assessment of Non-Destructive Tests for Determining the Pavement Layers Density"

- Asphalt Mixture and Bitumen Research Center(ABRC)
  - Master Researcher
  - Organizing research tasks and making connections with industry
  - Producing reports, documents and papers

Jul. 2007- Sep. 2007, University of Science and Technology, Tehran, Iran

Project title:"Laboratory Assessment of Performance of a Kind of Mineral Bitumen"

- Asphalt Mixture and Bitumen Research Center(ABRC)
  - Master Researcher
  - Organizing research tasks
  - Lab testing and data analysis
  - Producing reports, documents and papers

Jun. 2006-Mar 2007, ShahidChamran University, Ahwaz, Iran

Project title:"Path-finding of the Life-time Reduction Causes of Asphalt Pavement Overlays in Tropical Zones of Iran"

- Organizing research tasks
- Field investigation of pavement distresses and data analysis
- Producing reports, documents and papers

May 2009- Dec. 2009, University of Science and Technology, Tehran, Iran

Project title:"Path-finding of the Distresses Causes of Asphalt Pavement in Ahwaz and Holding Forth Executive Approaches for Improvements"

- Municipality of Ahwaz
  - Master Researcher
  - Organizing research tasks
  - Field investigation of pavement distresses and data analysis
  - Producing reports, documents and papers

Publications:

Journal Papers:

1. S. A. Tabatabaie, H. Ziari, **M. Khalili**, "Modeling Temperature and Resilient Modulus of Asphalt Pavements for Tropical Zones of Iran", Asian Journal of Scientific Researches, July 2008

Conference Papers:

1. S. A. Tabatabaie, **M. Khalili**, A. Safikhani, " Path-finding of the Life-time Reduction Causes of Asphalt Pavement Overlays in Tropical Zones of Iran ", 4th National Congress on Civil Engineering, 6-8th May 2008 (in Farsi)
2. S. A. Tabatabaie, **M. Khalili**, A. Safikhani "Assessment of Filler Gradation and Type on Asphalt Layer Distresses", 8th International Congress on Civil Engineering, 10-13th May 2009 (in Farsi)
3. S. A. Tabatabaie, **M. Khalili**, A. Safikhani "Lab. Investigating of Effective Factors on Asphalt Pavements Bleeding", 8th International Congress on Civil Engineering, 10-13th May 2009 (in Farsi)
4. S. A. Tabatabaie, **M. Khalili**, A. Safikhani "Using PMS on Obtaining Optimum Cost of Overlay Construction Projects, Case Study: Ahwaz-Andimeshk", 1th Constructiom Management Congress on Civil Engineering, 8-10th June 2009 (in Farsi)

Skills:

Computer:

- **Proficient in:**AutoCAD, Land Development, Microsoft Office, Geo Studio, UDEC
- **Familiar with:** FLAC, Plaxis, Pascal, Basic, Visual Basic

Language:

- **English:**Fluent
- **Farsi:** Mother tongue

References:

Dr. Moses Karakouzian, PhD, PE
Professor of Civil Engineering
University of Nevada Las Vegas
Department of Civil and Environmental Engineering
4505 Maryland Parkway, Box 454015
Las Vegas, NV 89154-4015
Tel: 702-895-0959
Fax: 702-895-3936
email: mkar@unlv.nevada.edu